CONTRACT NO. 94-347
FINAL REPORT
JULY 1998

Demonstration of a Heavy-Duty Vehicle Chassis Screening Test for Compliance Testing Heavy-Duty Engines

CALIFORNIA ENVIRONMENTAL PROTECTION AGENCY

AIR RESOURCES BOARD
Research Division

DEMONSTRATION OF A HEAVY-DUTY VEHICLE CHASSIS SCREENING TEST FOR COMPLIANCE TESTING HEAVY-DUTY ENGINES

Final Report
Contract No. 94-347

Prepared for:

California Air Resources Board
Research Division
2020 L Street
Sacramento, CA 95814

Prepared by:

Nigel N. Clark
David L. McKain
Jennifer A. Hoppie
Donald W. Lyons
Mridul Gautam

Department of Mechanical Engineering
West Virginia University
Morgantown, WV 26506-6106

July 1998

For more information about the ARB's Research Division, its research and activities, please visit our Web site:

http://www.arb.ca.gov/rd/rd.htm

Disclaimer

"The statements and conclusions in this report are those of the contractor and not necessarily those of the California Air Resources Board. The mention of commercial products, their source, or their use in connection with material reported herein is not to be construed as actual or implied endorsement of such products."

Acknowledgments

This report was submitted in fulfillment of ARB Contract 94-347 "Demonstration of a Heavy Duty Vehicle Chassis Screening Test for Compliance Testing Heavy Duty Engines" by the Mechanical and Aerospace Engineering Department of West Virginia University under the sponsorship of the California Air Resources Board. Work was completed as of May 22, 1998.

Abstract

Emissions testing of new heavy-duty engines is performed to ensure compliance with governmental emissions standards. This testing involves operating the engine through the heavy-duty diesel engine transient Federal Test Procedure (FTP). While in-use engine emissions testing would be beneficial in aiding regions to meet standards dictated by the Clean Air Act, the process of removing the engine from the vehicle, fitting it to an engine dynamometer, testing, and refitting the engine in the chassis, combined with costs associated with removing the vehicle from service, is prohibitively expensive. A procedure for screening engine emissions testing with the engine in the vehicle using a chassis dynamometer was developed to mimic the FTP. Data from two engines and vehicles (a 195 hp Navistar T 444E in a single axle straight truck and a 370 hp Cummins N-14 in a tandem drive axle tractor) is presented as well as correlation between engine and chassis emissions tests. Also included was data gathered to gauge the effects of engine tampering and malfunctioning on emissions levels. It was concluded that engine and chassis emissions levels were well correlated with respect to oxides of nitrogen, but less well so with respect to particulate matter.

Table of Contents

List of Figures

List of Tables

List of Symbols

NO_X – Oxides of Nitrogen
CO_2 – Carbon Dioxide
CO – Carbon Monoxide
HC - Hydrocarbons
PM – Particulate Matter
FTP – Heavy Duty Engine Transient Federal Test Procedure
CBD – Central Business District Test Driving Cycle (from SAE J1376)
BSFC – Brake Specific Fuel Consumption
GVW – Gross Vehicle Weight
MAP – Manifold Air Pressure
T – Torque
S – Speed
g - Grams
bhp-hr – Brake Horsepower - hours
ahp-hr – Axle Horsepower - hours
kg - Kilograms
ppm – Parts per Million (Volume)
σ - Standard Deviation
μ - Arithmetic Mean

Executive Summary

To certify the emissions levels of a heavy duty engine, the engine must be installed in a transient test cell and the emissions measured using a full scale dilution tunnel while the engine is exercised through a specific speed and torque schedule as specified in the Title 40 of the Code of Federal Regulations, Part 86, Subpart N. The speeds and torques are found from a list of relative speeds and torques following the operation of the engine to yield a full power map. Measured emissions are expressed in grams/ brake horsepower-hour. The test must meet requirements for calibration and for post-test regression on the torque, speed and power, but there is still latitude in these requirements that can lead to variation between facilities. This engine testing approach is unsuited to application in in-use compliance testing specifications because it is slow and costly, requiring the removal of the engine from the subject vehicle, and because protocols and procedures for testing an in-use engine remain inchoate. Also, certain failures that may lead to high emissions in the vehicle may not be exhibited when the engine is tested in isolation.

A chassis test method was proposed as a screening device for heavy duty vehicle emissions and it was the objective of this effort to assess the practicality of this approach, to devise a suitable chassis test, and to determine the degree of correlation between this chassis test and the engine certification test. In a chassis test, the whole vehicle is operated with the drivewheels on rollers, with the power removed either through the rollers or from the drive hubs. Existing heavy duty vehicle chassis tests consist of a vehicle speed versus time schedule, with the applied torque implied by the simulated vehicle weight and simulated wind and road losses, without implied presence of gradients. As a result the speeds and torques experienced by the engine are dependent on the nature of the transmission and behavior of the driver, so that existing chassis tests would prove unsuitable for screening work. A chassis test was proposed where the vehicle was mapped and tested in one chosen gear, with the axle speed and axle torque specified to mimic closely the engine torques and speeds associated with the engine certification test. Results could then be expressed in grams/ axle-horsepower-hour, with the axle power and engine power related by the efficiency of the drivetrain. Moreover, modern vehicles could have the fueling ("throttle", though there is no throttle in most diesel engines) controlled directly by a computer generated signal, since these engines are of the electronic "drive by wire" type.

The test program was executed using a Navistar T 444 E engine in a 6-speed single axle International chassis truck, and a Cummins N14 engine in a 10-speed over-the-road tractor that was configured to operate either with tandem drive axles or a single drive axle. Both engine and chassis emissions measurement were employed. Each engine was subjected to mapping and to hot and cold stock engine certification tests, and levels of carbon dioxide (CO_2), carbon monoxide (CO), oxides of nitrogen (NO_X), hydrocarbons (HC) and particulate matter (PM) were recorded. In addition, the engines were operated in various tampering modes to raise emissions levels with a view to correlating these elevated levels with the behavior when the engine was later tested in the chassis. The Navistar was tested with an alternate stock controller and three temperature sensor tampering modes that caused the engine to employ a cold start mode and elevated NO_X levels. For example, with the sensor input falsely set to correspond to 39 degrees Farenheit (4 degrees Centigrade), the hot test NO_X level was 15.25 grams/ brake horsepower-hour compared to 4.98 grams/ brake horsepower-hour for the stock case. The Cummins engine

was also operated with a disabled manifold air pressure sensor and a false manifold air pressure sensor signal that raised the level of PM measured.

Each engine was installed in the respective truck, and emissions testing was conducted using the West Virginia University Transportable Heavy Duty Emissions Testing Laboratory, which employs a full scale exhaust dilution tunnel and analyzers similar to those in the engine emissions certification test cell. Power was withdrawn directly from the vehicle hubs while the tires ran on rollers. Axle torque was measured using torque cells in the driveline and power was absorbed using eddy current dynamometers installed on the laboratory chassis dynamometer test bed. Motoring was not possible, so that some deviation between the engine behavior during the chassis and engine testing did occur. Each vehicle was mapped to yield a curve of full power axle torque, with one gear selected, through the engine speed range. The axle torque was referenced back to engine speed and was used to construct the target axle torque schedule during the subsequent emissions testing. Figure S.1 compares the engine torque for the stock Navistar engine with the axle torque using the single axle Navistar truck. Difference between the curves represents drivetrain losses. Resulting data provided for the development of a drivetrain and rolling tire loss model: efficiency was typically less than 80%. Emissions levels were measured for both trucks using stock and tampering modes, and the tractor was operated in three different gears and with tandem and single axle drive.

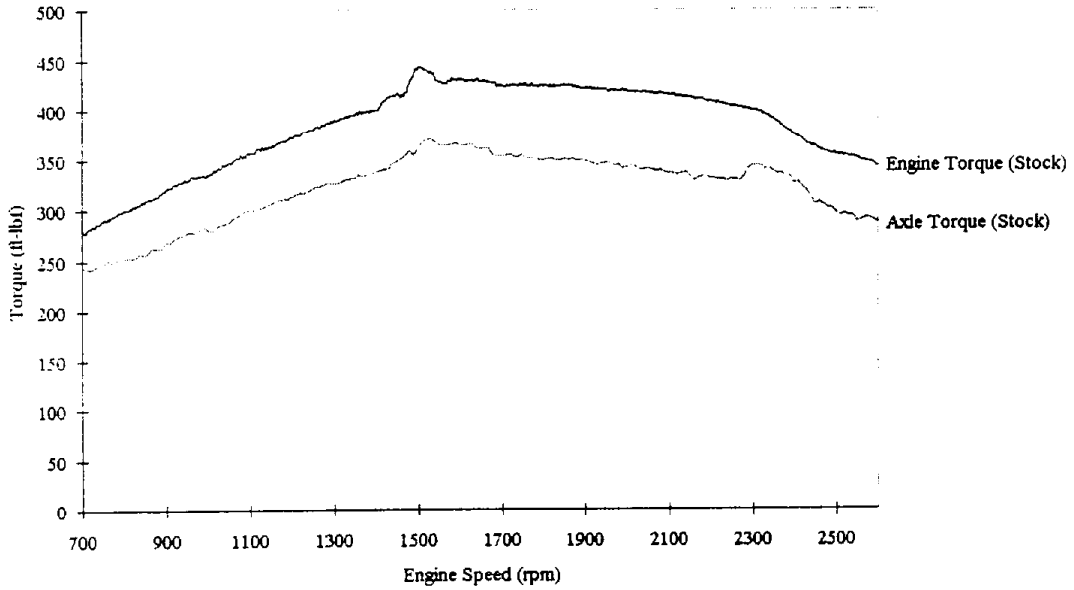

Figure S.1 – Comparison of Engine and Axle torque maps from the Navistar engine.

Chassis (in grams/ axle-horsepower hour) and engine (in grams per brake horsepower-hour) NO_X levels correlated well, for both the Navistar and Cummins engines, and for the combination of data from both engines. Figure S.2 shows all of the data, which shows that a best fit prediction is given by:-

$$\text{Engine } NO_X \text{ (g/bhp-hr)} = 0.775 \times \text{Chassis } NO_X \text{ (g/ahp-hr)}$$

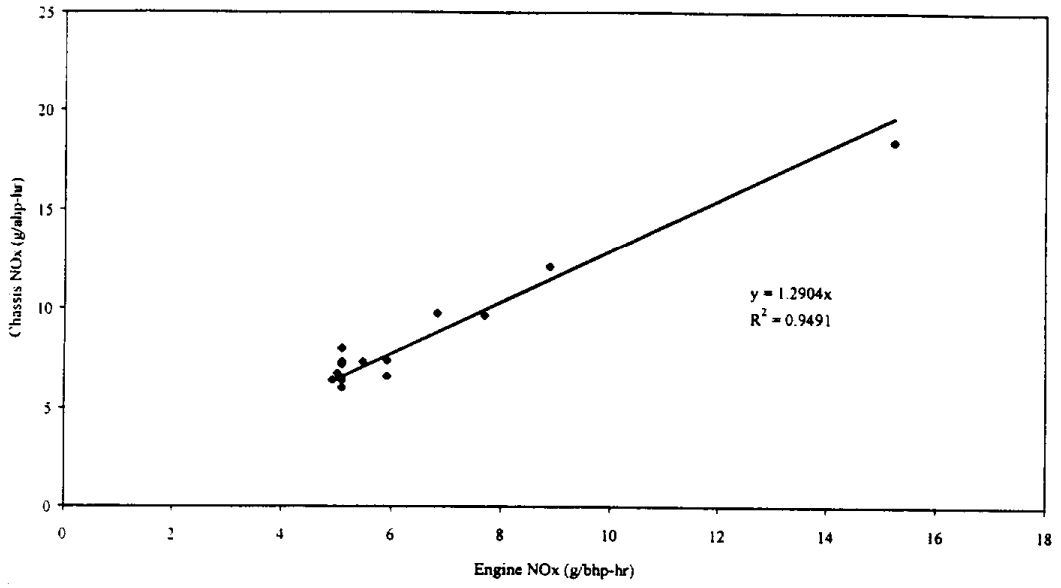

Figure S.2 – Linear curve fit to NO_X mass emissions data from both the Navistar and Cummins chassis testing to NO_X mass emissions data from engine testing. (Data representing both stock and tampered/malmaintained modes).

The excellence of this correlation can be attributed to the near linearity of NO_X with respect to engine power. A good correlation between chassis and engine tests was also found for NO_X/CO_2 ratios:

$$\text{Engine } NO_X/CO_2 = 0.98 \times \text{Chassis } NO_X/CO_2$$

Particulate matter was less well correlated, with the best fit as

$$\text{Engine PM (g/bhp-hr)} = 0.78 \times \text{Chassis PM (g/bhp-hr)}$$

Particulate matter emissions are clearly nonlinear with respect to engine load and escalate significantly as full power operation is approached. PM emissions are sensitive to the transient operation of turbocharged diesel engines. Also, PM measurements are known to be marred by dilution tunnel behavior, where factors such as thermophoresis, soot deposition on the tunnel wall and wall deposit shedding lead to variations between runs. The variation of PM measurements between certification laboratories during "round robin" tests is well known.

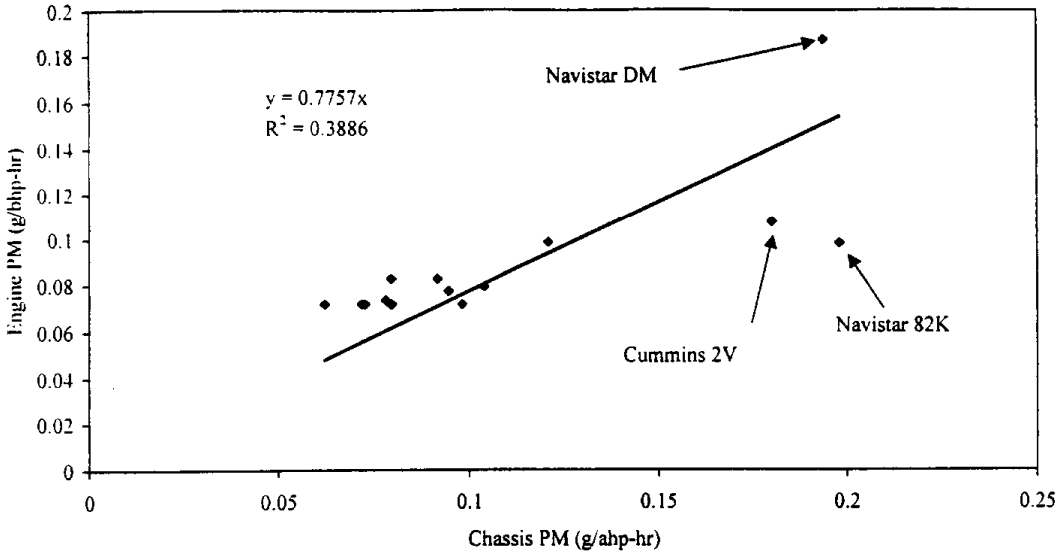

Figure S.3 – Comparison of chassis and engine particulate emissions from tests on both the Navistar and Cummins engines.

The correlations presented above should not be used as screening criteria without careful consideration of errors of omission and comission. To minimize the sum of vehicles passing the screening wrongly and failing the screening wrongly, the criterion that chassis NO_X (in g/ahp-hr) is greater than 1.6 times certification level NO_X (in g/bhp-hr) proved best for the 71 chassis tests generated by this research. Correlation between chassis and engine tests for HC was poor, while for CO correlation was good, but neither CO nor HC are typically of interest because they are emitted at low levels by diesel engines.

The investigators have concluded that the chassis test, with the vehicle operated in a single gear, is a viable approach to screening the emissions from heavy duty engines without removing the engine from the truck. Modest increases in NO_X can be detected, but only gross PM emitters can be detected. Although the practicality of the method is now well proven, it is recommended that the database of chassis and engine tests is enlarged before seeking to set any firm screening criteria.

1. Introduction

The goal of this research project was to develop a vehicle (chassis) test schedule to provide values of vehicle emissions levels that can be readily correlated with the current Federal Test Procedure (FTP) for heavy duty engine emissions certification. At present, heavy duty engines produced by third party manufacturers must be certified to have emissions of carbon monoxide, hydrocarbons, oxides of nitrogen, and particulate matter below legislated levels when the engine is exercised through a well defined transient speed and torque schedule as defined in the Code of Federal Regulations, Title 40, Part 86, Subpart N.

Comprehensive in-use engine degradation information is needed for the enforcement of emissions compliance and for improved atmospheric pollutant inventory. At the commencement of this project, there was no prescribed method for measuring the effects of engine degradation on engine emissions other than by removing the engine from the vehicle and testing using the customary engine transient test procedure. Customarily, this type of testing is precluded by the associated downtime, cost and liability involved with the engine removal and re-installation. The development of a chassis engine emissions testing cycle representative of the engine FTP would increase the ability to screen and monitor engine degradation without the difficulties involved in engine removal for testing.

A thorough literature review was performed to examine existing chassis cycles and determine how well they correlated in engine speed and torque to the heavy duty engine FTP but use of speed-time chassis cycles is clearly confounded by the use of transmissions. Since no chassis cycles were found that would be applicable towards achieving the objective of this project it was decided that a best correlation would be achieved using a chassis simulation of the engine FTP.

Initial testing was performed on a Ford tractor with the chassis dynamometer to aid in developing test procedures. Subsequently, two recent manufacture vehicle/engine combinations were examined, namely a Navistar straight truck with a Navistar T 444E (195 hp) diesel engine and an International Tractor with a Cummins N-14 (370 hp) diesel engine. The Navistar engine used for the testing was on a long term loan from Navistar for experimental research while the Navistar truck was obtained from Navistar specifically for this testing. The International truck and Cummins engine were rented from Ryder Truck Rental. Both engines were electronically controlled which enabled the researchers to develop an electronic pedal control system in lieu of a human driver for the chassis testing. Data gathered from the testing was analyzed by both WVU and by Optimation Inc.

In addition to testing as received, both engines were also tested in malmaintained and tampered configurations both on the engine and chassis dynamometers. This was done to gauge the effect of tampering and malmaintenence on emissions and form a better thesis on pass/fail criteria for the chassis emissions testing. Additional testing was also performed to examine the effects of different drivetrain configurations on both emissions and performance.

2. Discussion of Chassis and Engine Cycles

At present chassis tests are not recognized for the certification of heavy duty engine. An engine test is favored because in may cases, the vehicle is powered by an engine produced by a thrid party manufacturer. Since it is both time consuming and expensive to take a vehicle out of service to remove the engine for emissions testing, it would be advantageous to develop a cycle to test the engine in the vehicle using a chassis dynamometer. The following review of heavy-duty engine and chassis test cycles was performed to determine if an existing combination of chassis and engine cycles would produce comparable emissions.

2.1 CAPE-21

In the early 1970's, the EPA initiated the CAPE-21 study to address vehicle emissions by collecting data from in-use heavy duty vehicles. Fifty-five trucks and five buses in New York City and Los Angeles were instrumented, and travel data was collected for both freeway and urban operating conditions. Also included in this database were some data collected in the "Truck-Taxi Survey" conducted in 1963 by the Tri-State Transportation Committee in New York, New Jersey and Connecticut and traffic count data taken at approximately 275 cordon points in the three states from 6 a.m. to 8 p.m. for a typical weekday in 1962-63 [Cosby, 1973]. The goal of the Cape-21 study was to identify the composition, function and travel behavior of urban trucks, and characterize the function and use patterns of trucks operating over the urban streets and freeways.

The final CAPE-21 database consisted of the operating data for forty-four trucks and four buses in New York and forty-four trucks and three buses in Los Angeles. Gasoline and diesel fueled, as well as two and three axle tractor trailer configurations were represented in this study. Data acquisition instrumentation on each vehicle recorded ten data channels including date and time, engine and vehicle speed, load factor, road type, traffic density, throttle position, and engine temperature. This data was then conditioned and reduced to a form listing engine speed and load factors as percentages of engine speed and power, respectively. This set of data is the CAPE-21 database in its final form [EPA, July 1978].

In 1974, the EPA awarded Olson Laboratories the "Heavy-Duty Vehicle Cycle Development" contract for the purpose of developing software to process the CAPE-21 data base into a format suitable for generating engine dynamometer and chassis dynamometer cycles, developing software to generate cycles representative of the CAPE-21 data base, and generating candidate cycles for trucks and buses from the CAPE-21 data base [EPA, July 1978]. The collected data was used to formulate Monte Carlo simulations of NY non-freeway, LA freeway and LA non-freeway driving. These sub-cycles were combined to develop whole cycles that were sufficiently representative of real-life driving patterns [EPA, June 1978].

2.2 Cycles Derived From Real Data

Perhaps the most prominent of these statistically derived cycles are the Federal Test Procedure (FTP), **Figure 2.1**, for engine testing and the EPA Urban Dynamometer Driving Schedule for

Heavy-Duty Vehicles (Test D), **Figure 2.2**, for chassis testing, both listed in the CFR [Pt.86, App.1, 1996]. Note that the latter is a highly transient speed-time trace which cannot be attained readily with manual transmissions and low power to weight ratios that are frequently used by many in-use heavy-duty vehicles. Since 1984, the EPA have required transient emissions certification testing, using the FTP, of all heavy-duty on-road engines sold in the United States [SWRI, 1997].

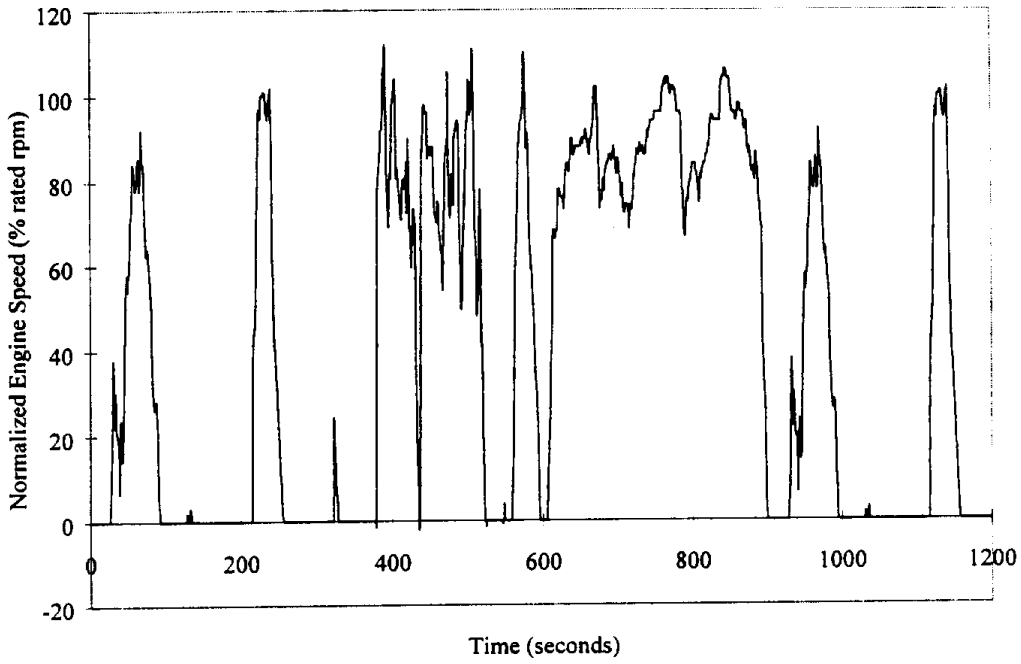

Figure 2.1 EPA Heavy-Duty Engine Transient Cycle Federal Test Procedure (FTP)

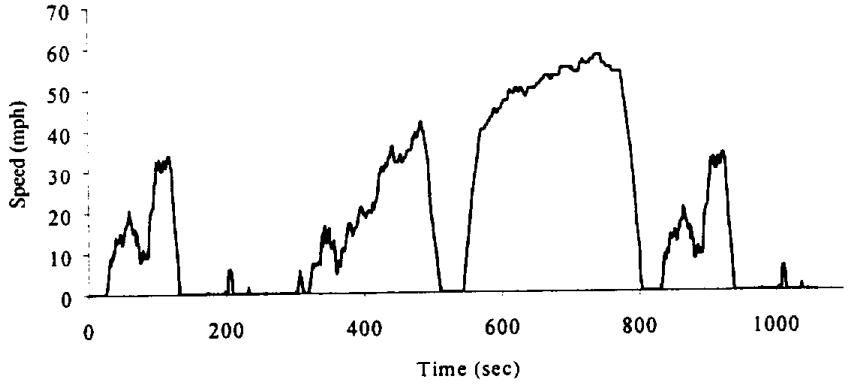

Figure 2.2 EPA Urban Dynamometer Driving Schedule for Heavy-Duty Vehicles (Test D)

Other tests derived from this actual vehicle data were the New York Bus **(Figure 2.3)**, New York Truck **(Figure 2.4)** and New York Composite Cycles **(Figure 2.5)** [EPA, July 1978]. These tests,

along with the EPA Test D, were used in Canada to test and compare ethanol and diesel bus emissions. Interestingly enough, the New York Bus Cycle, intended to simulate very low average speed operation in dense city traffic, consistently produced fuel consumption and CO_2 emissions in grams/mile, twice that of any other cycle. Very few cities have the degree of traffic congestion implied by this cycle; therefore, it is only applicable in high traffic areas such as New York City, Tokyo, Beijing or Mexico City [King et al., 1992].

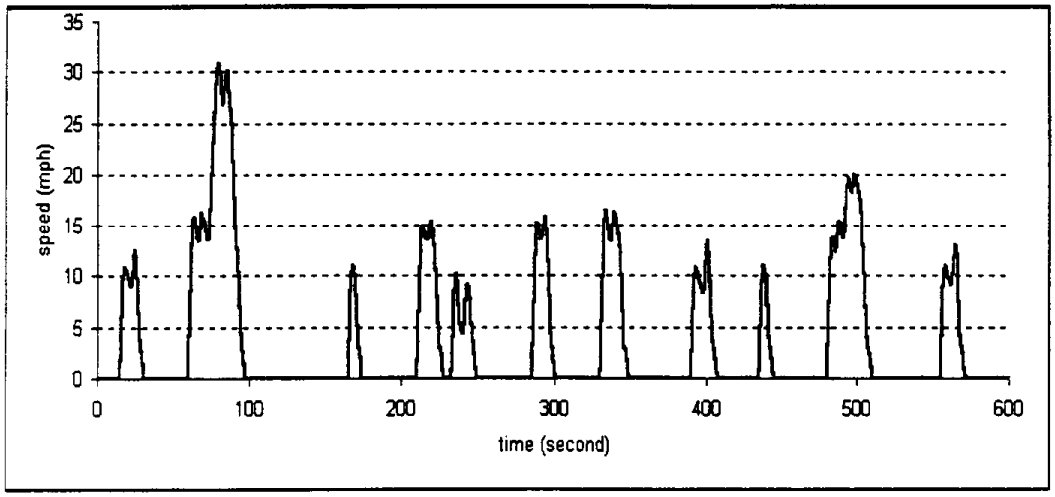

Figure 2.3 New York Bus Cycle [Wang, 1997]

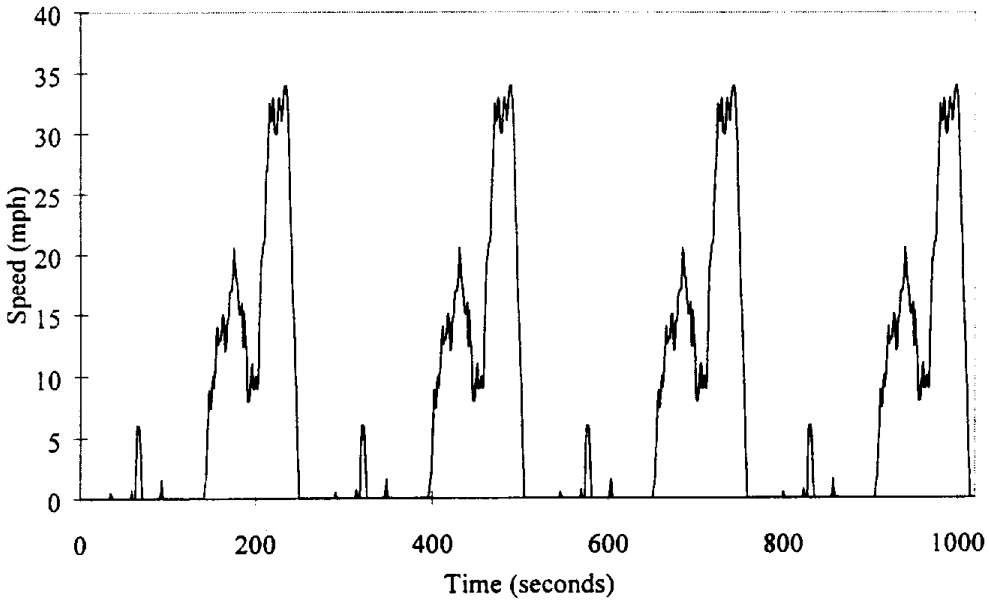

Figure 2.4 New York Truck Cycle

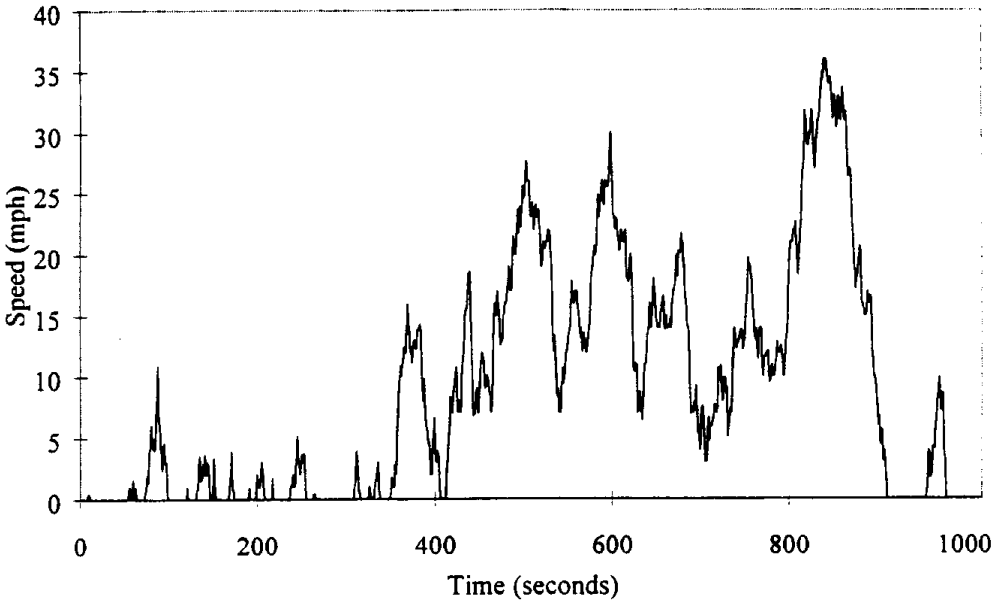

Figure 2.5 New York Composite Cycle

The New York Composite Cycle, **Figure 2.5,** was used by Chevron Corporation (referred to as the unfiltered bus cycle) to test emissions and fuel economy of a methanol bus with a 1988 DDC engine [Thompson et al., 1990]. Since it is not repetitious, it was thought to more fully explore engine performance. The high frequency components of the speed trace have not been removed, so this cycle is unsuited for emissions research and was not employed in any relevant testing.

2.3 Synthesized (or Geometric) Cycles

In contrast to cycles derived from data gathered from in-use vehicles, synthesized cycles represent characteristic driving patterns based on the typical operation modes: idle, acceleration, steady state and deceleration. The use of synthesized cycles eliminates the need to collect large banks of data from operating vehicles. Cycles derived from both methods are presently being used in emissions testing; yet neither is a true simulation of real life driving routines.

The composite nature of synthesized cycles causes the transitions between various modes to be somewhat artificial in nature [Barnes, 1985]. Defining these modes is necessary for proper analysis of the resulting data. The modes have been identified as follows [Bata et al., 1994]:

- Acceleration - The absolute acceleration of the vehicle is more than 0.03 m/s^2.
- Steady State - The absolute acceleration of the vehicle is less than 0.03 m/s^2 and the vehicle speed is greater than 0.3 m/s.
- Deceleration - The deceleration of the vehicle is greater than 0.03 m/s^2.
- Idle - The vehicle speed is less than 0.3 m/s.

Note: The indicated acceleration and deceleration rates and speeds are prescribed, but lower values may be necessary in order to compensate for the low power to weight ratios of heavy-duty vehicles.

Several synthesized test cycles exist and are used extensively in emissions research. The "local test cycles", **Figures 2.6** and **2.7,** and the "transit coach design operating profile duty cycle" in **Figure 2.8**, reported in SAE Standard J1376 [1993] proved suitable for determining fuel consumption but were not considered to be representative of in-service vehicles. The transit coach design operating profile duty cycle offers a set of "sawtooth" cycles for Central Business District Simulation (CBD), up to 8.94 m/s (20 mph) shown in **Figure 2.9**, Arterial Operation, up to 17.9 m/s (40 mph), and Commuter Operation, up to 24.6 m/s (55 mph). These three "mini-cycles" are combined to travel a total of 22.5 km (14 miles). The CBD phase, intended to simulate city driving, is comprised of 14 identical sections each of which consists of an idle, acceleration to 8.94 m/s (20 mph), steady state and deceleration back to idle. The 14 sections together simulate a distance of 3.2 km (2 mile) traveled. The Arterial Phase consists of four modes, each contains idle, acceleration to 17.9 m/s, steady state and deceleration. Finally, the Commuter Phase is a single 6.4 km (4 mile) mode that entails acceleration up to 24.6 m/s (15.3 mph), steady-state and deceleration. Perkins [1982] developed several analytical variations of the local test cycles, to be realistic cycles for testing heavy-duty vehicles. **Figure 2.10** is one of Perkins cycles.

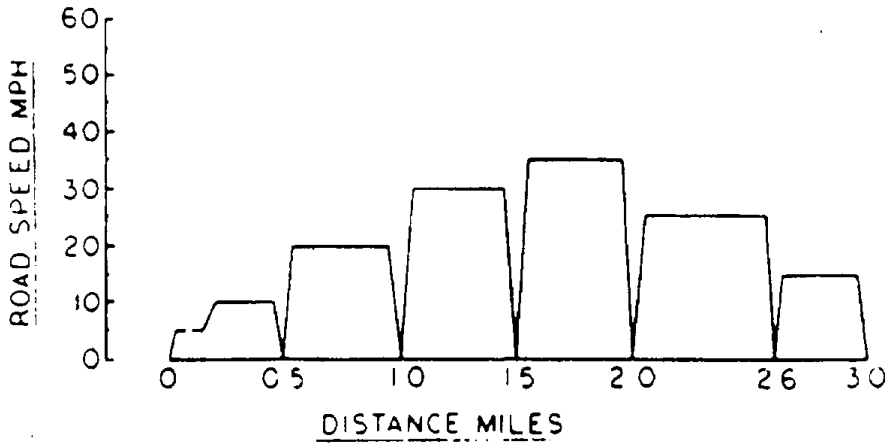

Figure 2.6 Preferred Local Test Cycle [SAE J1376, 1993]

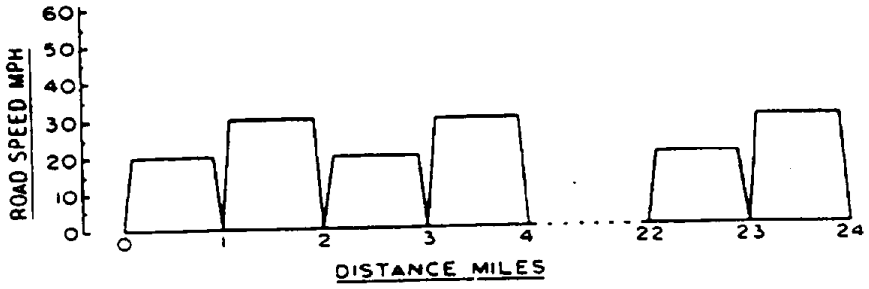

Figure 2.7 Local Test Cycle Without Suitable Test Track [SAE J1376, 1993]

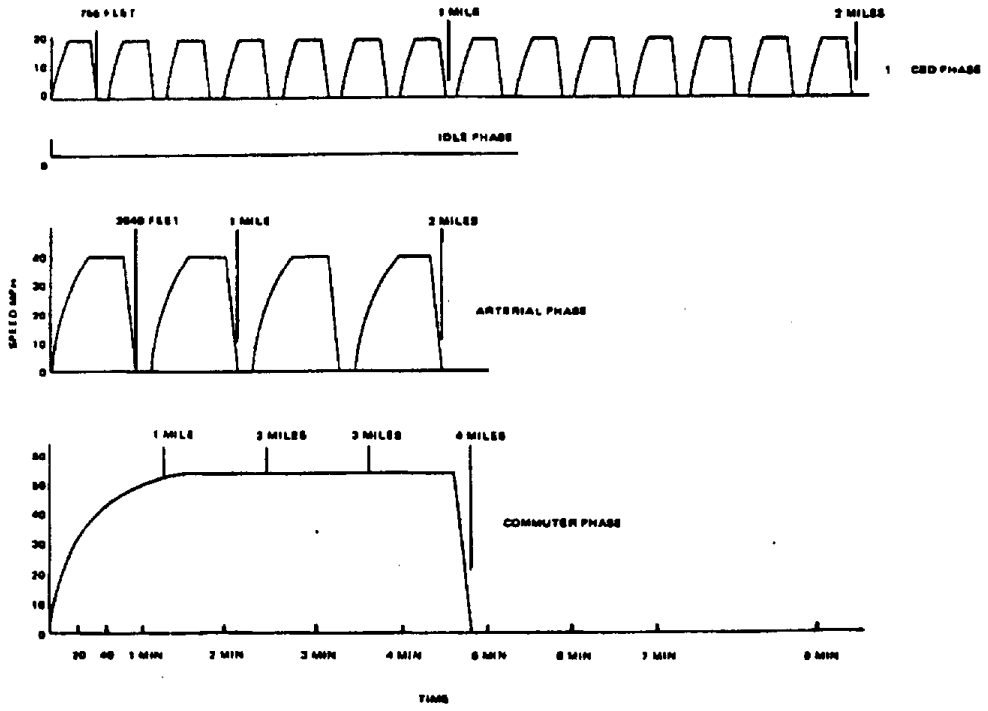

Figure 2.8 Transit Coach Design Operating Profile Duty Operation Cycle [SAE J1376, 1993]

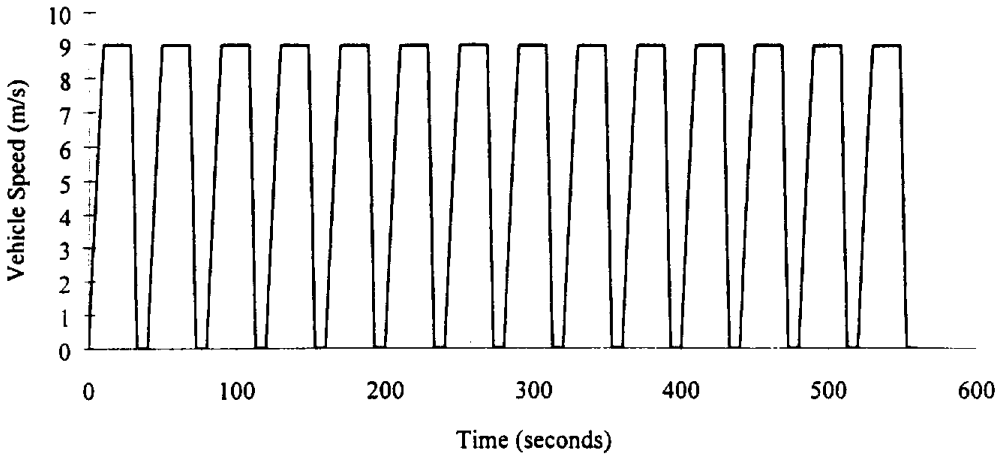

Figure 2.9 Central Business District (CBD)

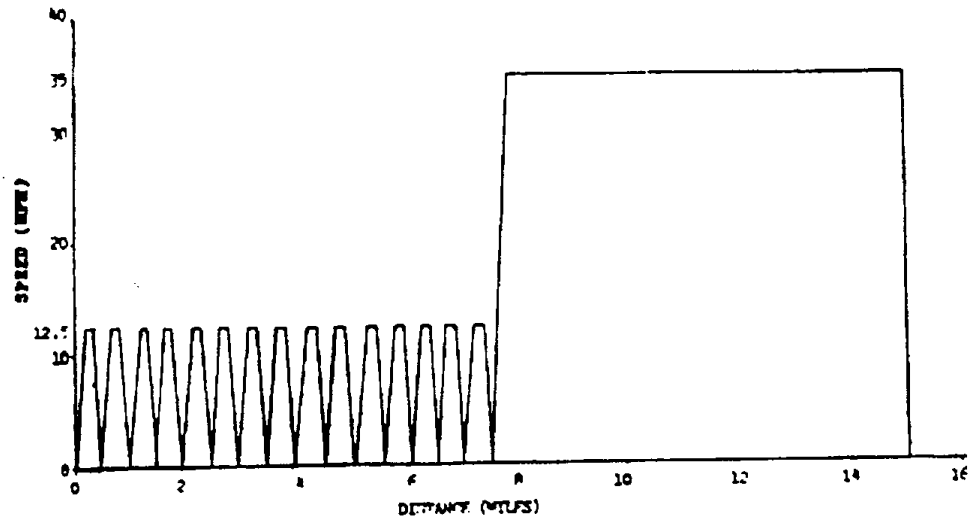

Figure 2.10 Perkins Local Truck Cycle [Perkins, 1982]

The WVU Transportable Heavy-Duty Emissions Testing Laboratory [Lyons et al., 1991 & Clark et al., 1994] has predominately used the CBD section of the transit coach design operating profile duty cycle to compare emissions from heavy-duty buses that use diesel, compressed natural gas (CNG), liquid natural gas (LNG) and alcohol based fuels. The short length of the CBD and its repetitive nature make it a simple cycle to use [Wang et al., 1993].

To test over-the-road tractors, the WVU Transportable Laboratory has employed a truck cycle similar to the CBD Phase of the transit coach cycle. This "Modified CBD" cycle, **Figure 2.11**, is similar to the original CBD, being 3.2 km (2 miles) long and having 14 peaks, but acceleration and braking rates are reduced to be more attainable by heavy-duty vehicles [Wang et al., 1993]. Clark et al. [1994] have also presented a "5 Peak West Virginia University" truck test cycle, **Figure 2.12**, which has been used successfully in testing snowplows and over-the-road tractors. The 5 peak WVU cycle along with the CBD cycle were also used to analyze the measurement delay caused by the exhaust collection system of the WVU Transportable Heavy-Duty Emissions Testing Laboratory [Messer et al., 1995].

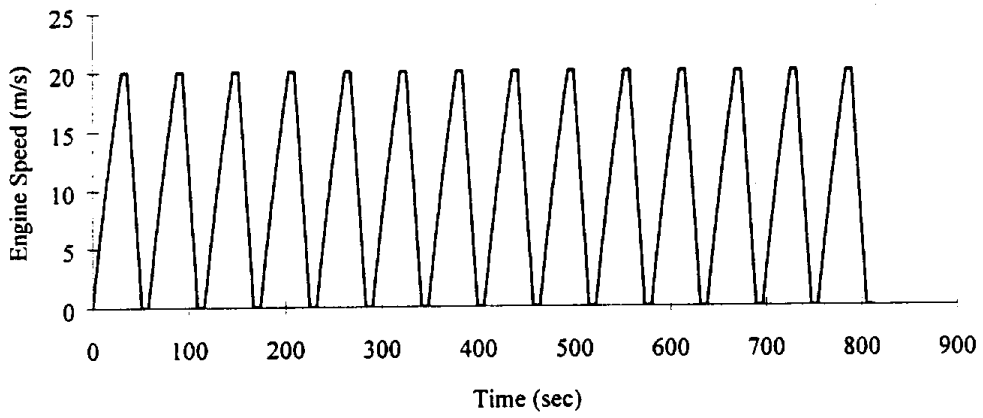

Figure 2.11 Modified CBD Cycle

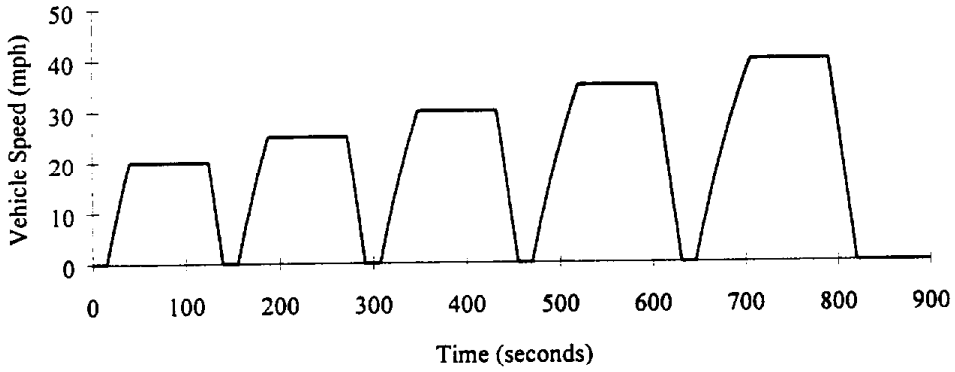

Figure 2.12 WVU 5 Peak Cycle

In an attempt to provide a quality control test for inspection and maintenance (I/M) operations at public transportation garages, Southwest Research Institute developed an I/M Short Emissions

test for buses. This short test was designed to correlate CO, NO_X, and PM emissions data gathered over two 30-second sampling intervals to the EPA transient cycle emissions of the same gases. The data gathered was found to correlate only marginally with the FTP cycle data and was not used in practice [Human et al., 1992].

2.4 Modal Cycles

The Japanese government uses a synthesized Heavy-Duty Diesel Six-Mode cycle to test diesel vehicles that weigh more than 2.5 tons or transport more than ten passengers. This cycle consists of six steady-state modes of varying speeds and loads lasting 3 minutes each. The results obtained during each mode are multiplied by weighting factors to give results that reflect urban driving conditions in Japan. **Table 2.1** gives the speed, load and weighting factor for this Japanese cycle [Degobert, 1995].

Mode Number	% of nominal speed	% loading rate	Weighting factor
1	0	0	35.5
2	40	100	7.1
3	40	25	5.9
4	60	100	10.7
5	60	25	12.2
6	80	75	28.6

Table 2.1 Japanese 6-mode cycle for diesel vehicles

The Economic Commission for Europe (ECE) R49 13 mode engine test cycle is used by the European Economic Community to test diesel engines. The ECE R49 cycle heavily weighs high temperature modes and produces particulate emissions unrepresentative of actual in-use urban driving patterns [Brown et al., 1996]. **Table 2.2** shows the speed, load and weighting factors for the ECE R49 13 mode cycle [Degobert, 1995].

Mode Number	Speed	Loading Rate (%)	Weighting Factors
1	Idle	---	0.25/3
2	Maximum torque	10	0.08
3		25	0.08
4		50	0.08
5		75	0.08
6		100	0.25
7	Idle	---	0.25/3
8	Maximum horsepower	100	0.10
9		75	0.02
10		50	0.02
11		25	0.02
12		10	0.02
13	Idle	---	0.25/3

Table 2.2 European ECE R49 13 Mode Test Cycle

Montgomery et al. [1996] from the University of Wisconsin - Madison, found the FTP transient test procedure to be applicable, but inconvenient for research in the United States. So they developed their own six mode steady state test cycle to simulate the FTP. This six-mode test, like

the Japanese test, consists of six steady state tests, each at different load and speed conditions in which emission rates and power are recorded. The results are multiplied by weighting factors that reflect the amount of time the FTP spends near the respective mode. The University of Wisconsin - Madison used this six mode test to examine the effects of EGR and multiple injections on reducing particulate and NO_X in heavy-duty diesel engines. These "mode" cycles may simulate the FTP in duration and in the amount of time spent in the entire test at these respected speeds, but there is no way of characterizing transients. Therefore, correlation with the FTP using modal test cycles is unlikely.

Degobert [1995] mentioned the 8-mode cycle developed by Cartellieri et al. in 1989, shown in **Table 2.3** used to simulate the FTP transient cycle. Although this 8-mode cycle does not account for transient operation of the vehicle, it proved to have a good correlation with the FTP for particulate and NO_X emissions. However, such good agreement must be predicated on an aggressive transient particulate control strategy on the part of the manufacturer.

% of Maximum Speed	% of Maximum Load	Weighting Factor
34	0	41.7
41	25	7.5
47	63	3.5
55	84	4.0
100	18	10.0
97	40	12.4
97	69	12.2
93	95	8.7

Table 2.3 Possible 8-Mode FTP Simulation

2.5 Units Conversion

Heavy-duty vehicle engines are certified using the FTP described in the Federal Register. The FTP speed versus time trace is shown in **Figure 2.1**. Emissions taken using the FTP and other engine tests are reported in g/bhp-hr whereas chassis emissions test results are reported in g/mile. Although it is possible to convert g/mile to g/bhp-hr employing the net energy delivered by the rear wheels during a chassis test, this chassis g/bhp-hr value cannot be compared to the engine test value because the speeds and torques which the engine experiences during the chassis tests are significantly different than during the engine tests.

Converting g/mile to g/bhp-hr requires a conversion factor (CF) of bhp-hr/mile:

$$\frac{g}{mile} = \frac{g}{bhp-hr} * \frac{bhp-hr}{mile} \qquad \textbf{2.1}$$

A conversion factor with units of bhp-hr/mile reported by the EPA in 1988 was calculated from brake-specific fuel consumption (BSFC), fuel density, and fuel economy (FE). **Equation 2.2** was used.

$$CF\left[\frac{bhp-hr}{mile}\right]=\frac{\rho\left[\frac{lb}{gal}\right]}{BSFC\left[\frac{lb}{bhp-hr}\right]*FE\left[\frac{mile}{gal}\right]} \qquad 2.2$$

This emissions conversion factor (CF) was calculated by gross vehicle weight (GVW) class for both gasoline and diesel powered vehicles, as BSFC and fuel economy (FE) vary with GVW and fuel type [Machiele, 1989]. The parameters of BSFC and FE were obtained questionably through statistical analysis of historical data. Conversion factors were then derived for each GVW class for each manufactured year. Therefore, the many CF's published are specific to GVW and engine manufactured date, they are at best approximations. Due to the specific parameters involved in their derivation and the questionable methods used to obtain them, the conversion factors that have been published are of arguable validity.

2.6 Attempted Chassis Simulations of the FTP

There seems to be no acceptable correlation between presently utilized chassis cycles and the FTP, unless the test is limited to *one engine type* in *one vehicle type*. A prior study by SWRI showed that attempted correlation using two different engines produced significantly different results. For example, SWRI found that the ratio of NO_x (in g/kg of fuel) obtained from the FTP, compared to the ratio of NO_X from the Test D chassis test, varied from 0.86 to 1.4 g/kg for six vehicles tested. The variation in g/km, assigning 10.3 km as equivalent distance traveled to the engine test, was even larger [Dietzmann et al., 1985]. These two tests should provide the most favorable comparison, since the FTP and Test D were derived from the same bank of original vehicle data.

Thompson et al. [1990] of Chevron Research and Technology Co. developed a stationary chassis dynamometer in 1985. This dynamometer was capable of testing heavy-duty vehicles at speeds up to 120 kph (75 mph) and was equipped with DC dynamometer motors that could handle power levels up to 373 kW (500 hp). The Chevron dynamometer could be operated in two ways "Road Simulation" to investigate vehicle performance, or "Engine Stand Emulation" to monitor engine output. In engine stand emulation mode engine speed was controlled by the DC dynamometer motors, and engine torque by a throttle positioner. The engine stand emulation method also required that an in-line torque transducer be installed between the vehicle's transmission and differential to measure driveline torque. Note that this does not measure actual engine torque. There were apparent engine test simulations using the FTP; however, only the difference between tests, not between test and setpoint, has been published by Chevron. The lack of details in this paper and the dearth of reports on further use of the engine stand emulation method do not permit a comprehensive evaluation of their technique, although they are most relevant to the issues discussed in this report.

Recently, Clark et al. [1995] examined the potential for developing a chassis test to mimic the FTP heavy-duty engine cycle for heavy-duty vehicles with manual transmissions. In preparing their analysis, assumptions of no road grade, continuously engaged clutch and no braking were

made. These assumptions, combined with a simple energy balance, yielded an equation to relate vehicle and engine energy outputs. One solution was ineffective due to steep accelerations in the FTP, while the other approach proved to be more successful. A specific test was derived using a simple simulation based on a 261 kW (350 hp), nine speed, 18,180 kg (40,000 lb) Mack truck with allowance for shift times, but it was recognized that this could not be universally applied to other vehicles. Moreover, the engine speeds and torques expected in the FTP engine test are not those customarily used when driving a heavy-duty compression ignition vehicle. However, this was employed as a method for deriving a test cycle to simulate on-road engine certification tests, by Harris et al. [1996], for emissions model development. The driver was unable to reproduce the original engine speeds and torques when operating the vehicle through the chassis test; however, the energy schedule was preserved. In other words, reproduction of the FTP engine conditions using a chassis test controlled only by speed vs. time is nearly impossible. A speed-time trace developed for a specific Mack truck is shown in **Figure 2.13**.

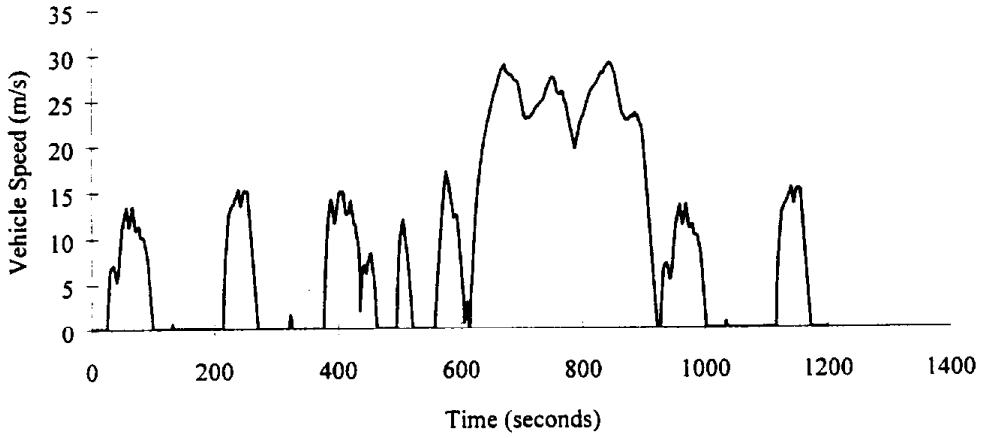

Figure 2.13 Chassis Cycle Developed by Clark and McKain for a specific Mack Truck

2.7 Chassis Test Weight Simulation

The simulated testing weight of the vehicle is another parameter that must be considered when performing chassis dynamometer tests. SAE Standard J1376 recommends both 50% and 100% gross vehicle weight (GVW) for the Local Truck Cycles and the Transit Coach Cycle. Test D prescribes the use of 50% of the gross weight, unless the weight as tested exceeds 50% of gross weight, in which case the as tested weight is used. The WVU Heavy-Duty Transportable Laboratory has tested at both 100% and 70% of the GVW, although in some cases even 70% is greater than the maximum simulation capability of the laboratory, using only flywheels [Lyons et al., 1991]. SWRI has also studied the role of testing weights on emissions with similar results [Dietzmann et al., 1985].

Table 2.4 [Messer et al., 1995] shows emissions results from a bus tested at 13,630 kg (32,000 lb) and 8,630 kg (19,500 lb) simulated weight using the CBD cycle. It is obvious from this data that the test weight has a profound effect on the emissions.

Simulated Bus Weight	13,630 kg	8,630 kg
CO (g/mile)	8.33	4.10
CO_2 (g/mile)	2488.0	2140.0
NO_X (g/mile)	25.25	19.27

Table 2.4 Effect of Simulated GVW on Emissions

2.8 Transmission and Rear End Considerations

One of the problems with vehicle emissions testing is variability introduced by variation in engine/transmission/rear end combinations. The same engine may be installed both in vehicles designed for relatively high speed use such as over-the-road tractors and in vehicles designed for heavy, low-speed hauling. Conversely, class 8 tractor-trailer engines may vary in power rating by a factor of three. The authors therefore believed that no conventional speed-time chassis test schedule will correlate broadly with the FTP, so that a novel approach was required for this program.

2.9 Summary

There is a desperate need for a standardized chassis dynamometer test for heavy-duty vehicles. Virtually all heavy-duty engines are tested and certified using the FTP cycle but a chassis test cycle of equal value does not exist. Several chassis test cycles derived using actual data were reviewed: the EPA Urban Dynamometer Schedule (Test D), the New York Bus Cycle, the New York Truck Cycle, the New York Composite Cycle also referred to as the "Unfiltered Bus Cycle" (all four derived from the same bank of data). Also covered were some synthesized cycles: the Local Test Cycles, the Transit Coach Design Operating Profile Duty Cycle, the Modified CBD Cycle, the WVU 5 Peak Cycle, the I/M Short Emissions Test for buses, the ECE R49, the Japanese 6 mode cycle, the 8-mode FTP simulation and several analytically developed local truck cycles. Consequently, many chassis dynamometer test cycles are currently being used to test vehicles, and although several are preferred, no real standard exists.

The many parameters involved in developing a chassis dynamometer test such as gear changes, lack of braking and motoring, testing weight, transmission and drivetrain losses, drag and friction simulation, etc. add to the complexity involved in developing a standard. It is also necessary in the application under present study that the results of the chassis tests be directly comparable to the FTP engine test results. This is essential in order to determine the effect of the specific vehicle configuration on the emissions, as well as to be able to follow an engine's performance over its life without having to remove it from a vehicle.

To reduce the effect of varying transmission and driveline ratios on emission test results, testing in a single gear was therefore pursued. In single gear chassis testing, a gear ratio was pre-selected, the vehicle was brought to an idle speed on the dynamometer, and the test was commenced with the engine following a torque and speed schedule that within practical limits was the same as the torque and speed schedule that the engine would follow on an engine test stand during the FTP. The single gear approach can be justified by considering the case of a chassis speed versus time cycle being applied two trucks with the same engine but different

numbers of gear speeds or gear ratio spacings. The truck with wider ratio spacings will cause the driver to lug the engine more than the truck with closer ratios. In other words, a different torque-speed envelope will be explored when the transmissions differ. Since electronically controlled engines employ versatile maps of injection timing and injection pulsewidth, it is essential that the speed and torque envelope explored in the chassis test is sufficiently similar to that of the engine test to insure that emmissions levels do not deviate from certification levels for ulterior reasons. The single gear approach avoids this issue.

In the present program, the gear was selected to provide modest torques, while avoiding high speeds on the dynamometer. In theory, any gear might be used, but in this program a gear that favored maximum speeds around 40 mph was chosen.

This approach has been developed for manual transmissions, but could be applied to automatic transmissions if one gear can be engaged and lockup can be effected.

3. Test Plan

The program test plan employed two engines, a Navistar engine and a Cummins Engine. The Navistar engine was installed in a Class 7 truck chassis. The Cummins engine was installed in a Class 8 tractor that could be configured as either a single axle (S/A) or a tandem tractor, thereby providing three engine/vehicle combinations. The Navistar powered vehicle was tested in only one gear. The Cummins powered vehicle was tested in three different gears. Both the Navistar and Cummins engines were subjected to various forms of tampering, which are described in detail in the "Tampering and Malmaintenance" chapter. Testing was performed with engines installed directly on the engine dynamometer, and with the engine installed in the chassis on the chassis dynamometer. In addition, two different pump fuels (No. 2 diesel) were used, but it was seen that fuel effects were not found to be significant.

The test matrix was not full, noting the number of variables discussed above. The test plan was executed with tests in the following order. A total of 41 engine and 71 chassis tests was performed during the course of the research project. Major data gathered during testing included engine speed, engine or chassis torque, emissions values, temperatures and flowrates.

Engine Type	Engine Configuration	# of tests
Navistar	Stock	7
Navistar	15K	4
Navistar	39K	4
Navistar	82K	4
Navistar	Disabled MAP	3
Navistar	Alternate Stock	4
Navistar	Failed Injector	4
Cummins	Stock	4
Cummins	Disabled MAP	3
Cummins	2V	4

Table 3.1 – Summary of Engine Testing Performed

Engine Type	Chassis Type	Axle configuration	Gear	Engine Configuraiton	# of tests
Navistar	Navistar 4700LPX	Single	3	Stock	6
Navistar	Navistar 4700LPX	Single	3	15K	4
Navistar	Navistar 4700LPX	Single	3	39K	4
Navistar	Navistar 4700LPX	Single	3	82K	4
Navistar	Navistar 4700LPX	Single	3	Disabled MAP	4
Navistar	Navistar 4700LPX	Single	3	Alternate Stock	8
Cummins	International COE	Tandem	8	Stock	15
Cummins	International COE	Tandem	7	Stock	9
Cummins	International COE	Tandem	9	Stock	4
Cummins	International COE	Tandem	8	Disabled MAP	4
Cummins	International COE	Tandem	8	2V MAP	4
Cummins	International COE	Single	8	Stock	4
Cummins	International COE	Single	7	Stock	4
Cummins	International COE	Single	9	Stock	4
Cummins	International COE	Single	7	Disabled MAP	4

Table 3.2 – Summary of Chassis Testing Performed
(note: COE refers to Cab-Over-Engine configuration)

4. Description of Laboratories

Chassis testing performed during this research was conducted at the West Virginia University Transportable Heavy Duty Emissions Laboratory. The transportable laboratory is designed to operate heavy-duty vehicles (transit buses, over-the-road tractors, and straight trucks) through prescribed torque and speed versus time cycles and driving routes to measure emissions. For engine testing, the flywheel of the engine was connected to a General Electric DC dynamometer (Figure 4.1) and operated over the desired test cycle while the engine exhaust was monitored using the comprehensive exhaust analysis facility in the WVU Stationary Engine Testing Laboratory.

4.1 Stationary Engine Testing Laboratory

Engine testing was conducted at the WVU Stationary Engine Testing Laboratory. The laboratory is equipped with a General Electric DC dynamometer capable of testing heavy duty engines up to 550 horsepower and 3000 rpm. The engine flywheel is connected to the dynamometer using a driveshaft with a protective shield and emergency failure cutout. The engine and dynamometer are mounted on a heavy duty skid. Exhaust from the engine is routed to an 18 inch dilution tunnel where the exhaust is mixed with conditioned air from the test cell. Valves are incorporated into the intake and exhaust of the engine so, prior to testing, intake and exhaust restrictions can be set as per manufacturers specifications. Engine cooling is accomplished by circulating the engine coolant through a surge tank with an overflow. When coolant temperature (measured in the surge tank) rises above a set temperature, fresh water is injected to the system to lower the temperature.

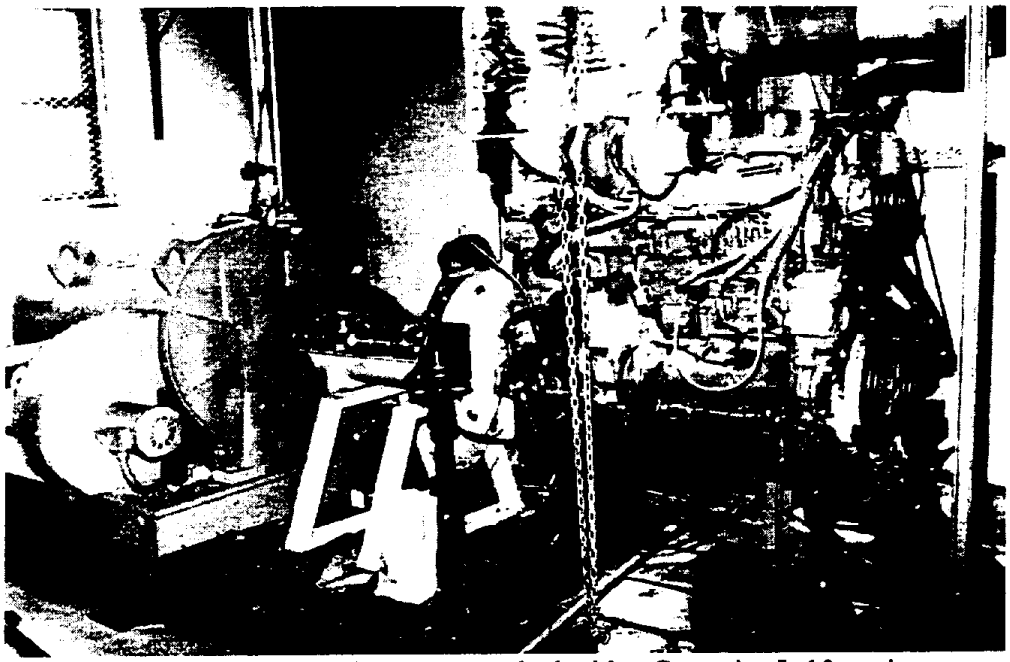

Figure 4.1 – Engine testing dynamometer bed with a Cummins L-10 engine mounted

The dilution tunnel is an 18 inch diameter stainless steel duct open at one end to receive exhaust and ambient or conditioned air and connected to a blower/venturi system on the other end to control flowrate. The venturi system incorporates three separate venturis each of which can be opened or blocked depending on the amount of dilution desired. An orifice near the entrance to the tunnel assists in mixing of exhaust and dilution air. Located ten diameters from the intake of the tunnel is the sample plane where heated probes withdraw the dilute exhaust for analysis.

Table 4.1 shows the analyzers used by the engine laboratory for analysis of hydrocarbons (HC), carbon dioxide (CO_2), carbon monoxide (CO), and oxides of nitrogen (NO_X). A substantial supply of calibration gases covering a wide range of concentrations was available for precise calibration of each analyzer. The analyzers in the laboratory receive regular in-house service and maintenance.

Hydrocarbons	Flame ionization detector	Rosemount Analytical Model 402
Carbon Monoxide	Non-dispersive infrared	Rosemount Analytical Model 880A
Carbon Dioxide	Non-dispersive infrared	Rosemount Analytical Model 880A
Oxides of Nitrogen	Chemiluminescent	Rosemount Analytical Model 955

Table 4.1 – Analyzers used for exhaust analysis during engine testing

Particulate matter was collected during the engine tests using 70mm particulate filters. Prior to testing the filters were conditioned at least 4 hours in an environmental chamber where temperature and humidity were precisely controlled. For each test, two filters (a primary and secondary) were weighed using a microbalance and placed in a stainless steel filter holder arranged in a series configuration. Flow through the filter assembly was monitored and adjusted throughout the test by a mass flow controller which was able to maintain a steady mass flowrate independent of sample stream temperature. As a check, a second integral flowmeter was used in conjunction to verify the first. After each test the filters were removed and placed back into the environmental chamber for at least 4 hours before being weighed again using the microbalance. The difference in weight was recorded for both the primary and secondary filters and then combined to obtain total sample particulate mass. Using the total volume of the sample and the total flow through the dilution tunnel (with additional correction factors associated with humidity) a total mass of particulate from the engine for the test was obtained.

Control of the engine, dynamometer, and emissions sampling system was accomplished using an in-house designed computer control and data acquisition system. A computer with an Intel 486 microprocessor and equipped with 4 Analog Devices RTI-815F data acquisition boards was able to monitor 96 individual data channels and control individual system components at the rate of 10 Hertz as well as perform the necessary computations during the test. This computer also was responsible for saving the desired information gathered during the test. All data recorded are available in electronic form.

4.2 – Chassis Testing Laboratory

The chassis dynamometer consists of inertial flywheels, eddy current power absorbers, and wheel

rollers mounted on a flat bed trailer. This unit is designed so that it can be lowered to the ground in order that vehicles can be driven on for testing and raised so that it can be attached to a tractor for transportation. WVU has two similar transportable laboratories: "Laboratory #1" was used for this ARB funded research and the laboratory was used at its home bas in Morgantown, WV. Detailed descriptions of the design, construction and use of these laboratories may be found in Bata et al. (1991), Clark et al. (1995), and Clark et al. (1997). A brief description is given below.

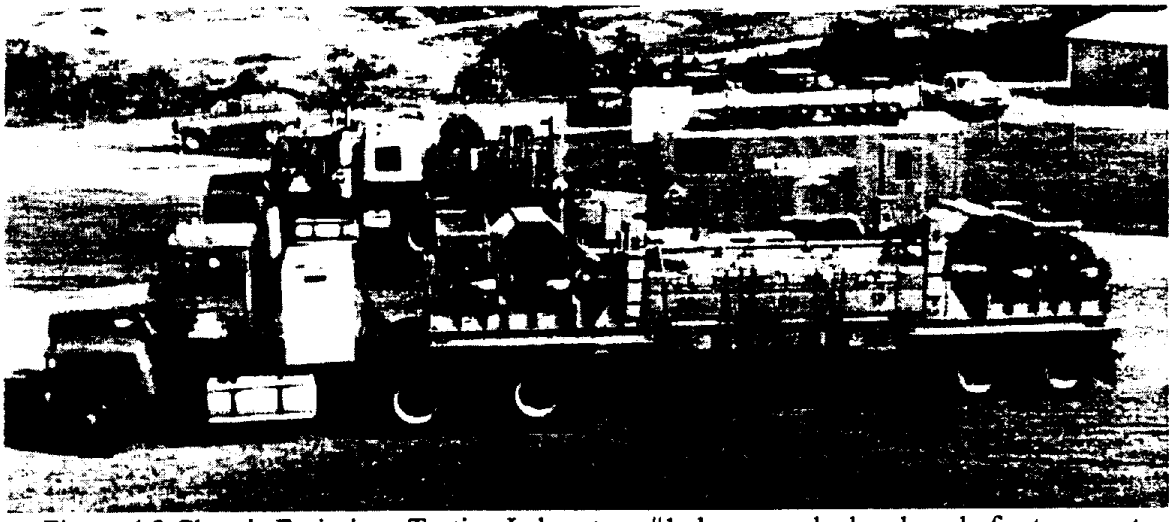

Figure 4.2 Chassis Emissions Testing Laboratory #1 shown packed and ready for transport.

The vehicle to be tested was driven onto the flat bed and positioned so that the drive axle of the vehicle were over the center section of the test bed and perpendicular to the length of the test bed. The wheels of the vehicle were positioned on rollers which were coupled such that the wheels on each side turned at the same speed. The outer wheels of the dual wheel set on each side of the vehicle were removed and special hub adapters were mounted to the drive axle connecting it to the drive shaft of the dynamometer units located to each side of the vehicle. In the case of testing of the tandem tractor, the power divider was locked and power was removed from the forward rear axle. Each dynamometer unit consisted of a power absorber and flywheel set. The flywheel set consisted of a group of individual flywheels which could be engaged or disengaged to simulate the inertial load of the vehicle. It was found that engagement of any flywheels during preliminary testing prevented the vehicle from following the extreme acceleration demanded by the FTP and therefore it was decided not to engage flywheels during this testing. Actual vehicle speed and torque were measured using speed transducers in the power absorber drive trains and load cells attached to the power absorbers.

The major difference between the transportable chassis dynamometer and stationary engine dynamometer which concerned this project involved the use of power absorbers by the chassis laboratory which, unlike the DC dynamometer used by the engine laboratory, are not capable of motoring the engine.

5. Test Engines and Vehicles

A Navistar International 4700LPX chassis was obtained on loan from Navistar to use in the first set of vehicle tests. This vehicle, as delivered, was equipped with a Navistar T 444E engine (serial no. 7.4HM2U003488). West Virginia University arranged transport for this vehicle from Illinois to West Virginia. The engine present in the vehicle as delivered was removed. After completion of the engine FTP testing, a Navistar T 444E engine already available at WVU was installed for the chassis testing. The chassis had a GVWR of 25,500 lbs and was equipped with an Eaton Midrange 6 speed transmission and a Spicer 4.11:1 ratio rear end.

The engine/chassis combination for the second series of transient testing was obtained from Ryder Truck Rental in Pittsburgh, PA. Specific requirements of the rental such as vehicle mileage, vehicle and engine year, and vehicle type were set up through Jim Salis at the Ryder Maintenance Facility in Miami, Florida. This vehicle was an International cab-over-engine tractor equipped with a Cummins N-14 370hp diesel engine (serial no. 11775178; Cummins Parts List (CPL) no. 1807), an Eaton-Fuller 10 speed transmission and a 3.9:1 ratio rear end.

For engine testing on the Cummins N-14, the engine was first removed from the vehicle by Cummins of Cumberland in Fairmont, WV, mounted to the DC dynamometer and instrumented at the Stationary Engine Testing Laboratory. After completing the engine testing phase, the engine was returned to Cummins of Cumberland where it was installed back into the vehicle for chassis testing. Although WVU had the capability to perform the engine change it was felt that having the work performed by an authorized shop would both satisfy the truck rental agency and ensure that the engine was installed according to manufacturer's specifications. Cost of professional engine removal and reinstallation was approximately $2,000, which emphasizes the costs associated with a program to assess in-use diesel emissions using engine dynamometer testing excluding the costs associated with vehicle downtime.

Engine	Navistar T 444E	Cummins N-14
Model Year	1994	1995
Cylinders	V-8	Inline-6
Displacement	7.4 liters	14 liters
Rated Power	195hp @ 2600 rpm	370hp @ 1800 rpm
Rated Torque	440 ft-lbf @ 1500 rpm	1300 ft-lbf @ 1300 rpm
Chassis	Navistar 4700LPX	International COE (Cab over engine) Sleeper
Transmission	Eaton Midrange (6 speed) 3rd gear (3.250) used	Eaton Fuller (10 speed) 7th gear (1.89) used 8th gear (1.38) used 9th gear (1.00) used
Rear End Ratio	4.11:1	3.90:1

Table 5.1 Vehicles Tested

6. Test Procedures

The FTP transient test is currently used to test new engines for compliance with current emissions standards. To meet the requirements of CFR Title 40, a cold start FTP, that is, a complete transient test initiated when the engine has been shut down for 12 hours with ambient air temperature between 20 and 30 degrees centigrade, must be performed at the beginning of a sequence of transient tests. While certification testing results are obtained using an average of cold and hot engine starts (1/6 cold test emissions + 5/6 hot test emissions), all chassis testing reported was performed with the engine warmed up since transmission losses in the dynamometer test bed, which affect torque at the wheels, were determined with the system at operating temperature. This criterion could not be met without operating the vehicle prior to the test. A minimum of three, and if possible four, complete test runs was performed in each engine/chassis configuration. Portions of the FTP call for negative torques and the chassis testing laboratory does not have the ability to apply torque to drive the vehicle with the exception of inertial flywheels which were not engaged for this testing and dynamometer bed component inertia which only came into play during decelerations. This resulted in the engine speed not matching the prescribed schedule speed during periods of the transient test which demanded high speed with negative torque. The dynamometer flywheels could be engaged reduce the rate at which engine speed decreased during these periods. Conversely, engagement of the flywheels prevented the vehicle from accelerating at the scheduled rate with the prescribed torque and had minimal effect of negative torque test portions on emissions (due to minimum fueling, "closed rack" operation). This led the researchers to conclude that engagement of the inertial flywheels was not beneficial. As additional support to this approach, negative torque is not taken into account when calculating the cumulative engine power and integrated emissions results according to prescribed Federal testing guidelines.

6.1 Engine Mapping

The first step in performing the transient Federal Test Procedure (FTP) was to determine maximum torque over the entire speed range of the engine: this is commonly known as mapping the engine torque. This process involved restricting the engine speed to a transient speed ramp (8rpm/second) while holding the engine to maximum power demand at that speed. The resulting torque versus speed map was then used to generate the transient test using prescribed data from the CFR.

6.2 Chassis Mapping

Since speed control with the DC dynamometer was straightforward, engine mapping was accomplished without significant difficulty. On the other hand, mapping the engine in the chassis necessitated a different approach. Since driveline efficiency (which was expected to vary with both speed and load) was not well known, chassis mapping and testing was performed in reference to torque at the driven wheels. Anecdotally, the transmission efficiency from engine to road is known to be between 80 and 90% but is poorly researched. Since the reduction ratio of the transmission was known, axle speed and torque were used to reveal engine speed and torque excluding losses in the drivetrain. Chassis test results were reported using axle horsepower (ahp)

and axle torque to differentiate from results of engine testing. The axle torque was measured using in-line torque cells between the wheel hubs and the dynamometer/flywheel drivetrains on either side of the vehicle. These torque cells were manufactured by Eaton-Lebow and were subject to regular shunt calibration. Since the overall gear ratio between the vehicle hubs and the engine was known axle torque could then be converted to an equivalent engine torque for comparison with engine dynamometer testing results.

To accomplish chassis engine mapping, the power absorbers were directed, using a computer control system, to control the rate of increase the engine speed at the same rate used for the engine mapping on the DC dynamometer. The resulting torque/speed data was used to generate an FTP schedule. Once the engine/chassis mapping procedure was complete, the data was used to develop an FTP test schedule using percent torque and speed data from the CFR. Figure 6.1 shows both engine and chassis maps of the Navistar engine for both stock and disabled MAP sensor conditions.

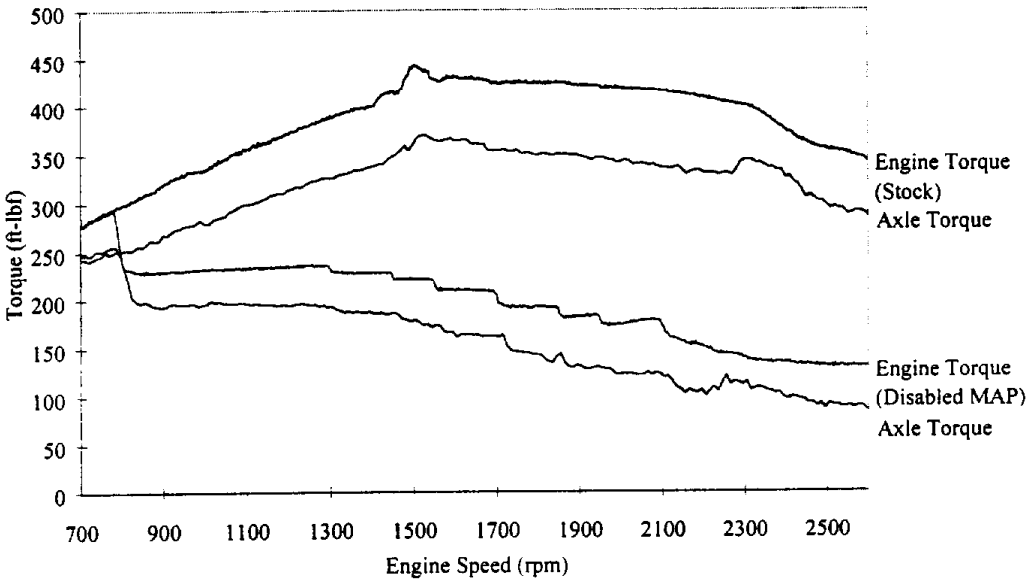

Figure 6.1 – Engine and chassis maps of the Navistar engine. The upper curve of each pair is the engine map while the lower is from the chassis map.

Initial scoping tests were performed using a "human" driver for both the mapping and driving portions of the research. However, it was found that variability in CO introduced by the driver was significant. This necessitated the development of a "computer" driver. An electronic device was constructed which enabled "pedal position" to be controlled from a proportional voltage signal from the laboratory's data acquisition computer. In the case of engine/chassis mapping, the pedal was set a 100% (corresponding to full power) while during transient tests the pedal position was varied using a software proportional-integral controller. In addition to reducing the variability in transient testing, this system allowed for precise pedal position, and thus power

control, for drivetrain efficiency testing since engine power could be precisely held independent of whether in or out of the chassis.

6.3 Chassis Testing

Chassis testing was accomplished on both vehicles using the WVU Transportable Heavy Duty Emissions Testing Laboratory. The first step in the testing procedure involved removing the outer wheels from the drive axle (front axle in the case of the tandem tractor) and installing hub adapters. After installing the adapters, the vehicle was driven onto the test bed and the hub adapters were connected to the dynamometer drivetrain. The rear axle(s) of the vehicle was lifted using bottle jacks placed on calibrated scales. This was done to obtain the actual weight on the rear axle(s) prior to testing. In the case of both vehicles, additional force was applied using an I-beam and tie-downs across the fifth wheel/frame. A calibrated scale was placed between the I-beam and the vehicle to monitor down force on the rear of the vehicle. The vehicle was secured to the test bed using heavy duty chain tie-downs to prevent the vehicle from moving either axially, laterally and vertically. Exhaust from the vehicle was routed to the dilution tunnel atop the laboratory emissions analysis trailer. To complete mounting and readying the vehicle, the electronic throttle control system was connected to the vehicle and tested.

Prior to testing the vehicle for emissions, an extensive calibration procedure was carried out. Using the calibration gas appropriate for the vehicle tested, each analyzer (CO, CO_2, HC, and NO_X) was calibrated using zero air (0ppm concentration), 100% calibration gas, and, using a gas divider, at 10% intervals from 0 to 100%. A multiple linear regression was performed to obtain calibration coefficients using the 11 calibration points from each analyzer. The microbalance used to weigh the particulate filters was calibrated using supplied calibration weights. Speed measurement devices on the dynamometer rollers and the power absorbers were calibrated by applying a square wave input to the instrument circuitry to ensure that the devices were working properly. As a part of the regular maintenance, all thermocouples used by the laboratory are periodically checked to ensure proper operation of both the thermocouples and their associated wiring. To ensure that the dilution system was operating at the correct flowrates, a complete calibration of the system was periodically performed using a subsonic venturi from the US EPA.

A set of standard weights was used to calibrate the side-arm load cells on the power absorbers. For normal operation of the laboratory these weights were hung from a point on the stator of each power absorber. In the case of this project, higher range load cells were used and a special set of extension arms were constructed to allow the same weights for that range of calibration. Two procedures were used to check the operation of the in-line hub torque cells since they could not be calibrated in-house. The first of these checks was a shunt calibration where the strain gauges in the torque cell were checked against standard resistors. This process was performed to determine that no plastic deformation (which would severely affect the operation of the torque cell) had occurred. As a second check, power absorber torque from the side-arm load cells was compared to the torque at the in-line torque cells.

6.4 Nomenclature

A standardized system for identifying chassis and engine tests was employed to eliminate confusion in examining test results. Figure 6.1 presents a breakdown of the system which explains the meaning of each numeral/digit in the test code.

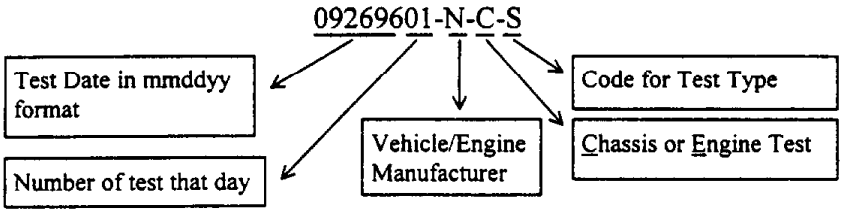

Figure 6.2 - Test numbering system outline

As an example, test number 09269601-N-C-S would identify the first Navistar chassis test taken on September 26, 1996 using a stock configuration. Test codes, shown in Table 6.1, were assigned to each different type of test.

S	Stock
AS	Alternate Stock
DM	Disabled MAP sensor
WU15	Temperature sensor replaced with 15KΩ resistor
WU39	Temperature sensor replaced with 39KΩ resistor
WU82	Temperature sensor replaced with 82KΩ resistor
2V	MAP Sensor set at 2V

Table 6.1 – Test codes used for Navistar and Cummins transient chassis and engine testing

Additional test codes for the Cummins chassis testing were used to denote what fuel was used for the test (N-new pump diesel, T-original test fuel) and if the rear axle was disconnected (RD). For example, test number 06269703-N14-C-RDT8 was a Cummins chassis test performed on June 26, 1997 with the rear axle disconnected and the transmission in 8th gear using the original test fuel.

7. Quality Control

7.1 Propane Injections

In order to ascertain the performance of the dilution tunnel, venturis, and associated blowers for each laboratory, a propane injection procedure was performed. This procedure was useful in determining whether any leaks were present in the lines between the dilution tunnel sample zone and the intake to the blower venturis. This also revealed if the venturi system is operating as designed. Using a calibrated orifice, propane gas was fed into the entrance to the dilution tunnel. While the injection was in progress, a continuous sample was drawn and analyzed using the hydrocarbon analyzer and a continuous background sample was retained in a Tedlar sample bag. The test was run for a total of 5 minutes. At the conclusion of the test, the background bag was analyzed and the amount of hydrocarbons present was subtracted from the continuous result to get a total volume of the propane recovered from the tunnel. This amount was then compared to the amount injected to determine a percent over/under recovery. In agreement with the Code of Federal Regulations, propane injections were considered satisfactory if the absolute percent error in volume recovered against volume injected was less than 2% and the error between three subsequent injections was within 1%. Both the chassis and engine laboratories successfully performed propane injections prior to the correlation tests.

7.2 Laboratory Correlation Testing

Correlation tests between the chassis emissions laboratory and the engine emissions testing laboratory were performed using the Navistar T-444E engine installed on the GE engine dynamometer to generate emissions. To perform the tests, the gas analysis trailer from the chassis emissions laboratory was stationed in the building housing the engine emissions laboratory and engine test dynamometer such that the exhaust from the engine could be routed to the dilution tunnels of both laboratories. Initial testing revealed that while good agreement between the laboratories was realized on carbon monoxide (CO), carbon dioxide (CO_2), oxides of nitrogen (NO_X), and particulate matter (PM), there was a significant difference in hydrocarbons (HC). Discrepancies in propane injections, which are used to check the flowrate through the dilution tunnels, were investigated prior to recommencing emissions tests. Due to dynamometer scheduling time constraints, the final correlation tests were performed using a Cummins L-10 diesel engine installed on the engine dynamometer.

7.3 Results of Correlation Testing

Results of the correlation tests from the engine laboratory are contained in Table 7-1 and for the chassis laboratory in Table 7-2 with comparison data in Table 7-3.

	HC (g/bhp-hr)	CO (g/bhp-hr)	CO_2 (g/bhp-hr)	NO_X (g/bhp-hr)	PM (g/bhp-hr)
Warmup	0.345	1.235	585	4.730	0.133
Hot FTP #1	0.316	1.463	574	4.654	0.103
Hot FTP #2	0.310	1.303	574	4.693	0.113
Hot FTP #3	0.314	1.215	572	4.636	0.098
Hot FTP #4	0.288	1.386	574	4.668	0.086
Average	0.315	1.320	576	4.676	0.107
CV%	6.47%	7.88%	0.88%	0.78%	16.58%

Table 7.1 - Emissions test results from the Engine Emissions Testing Laboratory. (warmup test data was not included in the statistical analysis)

	HC (g/ahp-hr)	CO (g/ahp-hr)	CO_2 (g/hp-hr)	NO_X (g/ahp-hr)	PM (g/ahp-hr)
Warmup	0.22	1.16	585	4.91	0.123
Hot FTP #1	0.26	1.18	565	4.78	0.099
Hot FTP #2	0.24	1.24	570	5.20	0.095
Hot FTP #3	0.25	1.28	580	4.95	0.094
Hot FTP #4	0.26	1.24	565	4.98	0.092
Average	0.25	1.22	573	4.96	0.101
CV%	6.77%	4.02%	1.57%	3.08%	12.40%

Table 7.2 - Emissions test results from the Chassis Emissions Testing Laboratory.

	HC (g/bhp-hr)	CO (g/bhp-hr)	CO_2 (g/bhp-hr)	NO_X (g/bhp-hr)	PM (g/bhp-hr)
Engine Average	0.315	1.320	576	4.676	0.107
Chassis Average	0.246	1.220	573	4.963	0.101
Percent Difference	24.46%	7.90%	0.50%	-5.96%	5.80%

Table 7.3 - Comparison of correlation test emissions results.

The values of CV% are acceptable. WVU is in posession of a bank of data to generate values of CV% for its own laboratories and other laboratories capable of producing the transient test, and the WVU values during this testing proved to be expected and acceptable.

Between laboratory differences for NO_X, CO, and CO_2 were of the same order of magnitude as the CV% values for each laboratory, which implies that there was no significant bias between laboratories. Total hydrocarbon (HC) differences between laboratories was 24.46 percent.

HC was deemed less important than NO_X in this program. In addition, the HC values measured in this correlation were about one fourth of the current Federal engine emissions certification standards. However, the difference merits discussion. It was attributed in this testing to the difference in exhaust lengths and tunnels used between the laboratories. The exhaust length ran from the engine to each laboratory's tunnel. In addition, the two tunnels had different dilution air temperatures ($78^{O}F$ average for the Engine Laboratory and $89^{O}F$ average for the Chassis Laboratory) since only the engine tunnel has full tunnel intake air conditioning.

McKain et al. (1996) have shown that heavy hydrocarbons associated with diesel fuel are readily adsorbed onto the tunnel walls and indeed the balance between heavy hydrocarbons and particulate matter detection is inchoate. In particular, they showed that heavy paraffins (C14 and C16) associated with diesel fuel were hung up on the tunnel walls and could continue to be eluted for some time after completion of the test. In this way tunnel conditions may well affect HC results. Confidence in HC measurement ability of each laboratory is confirmed by successful propane injection. However, propane is far more volatile than the hydrocarbons associated with diesel fuel and lubricating oil. The investigators believed that at this stage the between laboratory agreement had been verified so that testing could proceed.

7.4 Gas Bag Analysis

In addition to correlation using exhaust from the Navistar T 444E and Cummins L-10 diesel engines, results of the analysis of prepared bag samples from each laboratory were compared to check the performance of their analyzers. After both laboratories had performed routine calibrations on all of their respective analyzers, a standard Tedlar sample bag was partially filled with propane, carbon monoxide (CO), carbon dioxide (CO_2), and oxides of nitrogen (NO_X) calibration gas. The bag was analyzed by both the engine and chassis laboratories using their bag sample analysis procedures. Results of this testing were recorded and the bag was analyzed repeatedly by both laboratories separately until each laboratory had analyzed the bag a total of four times. The results of this testing are shown in Table 7-4.

	HC (ppm)	CO (ppm)	CO_2 (ppm)	NO_X (ppm)
Engine Laboratory Average	79.1	313	11760	83.0
Engine Laboratory CV%	0.53%	0.97%	0.83%	1.51%
Chassis Laboratory Average	80.0	306	11650	84.2
Chassis Laboratory CV%	0.15%	1.50%	2.53%	1.18%
Percent Difference	-1.13%	2.30%	0.94%	-1.44%

Table 7.4 - Results of Gas Bag Analysis, CV% values denote one standard deviation based on data from four tests.

Close agreement between analysis of the bags confirms that tunnel and exhaust effects were responsible for variations in hydrocarbon measurements between laboratories.

8. Tampering/Malmaintenance Testing

Of interest to this project was the effect of tampering and malfunction/malmaintenance on engine emissions performance. Specifically, these tests were designed to determine by what magnitude emissions would change as a result of tampering and malmaintenance. A major motive was to cause the engine to change emissions rates under engine test conditions and to see whether there elevated levels were reflected in the chassis test data. In this way correlation between engine and chassis laboratories was possible for a wide range of PM an NO_X levels. Various tampering and malmaintainence methods/configurations were selected after considering opinions of experienced diesel engine mechanics and truck drivers as well as technical knowledge the researchers had relating to the operation of diesel engines. What made the tampering portion of the project more difficult than originally thought was the advances in electronic engine control over the last decade. Older engine technology was readily understood and certain operators might elect to override crude puff limiting devices and "turn-up" mechanical fuel injection systems. Upon completion of the project it was found that although newer electronic devices may inhibit tampering, they are still vulnerable when approached by persons with the correct skill and knowledge of their operation.

8.1 Navistar

The Navistar engine was operated in the following modes: Stock, Alternate Stock (AS), three temperature sensor tampering modes (15K, 39K, and 82K), Disabled MAP sensor (DM) as well as with a failed injector. As one of the tampering modes, the Navistar T444E engine's behavior was altered by replacement of temperature sensors with resistors to prevent the engine control system from modifying injection parameters as the engine temperature increased. An initial test was performed by disconnecting the coolant temperature sensor and replacing it with a 39 kΩ resistor to send a false signal of approximately 64°F to the engine control system. When this test resulted in no discernible change in engine performance, both the oil and intake air temperature sensors were also replaced by 39 kΩ resistors in addition to the coolant sensor.

It was later found that the oil temperature sensor input was the controlling parameter. Since the injection system was driven using oil actuation, the higher viscosity of lower temperature oil at cold startup necessitated the control system to energize the injector solenoids for a longer time period than when at normal operating temperature.

With the resistors in place, this injection scheme resulted in a greater amount of fuel than normal being delivered under normal temperature operation and thus, an increase in engine power. Such tampering would also interfere with injection timing. As a result, the engine emissions of NO_X and CO were greater. Navistar testing was performed with the engine actually at operating temperature, but with the control system believing that the oil was at 4, 19 and 43°C (resistors of 82, 39 and 15 kΩ were substituted for the oil, coolant, and intake air sensors). Figure 8-1 shows the temperature resistance curve for the Navistar temperature sensors. This data was acquired by measuring the resistance of a Navistar temperature sensor at various temperatures. The exact resistors were employed in both engine and chassis testing. These three tampering modes have been designated "82K", "39K", and "15K".

These tampering modes produced changes in engine power output and in this way altered the engine maps that resulted. Figure 8.1 shows maps form each of the Navistar tampering scenarios. The fact that tampering or failures can alter engine power suggests that in performing screening tests the actual power and torque of the engine will need to be recognized in generating the test schedule. Use of manufacturer rating will not prove satisfactory for this purpose.

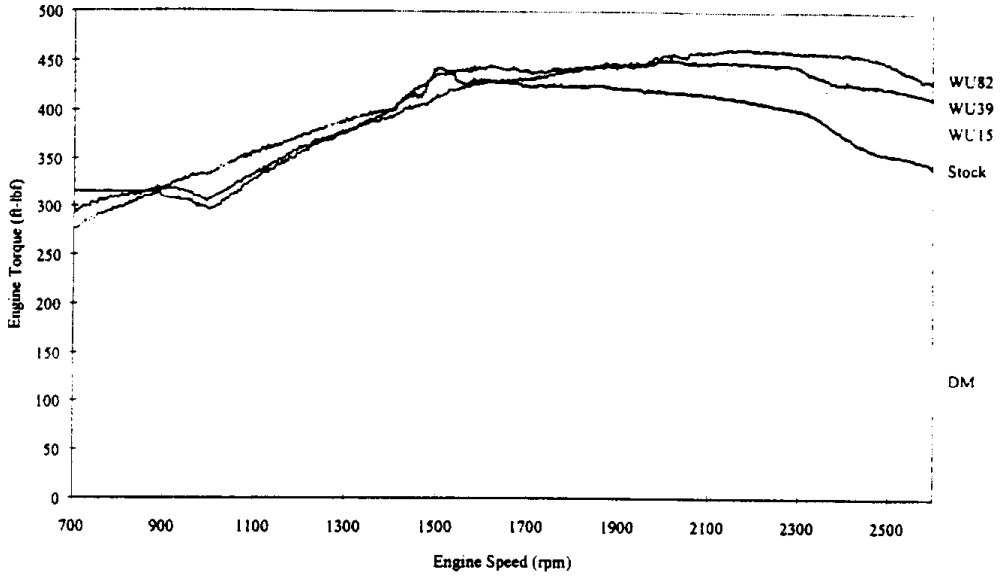

Figure 8.1 – Engine torque maps from the Navistar T 444E in stock and tampered modes

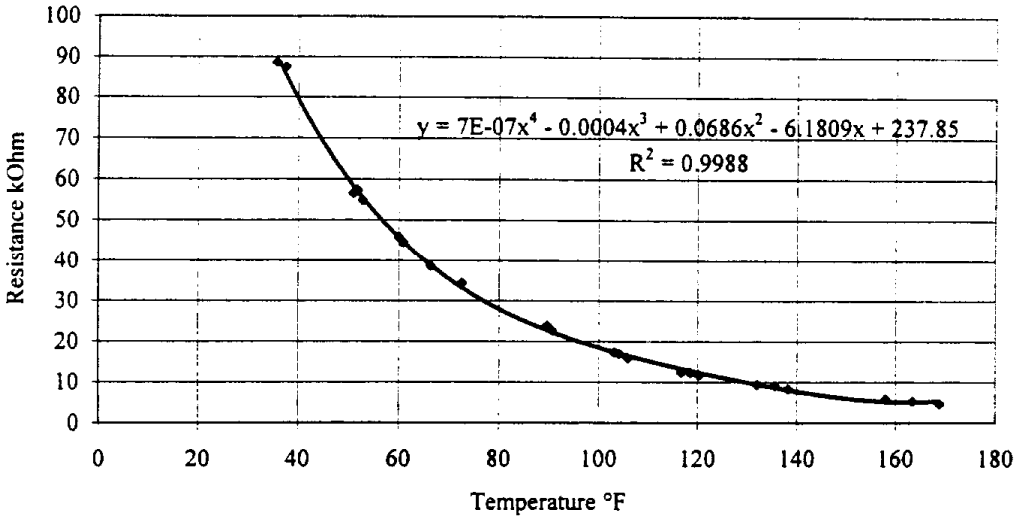

Figure 8.2 - Temperature - resistance plot for engine temperature sensors

In addition, the Navistar engine was also operated with the manifold air pressure sensor disconnected (designated DM), which reduced power output considerably. While this did accomplish the goals of the tampering/malmaintenance phase of the study, it was readily apparent that the vehicle would not be driveable in this mode and such would most likely not be encountered in any real-world situation. Hence, less attention was paid to this mode than for the modified temperature sensor modes.

The Navistar T 444 engine is configured by its electronic control and personality modules and is available in the marketplace in various torque and speed ratings. Since the both the engine in possession of the University (with the "stock" controller) and the vehicle used for the testing had different electronic control modules (ECMs), runs were conducted in an "alternate stock" where the test engine was connected to the ECM supplied with the vehicle rather than its own. This mode, designated "AS", was investigated since modification or replacement of the original ECM could result in significant changes in engine performance when compared to original engine performance as indicated by the vehicle identification number (VIN). The ECM Is usually associated with the vehicle and acts independently of the engine. For example, if a vehicle is supplied with a 210 horsepower engine and an engine of the same family originally rated at 175 horsepower is installed, that engine will now produce 210 horsepower.

The engine was also operated with a failed injector. In these tests, the connection to the #8 fuel injector was disconnected and the engine was run through the normal mapping and FTP test procedures. Although the engine was expected to produce considerably less than the 88% of the integrated power due to the failure of one cylinder and parasitic losses from that cylinder, the engine was able to produce almost 92% of integrated power. While further investigation of the engine control strategy regarding a failed injector was felt to be beyond the scope of this study it is the opinion of the researchers that the ECM, detecting a failed injector, can modify injection timing to make up for power lost. This mode of operation resulted in a 10% reduction in hydrocarbon emissions and a 5% reduction in particulates.

8.2 Cummins

The Cummins engine was operated in three modes: Stock, Disabled MAP (DM) and 2 volt MAP (2V). The malfunctioning modes investigated for the Cummins N-14 engine involved both disabling the (DM) and modifying the manifold air pressure (MAP) sensor signal to the engine control system. Since the engine control system depends on the MAP sensor to determine fuel delivery, a disabled sensor forced the system to deliver fuel based on an engine speed and fixed manifold pressure algorithm thus damaging the intended purpose (puff control) of the sensor. In modifying the MAP sensor input to the engine control system, where manifold air pressure was translated to a voltage, a 2 volt supply (2V) corresponding to full boost pressure was substituted. This caused the engine to overfuel, that is to decrease the air-fuel ratio below design specifications, and resulted in corresponding increases in engine power and emissions.

8.3 Manual Operation

In order to compare operation of an engine with a driver and a computer, a throttle pedal was arranged so that the engine torque could be controlled by the operator while the Navistar engine was installed on the engine dynamometer. While the operator was not able to follow the torque schedule as closely as the computer, emissions were generally lower. This can be attributed to the difference in driving characteristics where the computer was much more aggressive in drive-by-wire mode and could react more quickly than the human operator. A comparison of data from both computer and manual FTP testing is shown in Table 3. This data is the average of 3 hot starts for the computer driven FTPs and the average of 2 hot starts for the manually driven tests.

	Manually Driven	Computer Driven	% Difference
Bhp-Hr	11.4	10.76	-5.8
HC (g/bhp-hr)	0.45	0.67	+39.7
CO (g/bhp-hr)	2.04	2.34	+13.7
NO_X (g/bhp-hr)	5.36	5.58	+3.9
PM (g/bhp-hr)	0.11	0.14	+28.3

Table 8.1 - Data from the Navistar engine FTP tests with stock engine setup using both computer and manual throttle control.

Although this manual operation of the Navistar engine was not pursued further, it did indicate that there was potential for driver induced error if manual chassis testing were attempted.

9. Data Gathered

9.1 Preliminary Test Data from a Ford Tractor

Before the two primary subject vehicles were tested in the program, preliminary research was performed using a 1985 model year tractor on the dynamometer. The engine in this tractor was not removed for testing as part of the test program. Since the engine was mechanically injected, a driver was used in place of the electronic control used on the primary subject vehicles. Data gathered from the preliminary test vehicle (Ford with Cummins 350 diesel engine) was examined to determine how drivers' experience level and driver-to-driver variability effect repeatability between both engine parameters (speed and torque) and emissions from test to test. Engine data were also examined to determine how well the driver met schedule speed and torque. Analysis was performed using correlation coefficients (ρ_x and ρ_y) determined using the formula

$$\rho_{x,y} = \frac{Cov(X,Y)}{\sigma_x \cdot \sigma_y}$$

where

$$-1 \le \rho_{x,y} \le 1$$

and

$$Cov(X,Y) = \frac{1}{n}\sum_{i=1}^{n}(x_i - \mu_x)(y_i - \mu_y)$$

where ρ is the correlation coefficient, X and Y are the data sets being correlated, σ_x and σ_y are the standard deviations of each data set, n is the number of data points, and μ_x and μ_y are the mean values of X and Y respectively. For example, when comparing actual engine torque to schedule engine torque, X is the second-by-second schedule torque data while Y is the second-by second actual engine torque. The first data correlated were test torque and speed the results of which are shown in Table 9.1.

Test Number	Driver – Test Number	ρ_{Torque}	ρ_{Speed}
041203	#1-1	0.925	0.855
041204	#1-2	0.914	0.858
041503	#2-1	0.880	0.807
041504	#2-2	0.889	0.803
041505	#2-3	0.904	0.818
041506	#3-1	0.900	0.866
041507	#3-2	0.906	0.880
041508	#3-3	0.890	0.846

Table 9.1 - Correlation of engine data to schedule data from testing performed on the preliminary test vehicle. Three drivers, designated #1, #2 and #3 were used for this set of tests.

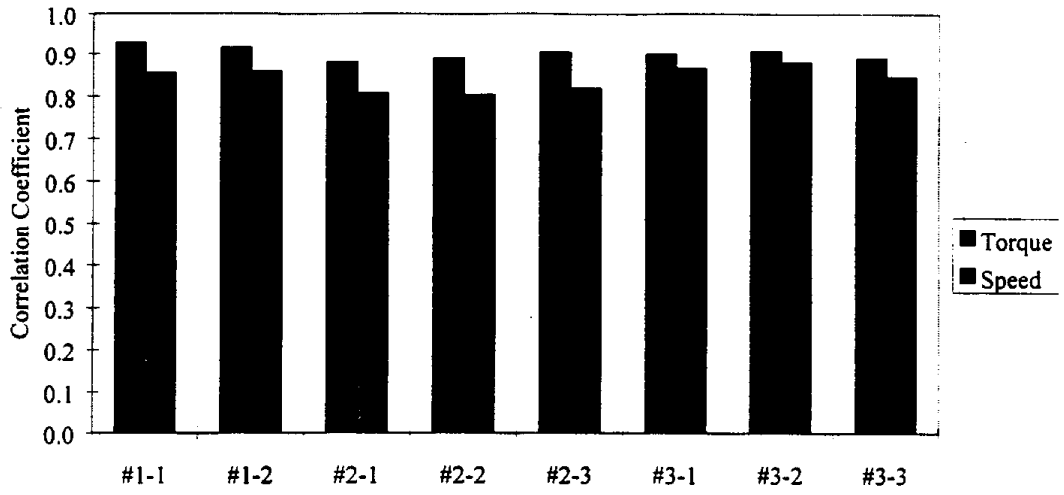

Figure 9.1 - Correlation coefficients (individual tests) for engine parameters from preliminary vehicle tests.

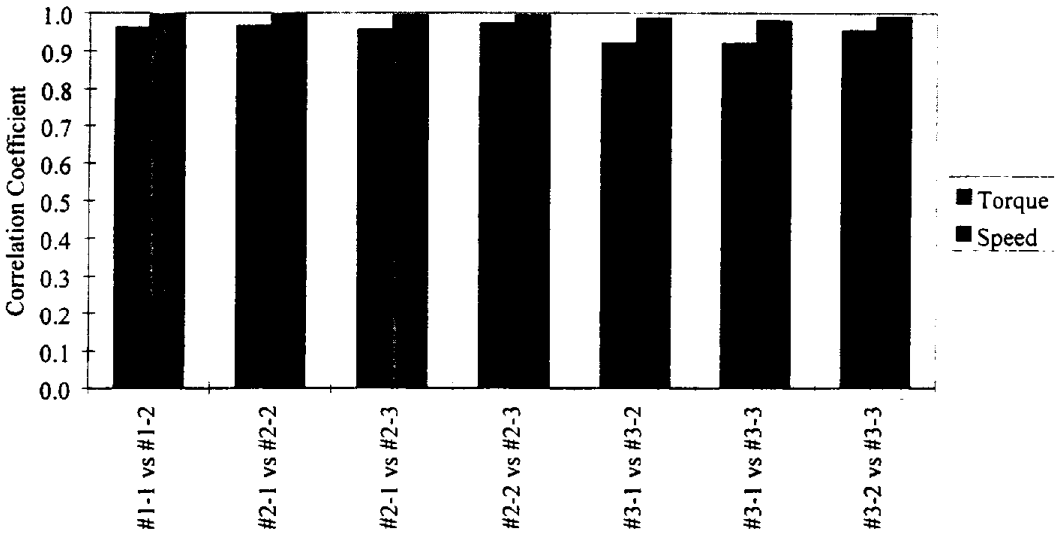

Figure 9.2 - Correlation coefficients (test to test, same driver) for engine parameters from preliminary vehicle tests.

Figure 9.1 shows that correlation of schedule and actual torque and speed were consistent for each driver while driver #2 did not meet the speed schedule as well as the other drivers. Figure 9.2 shows that correlation of actual speed and torque from test to test for each driver is also consistent with the exception of the correlation for driver #3 where tests 2 and 3 correlated better against each other than against test 1. This would indicate that the driver may have better learned

how to drive the schedule after the first test. In addition to engine data, emissions data were also correlated to determine their repeatability both from test to test and from driver to driver.

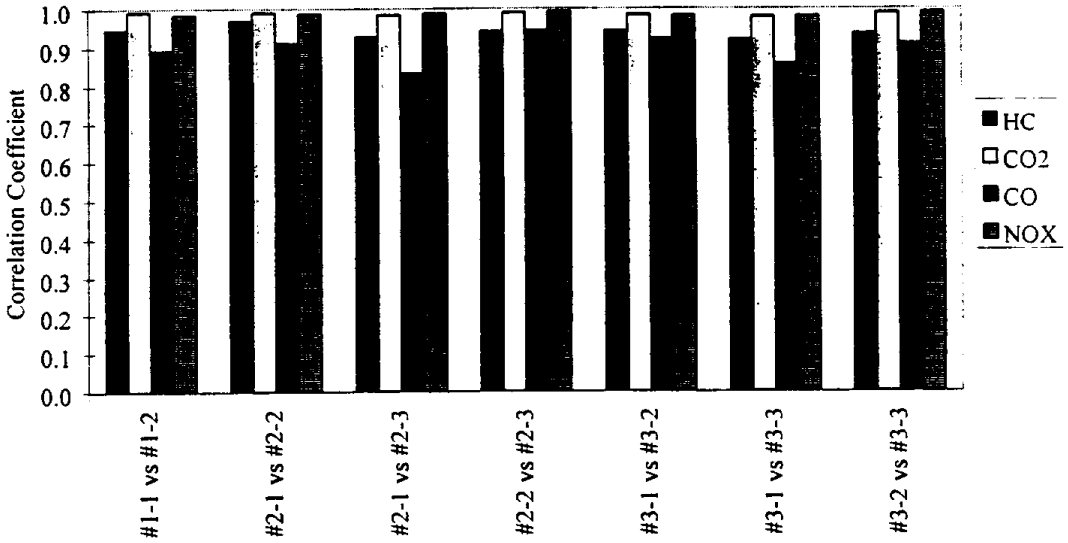

Figure 9.3 - Correlation coefficients (test to test, same driver) for emissions data from preliminary vehicle tests.

Figure 9.3 shows that the correlation of carbon dioxide (CO_2) and oxides of nitrogen (NO_X) from test to test with the same driver were excellent while hydrocarbons (HC) and carbon monoxide (CO) were lower. For CO_2 this could be expected due to its direct correlation to engine power and NO_X usually proves to be a stable and reproducible species in the experience of the investigators. PM data were not gathered for the preliminary testing.

The conclusion is that when a driver, rather than an electronic controller, is used for chassis testing, additional error will be incurred as a result of variations between drivers and between tests. However, for NO_X emissions, the driver-to-driver and test-to-test variations were less than 2%.

9.2 – Navistar and Cummins Data Collected

The two primary subject vehicles were subjected to engine testing according to the plan tabulated in Chapter 3. The Navistar engine was installed in the single axle chassis and chassis tests were performed as shown in the plan in Chapter 3. Similarly, the Cummins engine was tested in the tractor in single and tandem axle modes.

Table 9.2 presents the emissions data in g/bhp-hr for each engine test performed. Table 9.3 presents the chassis test data, in g/axle-hp-hr, for each chassis test performed. Table 9.4 summarizes the averages for the first three hot engine tests performed in each mode of operation. Table 9.5 summarizes the averages for the first three hot chassis tests performed in each mode of operation. In examination of these data, the work of Kittelson and Johnson (1991) on variations

within and between laboratories was considered. Table 9.6 provides data showing the effect of two different batches of fuel on emissions measured.

Test Sequence Number	Power (bhp-hr)	HC (g/bhp-hr)	CO (g/bhp-hr)	CO_2 (g/bhp-hr)	NO_x (g/bhp-hr)	PM (g/bhp-hr)
12109602-N-E-S	11.59	0.353	1.096	625	4.996	0.081
12109603-N-E-S	11.56	0.338	1.091	614	4.969	0.078
12109604-N-E-S	11.58	0.325	1.012	611	4.976	0.079
12109605-N-E-S	11.53	0.353	1.042	627	5.005	0.079
12169601-N-E-S	11.59	0.422	1.210	643	4.964	0.080
12169602-N-E-S	11.59	0.375	1.111	632	4.970	0.069
12169603-N-E-WU15	12.52	0.291	1.327	613	5.346	0.068
12169604-N-E-WU15	12.53	0.310	1.251	609	5.405	0.073
12169605-N-E-WU15	12.53	0.302	1.291	603	5.466	0.086
12169606-N-E-WU15	12.54	0.323	1.291	594	5.641	0.091
12169607-N-E-WU39	12.69	0.305	1.957	611	7.732	0.086
12169608-N-E-WU39	12.69	0.301	1.882	611	7.782	0.092
12169609-N-E-WU39	12.72	0.321	1.801	611	7.783	0.100
12169610-N-E-WU39	12.67	0.316	1.886	619	7.771	0.088
12199601-N-E-WU82	13.28	0.263	2.490	606	15.160	0.090
12199602-N-E-WU82	13.40	0.257	2.407	604	15.136	0.088
12199603-N-E-WU82	13.36	0.252	2.354	604	15.288	0.110
12199604-N-E-WU82	13.36	0.253	2.299	606	15.314	0.105
12189601-N-E-AS	11.67	0.323	1.223	638	4.938	0.068
12189602-N-E-AS	11.71	0.328	1.139	625	4.924	0.077
12189603-N-E-AS	11.68	0.327	1.165	625	4.887	0.078
12189704-N-E-AS	11.70	0.360	1.168	628	4.893	0.072
04289701-N14-E-S	22.42	0.156	0.958	559	4.923	0.071
04289702-N14-E-S	22.44	0.185	0.903	556	4.960	0.069
04289703-N14-E-S	22.48	0.191	0.920	554	5.060	0.069
05069701-N14-E-S	22.58	0.153	1.105	596	5.394	0.079
05019701-N14-E-DM	20.00	0.155	1.409	581	6.250	0.086
05019702-N14-E-DM	20.81	0.223	1.193	574	5.757	0.085
05019703-N14-E-DM	20.79	0.264	1.130	575	5.703	0.078
05029701-N14-E-2V	23.35	0.241	2.400	529	8.686	0.108
05029702-N14-E-2V	23.36	0.246	2.408	528	8.821	0.096
05029703-N14-E-2V	23.36	0.242	2.402	530	8.919	0.114
05069704-N14-E-2V	23.15	0.216	2.387	535	9.079	0.112

Table 9.2 – Emissions data from the Navistar and Cummins Engine tests

Test Sequence Number	Power (ahp-hr)	HC (g/ahp-hr)	CO (g/ahp-hr)	CO_2 (g/ahp-hr)	NO_x (g/ahp-hr)	PM (g/ahp-hr)
10089602-N-C-S	10.72	0.29	0.81	821	7.16	0.092
10089603-N-C-S	10.76	0.31	1.08	820	6.90	0.091
10089604-N-C-S	10.82	0.32	1.05	820	6.79	0.084
10089605-N-C-S	10.76	0.35	1.15	834	6.82	0
10099607-N-C-S	10.76	0.29	1.16	816	6.56	0.116
10099608-N-C-S	10.78	0.29	1.25	799	6.42	0.089
10079607-N-C-WU15	11.64	0.25	1.31	774	7.36	0.120
10079608-N-C-WU15	11.98	0.24	1.56	769	7.36	0.111
10079609-N-C-WU15	12.02	0.27	1.68	785	7.34	0.094
10079610-N-C-WU15	12.04	0.26	1.76	797	7.32	0.091
10079602-N-C-WU39	12.90	0.18	1.92	743	9.72	0.129
10079603-N-C-WU39	12.90	0.23	2.13	761	9.81	0.115
10079604-N-C-WU39	12.94	0.23	2.05	749	9.62	0.115
10079605-N-C-WU39	12.86	0.23	2.07	752	9.49	0.126
10099602-N-C-WU82	14.34	0.23	4.26	725	18.53	0.190
10099603-N-C-WU82	14.30	0.24	4.22	754	18.73	0.194
10099604-N-C-WU82	14.26	0.23	4.65	743	18.18	0.189
10099605-N-C-WU82	14.28	0.25	4.65	759	18.46	0.219
10179602-N-C-AS	15.64	0.20	0.78	769	6.31	0.092
10179603-N-C-AS	15.62	0.18	0.68	772	6.34	0.085
10179604-N-C-AS	14.50	0.22	1.04	806	6.53	0.083
10179605-N-C-AS	14.52	0.29	1.35	877	6.80	0.097
10249602-N-C-AS	15.56	0.20	0.86	744	6.28	0.072
10249603-N-C-AS	15.72	0.21	0.73	766	6.30	0.066
10249604-N-C-AS	15.90	0.20	0.82	761	6.46	0.066
10249605-N-C-AS	15.84	0.20	0.88	750	6.36	0.065
06059704-N14-C-SN8	19.24	0.34	1.13	725	7.44	0.071
06059705-N14-C-SN8	19.07	0.34	1.04	746	7.38	0.066
06059706-N14-C-SN8	19.13	0.34	1.17	747	7.43	0.065
06059707-N14-C-SN8	19.01	0.38	1.21	761	7.36	0.071
06099702-N14-C-SN7	18.91	0.35	0.91	704	6.95	0.087
06099703-N14-C-SN7	19.38	0.33	1.00	721	6.75	0.071
06109702-N14-C-SN7	18.89	0.39	1.15	702	7.52	0.080
06109703-N14-C-SN7	19.66	0.35	1.04	756	7.61	0.080
06169701-N14-C-SN9	19.17	0.36	1.79	785	8.42	0.117
06169702-N14-C-SN9	18.76	0.35	1.75	761	8.09	0.091
06169703-N14-C-SN9	18.58	0.31	1.75	758	7.81	0.089
06169704-N14-C-SN9	19.08	0.33	1.71	775	7.66	0.095
06189702-N14-C-SN7	19.49	0.32	1.17	704	7.14	0.076
06189703-N14-C-SN7	19.41	0.33	1.12	687	6.93	0.078
06189704-N14-C-SN7	20.14	0.34	1.02	723	6.07	0.072
06199701-N14-C-SN7	19.55	0.38	1.03	716	7.16	0.086
06199702-N14-C-SN7	19.52	0.33	1.06	704	7.01	0.072
06199705-N14-C-ST8	19.04	0.33	1.21	733	7.55	0.095
06199706-N14-C-ST8	19.18	0.32	1.02	733	7.38	0.070
06199707-N14-C-ST8	19.04	0.32	1.17	721	7.06	0.073
06259701-N14-C-ST8	19.05	0.31	1.21	708	6.89	0.081
06259702-N14-C-ST8	19.03	0.31	1.29	719	6.83	0.072
06259703-N14-C-ST8	19.03	0.35	1.24	726	6.76	0.081
06269704-N14-C-DMT8	18.18	0.30	1.40	741	7.83	0.098
06269705-N14-C-DMT8	18.06	0.32	1.52	720	7.32	0.088
06269706-N14-C-DMT8	18.00	0.35	1.40	733	7.26	0.089
06269707-N14-C-DMT8	17.94	0.31	1.36	703	7.20	0.092
06279703-N14-C-RDT8	19.70	0.28	0.88	652	6.47	0.064

Table 9.3 – Emissions data from chassis tests on the Cummins and Navistar engines

06279704-N14-C-RDT8	19.66	0.30	0.93	652	6.28	0.056
06279705-N14-C-RDT8	19.56	0.31	0.84	656	6.38	0.064
06279706-N14-C-RDT8	19.72	0.31	1.00	672	6.49	0.066
06309703-N14-C-RDT9	19.95	0.28	1.06	669	6.72	0.070
06309704-N14-C-RDT9	19.80	0.28	1.15	669	6.60	0.072
06309705-N14-C-RDT9	19.77	0.30	1.25	691	6.47	0.074
06309706-N14-C-RDT9	19.76	0.30	1.25	682	6.25	0.075
07019704-N14-C-RDT7	20.08	0.32	0.95	657	5.96	0.070
07019705-N14-C-RDT7	20.34	0.32	0.84	663	5.87	0.075
07029701-N14-C-RDT7	19.74	0.31	0.97	665	6.25	0.074
07029702-N14-C-RDT7	19.70	0.31	1.00	660	6.08	0.069
07029704-N14-C-RDDMT7	18.45	0.30	1.41	701	6.82	0.078
07029705-N14-C-RDDMT7	18.62	0.32	1.45	694	6.45	0.082
07029706-N14-C-RDDMT7	18.47	0.32	1.28	685	6.66	0.077
07029707-N14-C-RDDMT7	18.23	0.29	1.35	707	6.53	0.081
07039701-N14-C-2VT8	18.92	0.31	4.60	711	12.49	0.190
07039702-N14-C-2VT8	18.86	0.32	4.25	716	11.99	0.178
07039703-N14-C-2VT8	18.74	0.33	4.07	710	11.90	0.179
07039704-N14-C-2VT8	18.67	0.31	4.11	701	12.11	0.173

Table 9.3 – Emissions data from Chassis tests on the Cummins and Navistar engines (cont.)

Test Conditions	Work (bhp-hr)	HC (g/bhp-hr)	CO (g/bhp-hr)	CO_2 (g/bhp-hr)	NO_x (g/bhp-hr)	PM (g/bhp-hr)
Navistar Engine Stock	11.58	0.34	1.07	616.86	4.98	0.08
Navistar Engine WU15	12.53	0.30	1.29	608.17	5.41	0.08
Navistar Engine WU39	12.70	0.31	1.88	611.24	7.77	0.09
Navistar Engine WU82	13.35	0.26	2.42	604.66	15.19	0.10
Navistar Engine Alt Stock	12.36	0.30	1.64	619.87	9.07	0.09
Cummins Engine Stock	22.50	0.18	0.98	569.06	5.14	0.07
Cummins Engine DM	20.53	0.21	1.24	577.14	5.90	0.08
Cummins Engine 2V	23.36	0.24	2.40	529.50	8.81	0.11

Table 9.4 – Average emissions data from Navistar and Cummins engine tests (warm starts only)

Test Conditions	Work (ahp-hr)	HC (g/ahp-hr)	CO (g/ahp-hr)	CO_2 (g/ahp-hr)	NO_x (g/ahp-hr)	PM (g/ahp-hr)
Navistar Chassis Stock	10.77	0.31	0.98	820.75	6.95	0.09
Navistar Chassis WU15	11.88	0.25	1.52	776.08	7.35	0.11
Navistar Chassis WU39	12.91	0.21	2.03	750.81	9.71	0.12
Navistar Chassis WU82	14.30	0.23	4.38	740.79	18.48	0.19
Navistar Chassis Alt Stock	15.25	0.20	0.83	782.50	6.39	0.09
Cummins Chassis Stock	19.09	0.32	1.13	729.11	7.33	0.08
Cummins Chassis DM	18.08	0.32	1.44	731.34	7.47	0.09
Cummins Chassis 2V	18.84	0.32	4.31	712.31	12.13	0.18

Table 9.5 – Average emissions data from Navistar and Cummins Chassis testing (Cummins chassis data from each gear is combined for each average)

Test Conditions	Work (ahp-hr)	HC (g/ahp-hr)	CO (g/ahp-hr)	CO_2 (g/ahp-hr)	NO_x (g/ahp-hr)	PM (g/ahp-hr)
Cummins Chassis Stock (Original Test Fuel)	19.15	0.34	1.11	739.16	7.42	0.07
Cummins Chassis Stock (BP Pump Fuel)	19.09	0.32	1.13	729.11	7.33	0.08

Table 9.6 – Effect of fuel on Cummins chassis emissions

It is not possible to present all of the continuous data generated in the space restraints of this report. However, one batch of continuous data has been included for the Navistar engine in stock condition and one batch of continuous data for the Cummins engine. In addition, comparative

data has been presented to show differences between continuous NO_X emissions between engine and chassis tests. Figures are as follows.

Figure 9.4: Schedule and actual engine speed from FTP testing performed on the Navistar engine in stock mode.

Figure 9.5: Schedule and actual engine torque from FTP testing performed on the Navistar engine in stock mode. The schedule torque was generated from the map in Figure 6.1.

Figure 9.6: Hydrocarbon emissions from the Navistar engine stock FTP testing.

Figure 9.7: Carbon monoxide emissions from the Navistar engine stock FTP testing.

Figure 9.8: Carbon dioxide emissions from the Navistar engine stock FTP testing.

Figure 9.9: Oxides of nitrogen emissions from the Navistar engine stock FTP testing.

Figure 9.10: Schedule and actual engine speed from FTP testing performed on the Cummins engine in stock mode.

Figure 9.11: Schedule and actual engine torque from FTP testing performed on the Cummins engine in stock mode. The schedule torque was generated from the map in Figure 6.2.

Figure 9.12: Hydrocarbon emissions from the Cummins engine stock FTP testing.

Figure 9.13: Carbon monoxide emissions from the Cummins engine stock FTP testing.

Figure 9.14: Carbon dioxide emissions from the Cummins engine stock FTP testing.

Figure 9.15: Oxides of nitrogen emissions from the Cummins engine stock FTP testing.

Figure 9.16: Schedule and actual engine speed from chassis FTP testing on the Cummins engine.

Figure 9.17: Schedule and actual axle torque from chassis FTP testing of the Cummins engine. The torque schedule was developed using chassis map data from Figure 6.4.

Figure 9.18: Oxides of Nitrogen emissions from chassis FTP testing with the rear axle disconnected (single axle).

Figure 9.19: Oxides of Nitrogen emissions from chassis FTP testing with both axles connected (dual axle).

Figure 9.20: Integrated axle power from Navistar transient chassis testing.

Figure 9.21: Integrated hydrocarbon emissions from Navistar transient chassis testing.

Figure 9.42: Average oxides of nitrogen emissions from transient engine tests.

Figure 9.43: Average oxides of particulate matter emissions from transient engine tests.

Figure 9.44: Average work from transient chassis tests.

Figure 9.45: Average hydrocarbon emissions from transient chassis tests.

Figure 9.46: Average carbon monoxide emissions from transient chassis tests.

Figure 9.47: Average carbon dioxide emissions from transient chassis tests.

Figure 9.48: Average oxides of nitrogen emissions from transient chassis tests.

Figure 9.43: Average particulate matter emissions from transient chassis tests.

The results and discussion chapter is concerned with the processing of the integrated data shown in Tables 9.2 and 9.3 rather than the continuous data.

Figure 9.4 - Schedule and Actual Engine Speed from Navistar Engine (06199602)

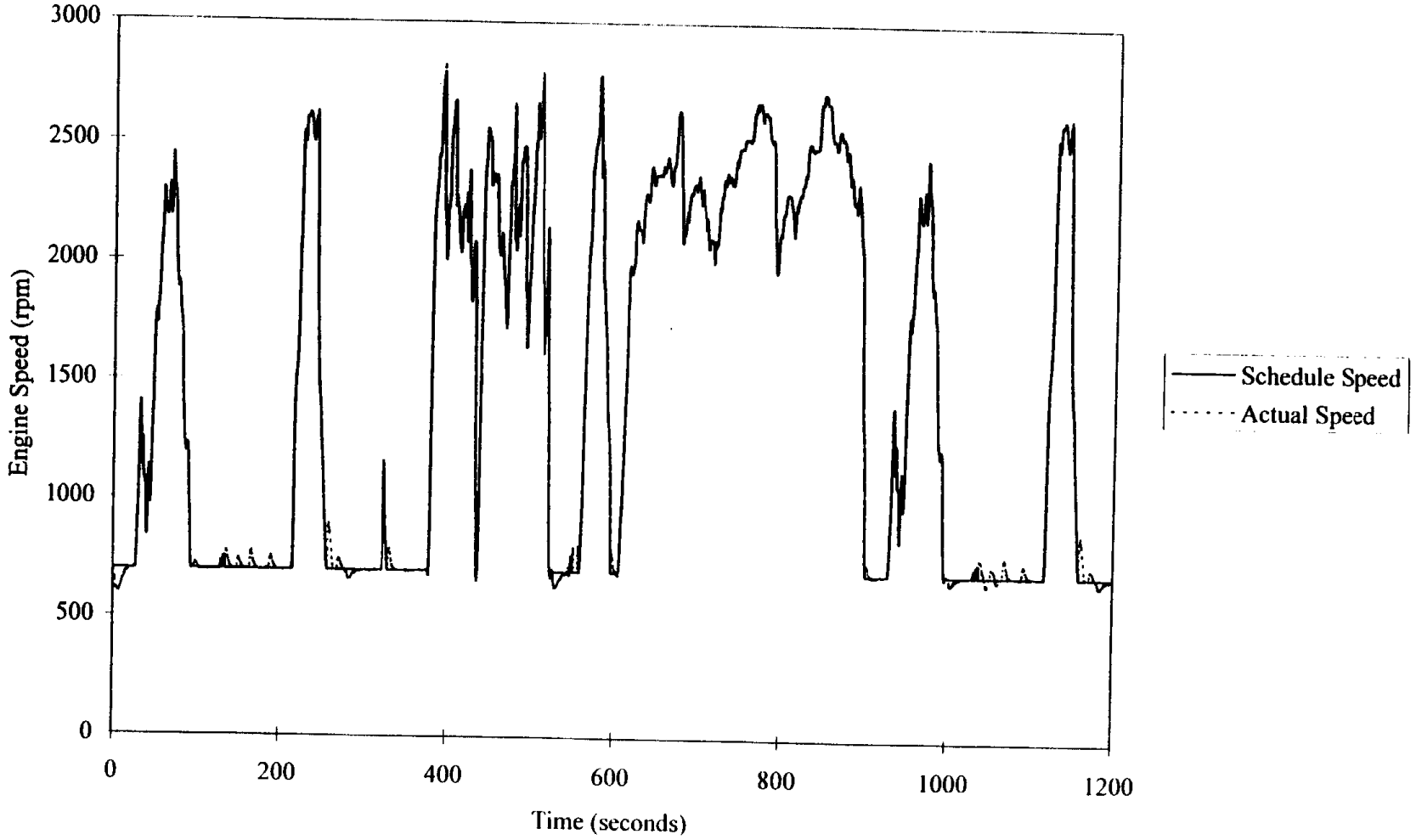

Figure 9.5 - Schedule and Actual Torque from Navistar Engine (06199602)

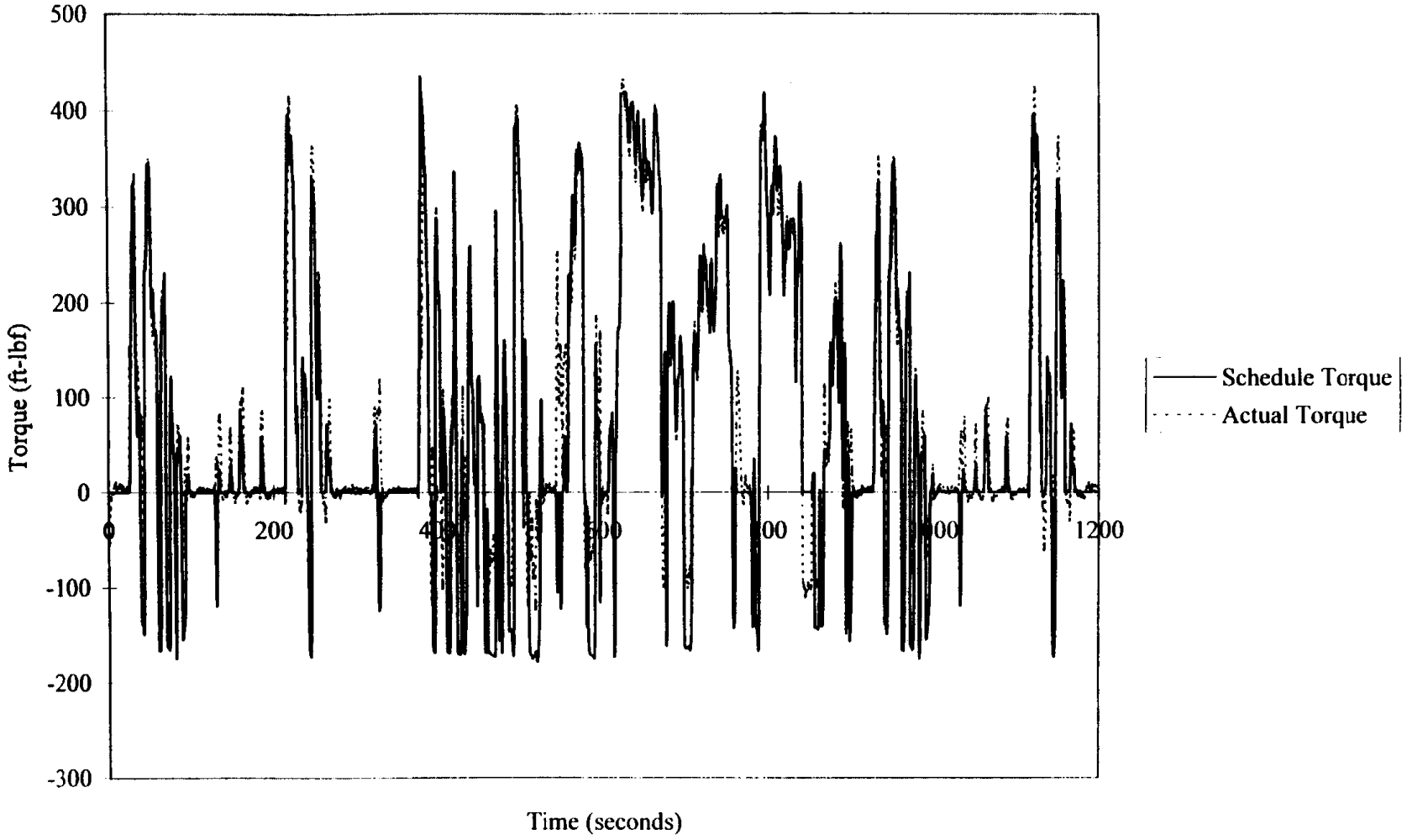

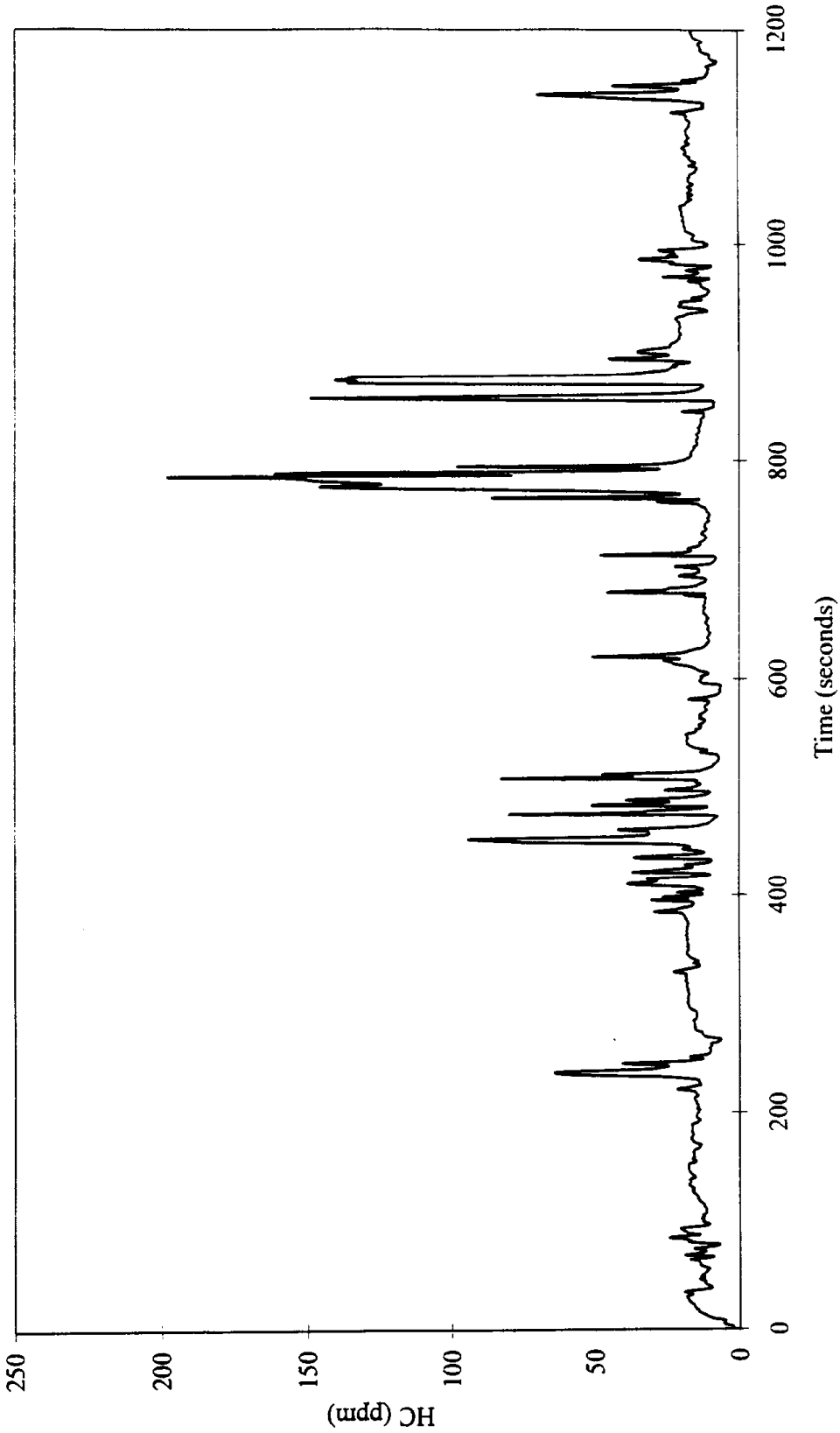

Figure 9.6 - Hydrocarbon Emissions from the Navistar Engine (09169602)

Figure 9.7 - Carbon Monoxide Emissions from the Navistar Engine (09169602)

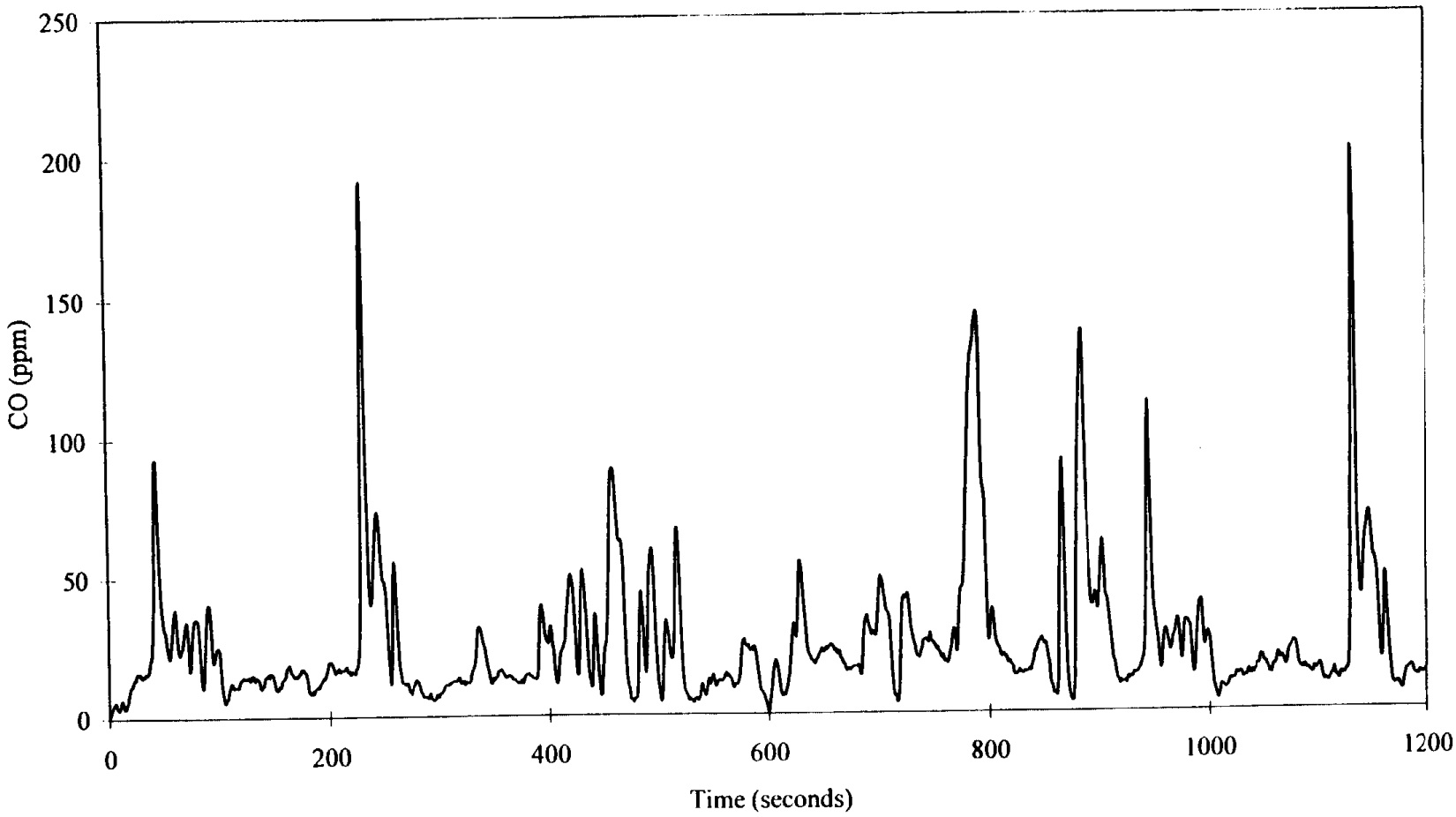

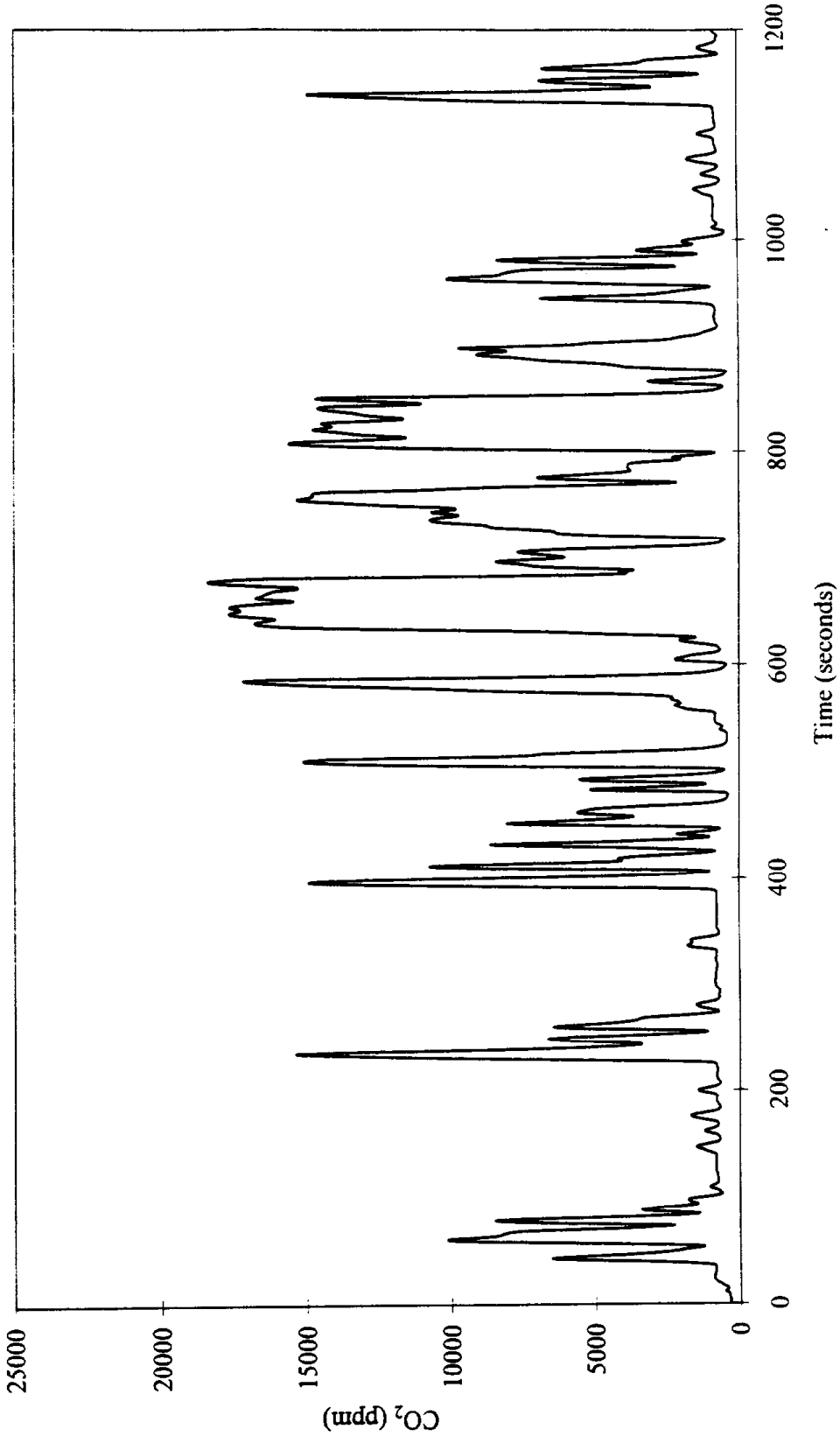

Figure 9.8 - Carbon Dioxide Emissions from the Navistar Engine (09169602)

Figure 9.9 - Oxide of Nitrogen Emissions from the Navistar Engine (09169602)

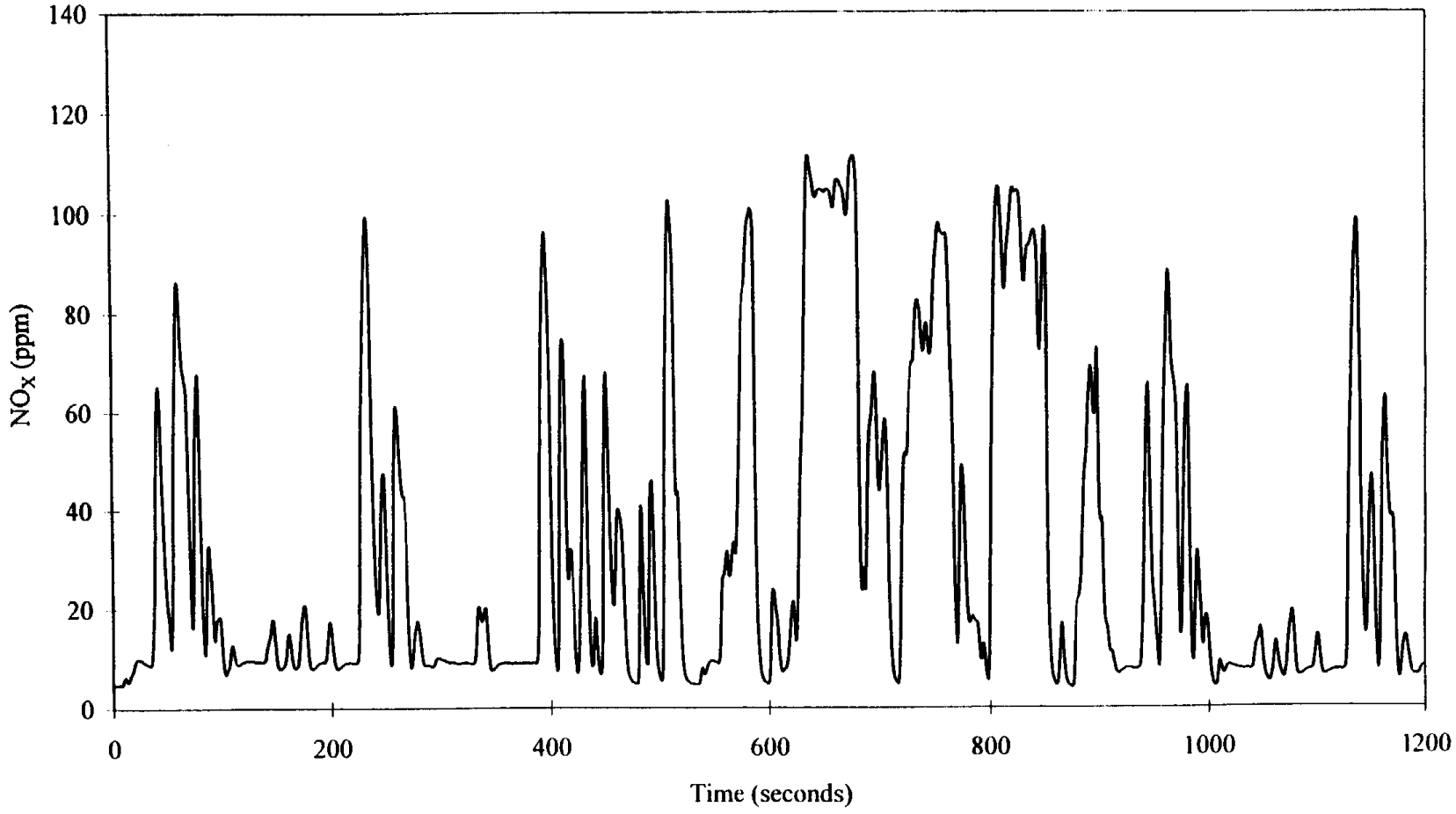

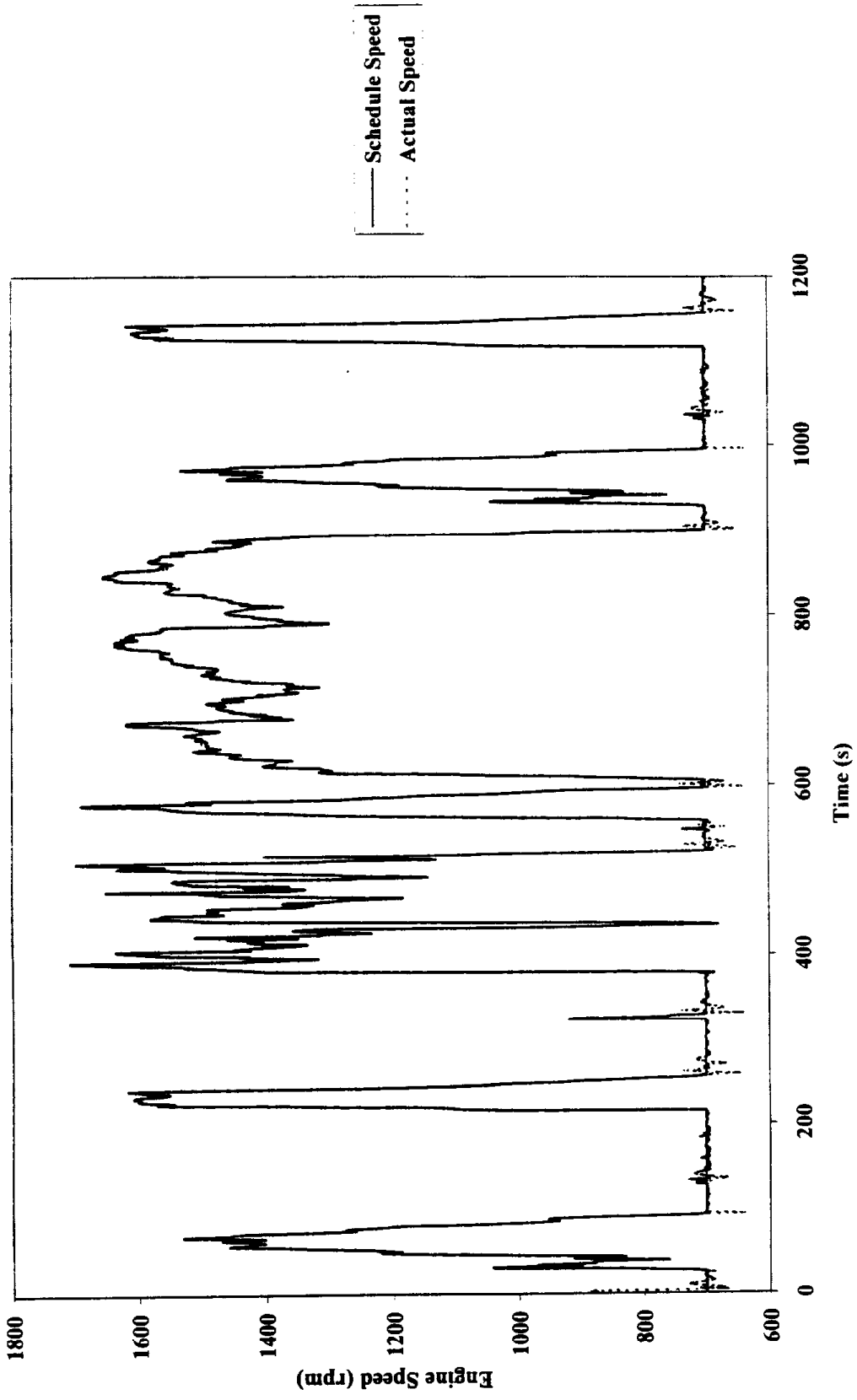

Figure 9.10 - Schedule and Actual Speed from the Cummins Engine (04289602)

Figure 9.11 - Schedule and Actual Torque from the Cummins Engine (04289602)

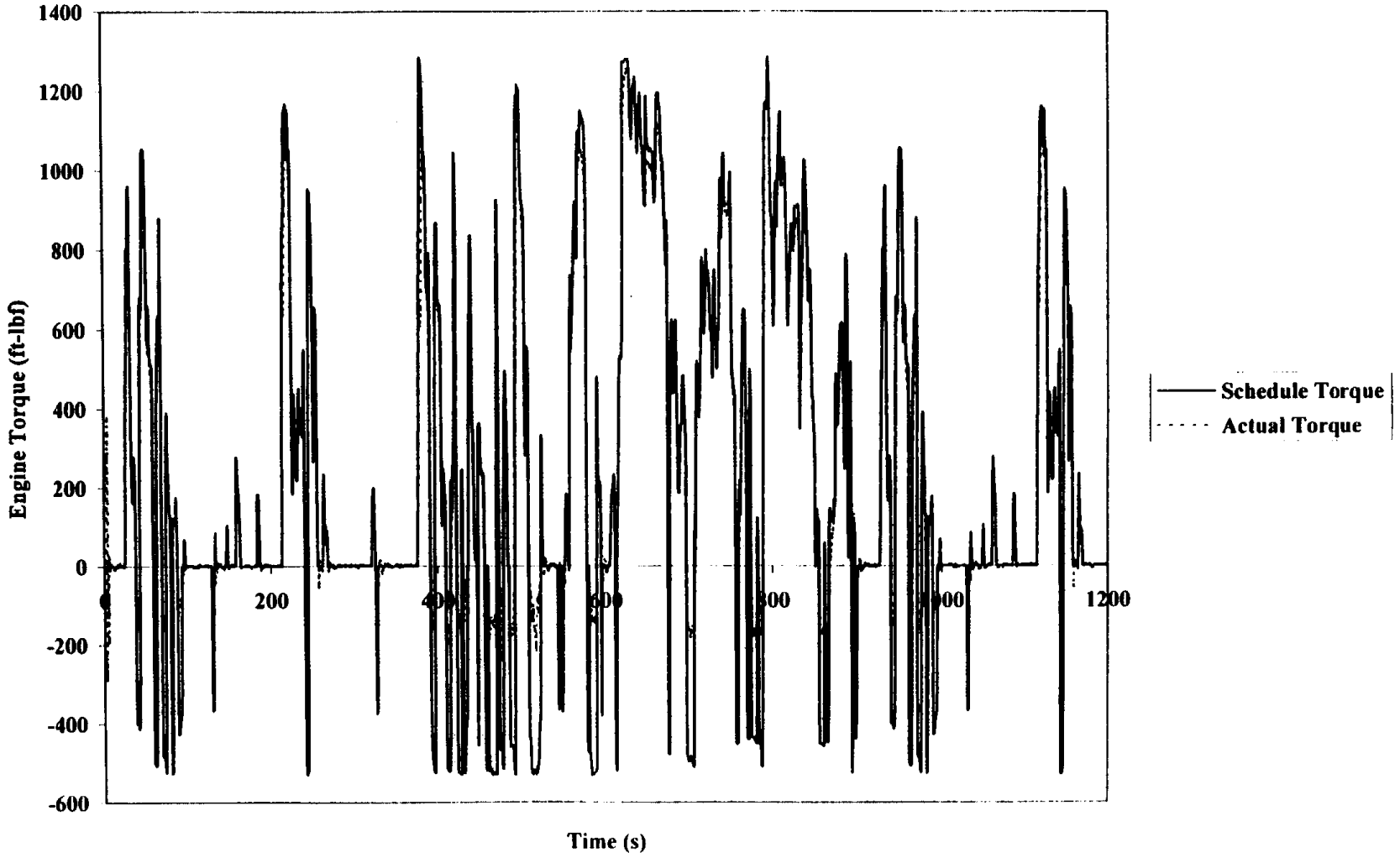

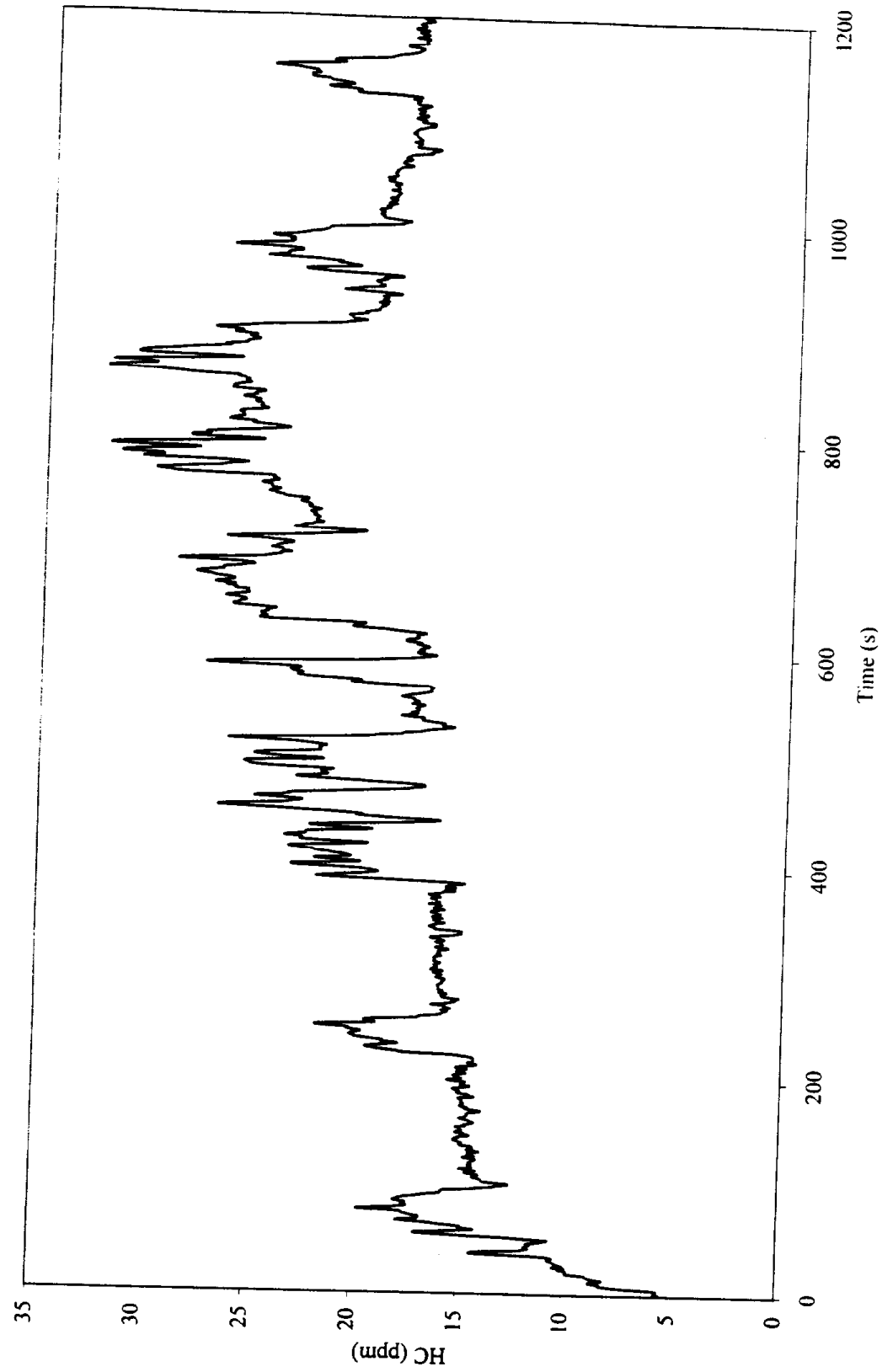

Figure 9.12 - Hydrocarbon Emissions from the Cummins Engine (04289702)

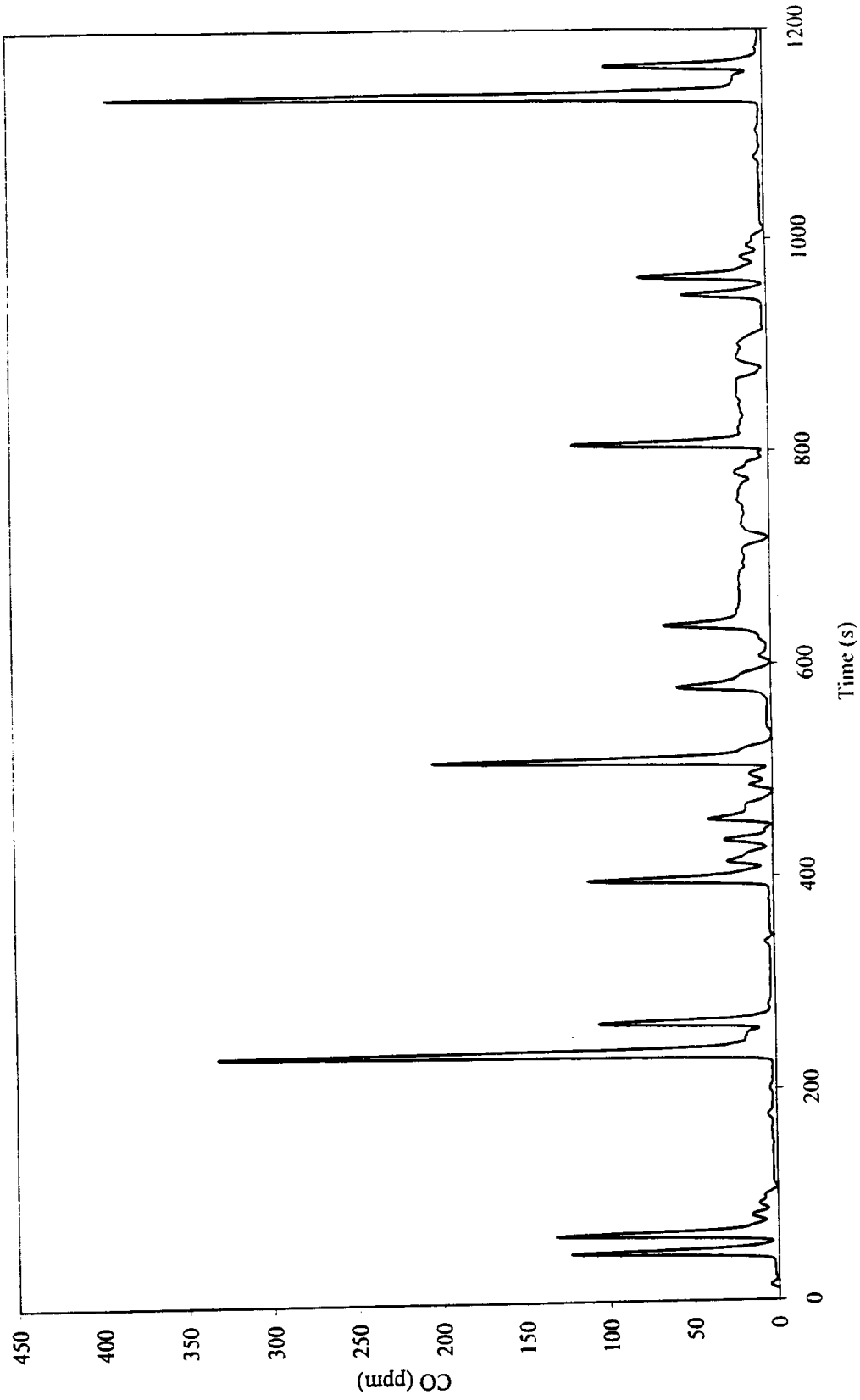

Figure 9.13 - Carbon Monoxide Emissions from the Cummins Engine (04289706)

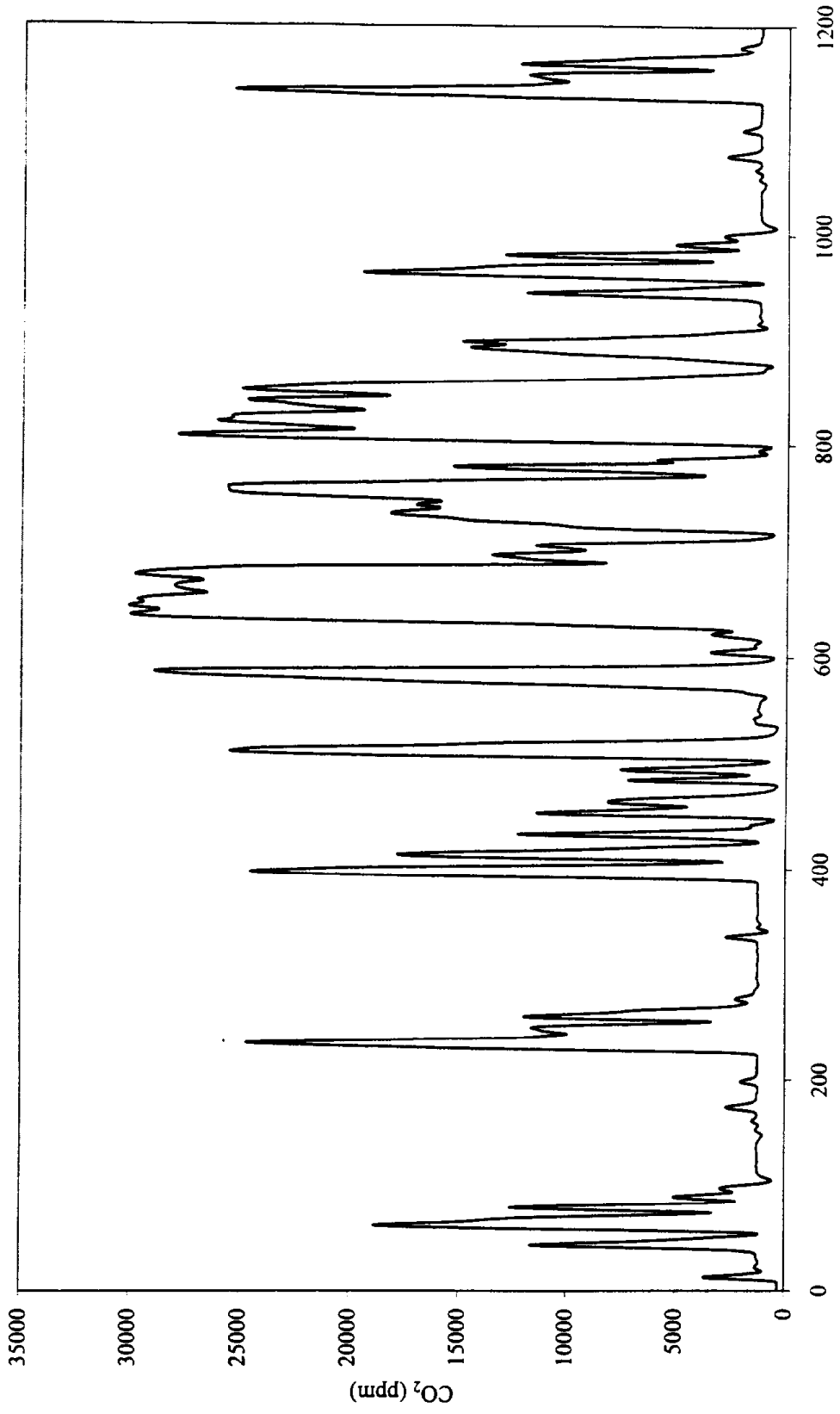

Figure 9.14 - Carbon Dioxide emissions from the Cummins Engine (04289702)

Figure 9.15 - Oxides of Nitrogen Emissions from the Cummins Engine (04289702)

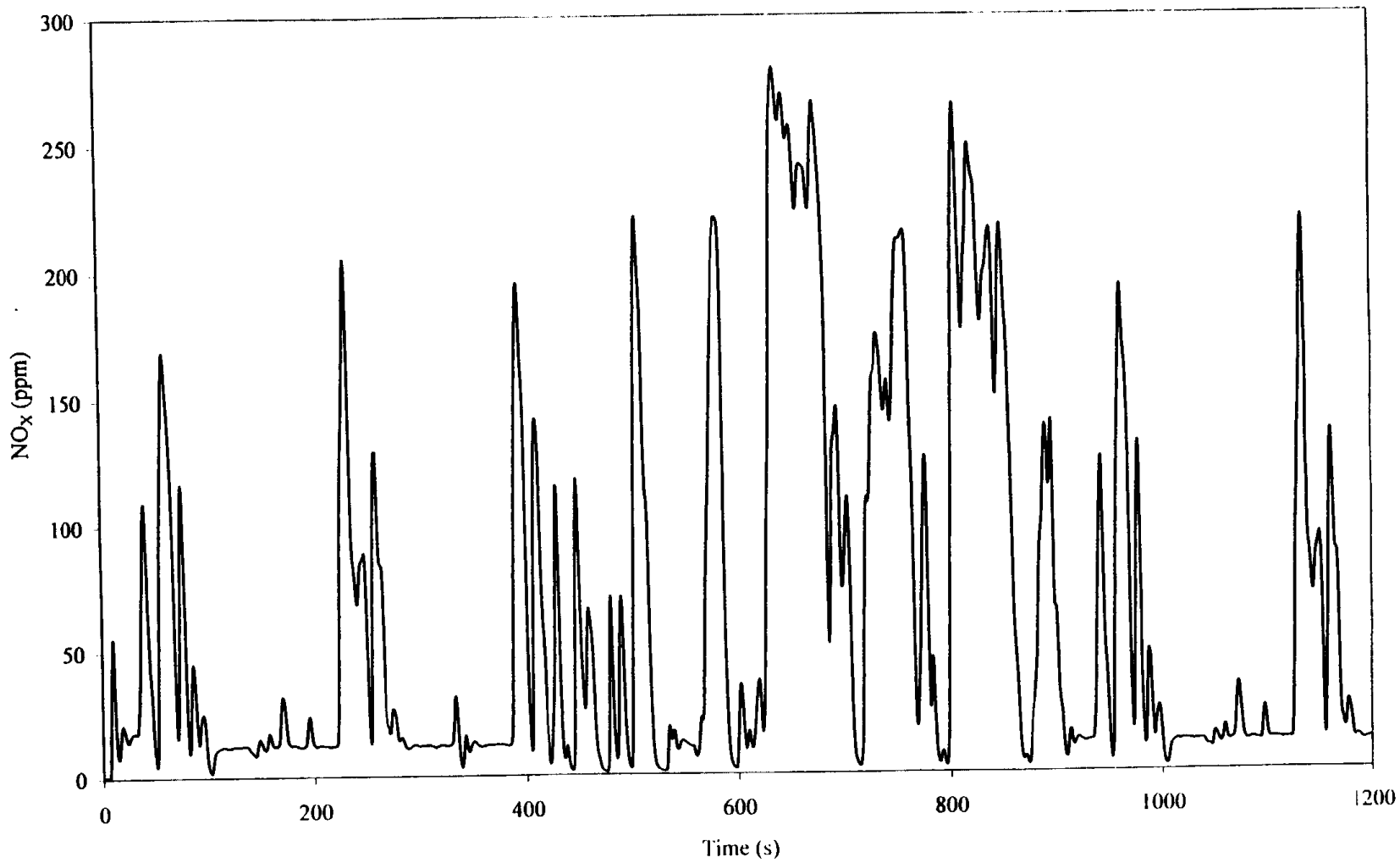

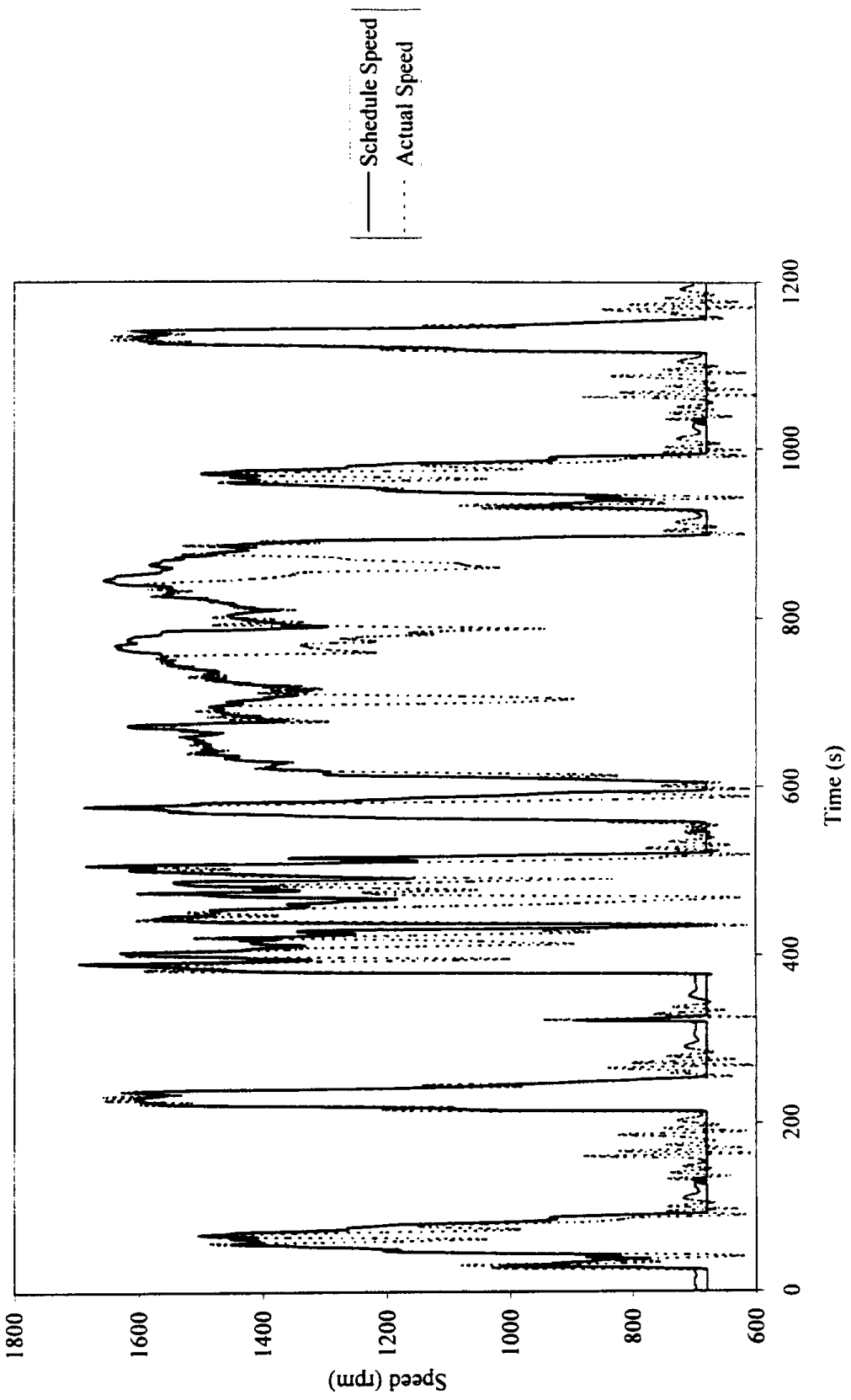

Figure 9.16 - Engine Speed from the Cummins N-14 Chassis (06199706)

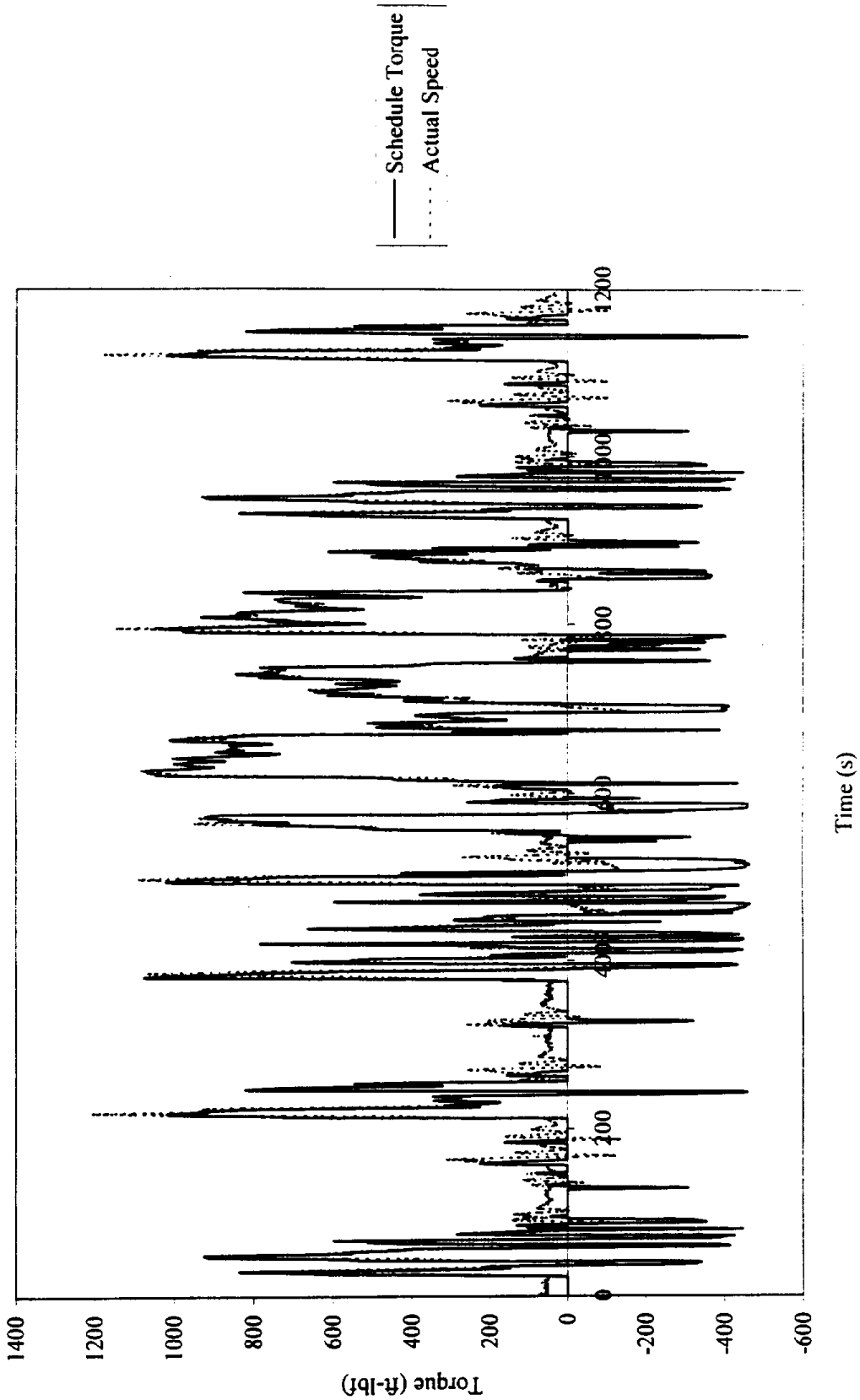

Figure 9.17 - Axle Torque from the Cummins N-14 Chassis (06199706)

Figure 9.18 - Oxides of Nitrogen Emissions from the Cummmins Chassis, Stock Engine with Single Axle (07019703)

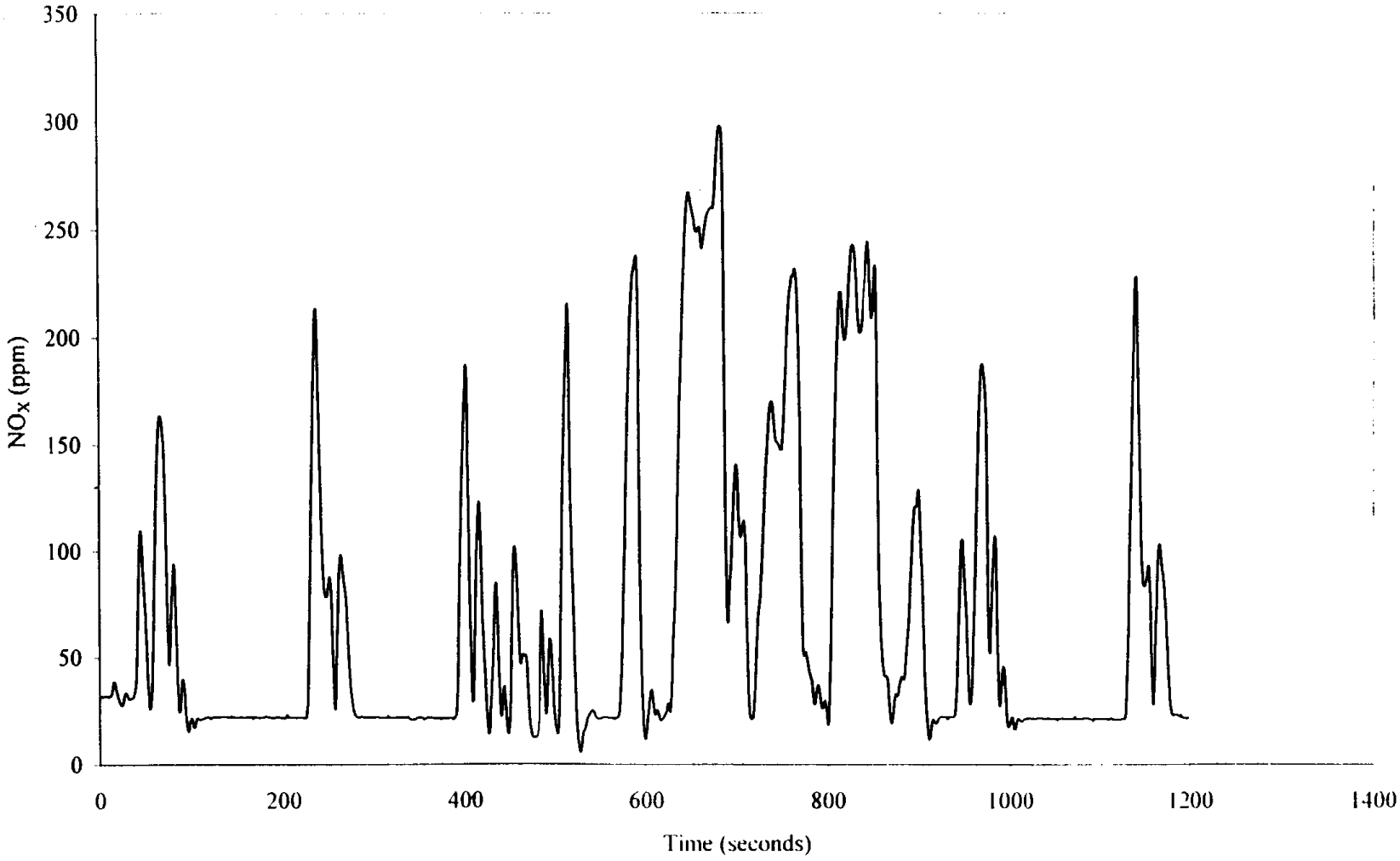

Figure 9.19 - Oxides of Nitrogen Emissions from the Cummins Chassis, Stock Engine with Tandem Axle (06199706)

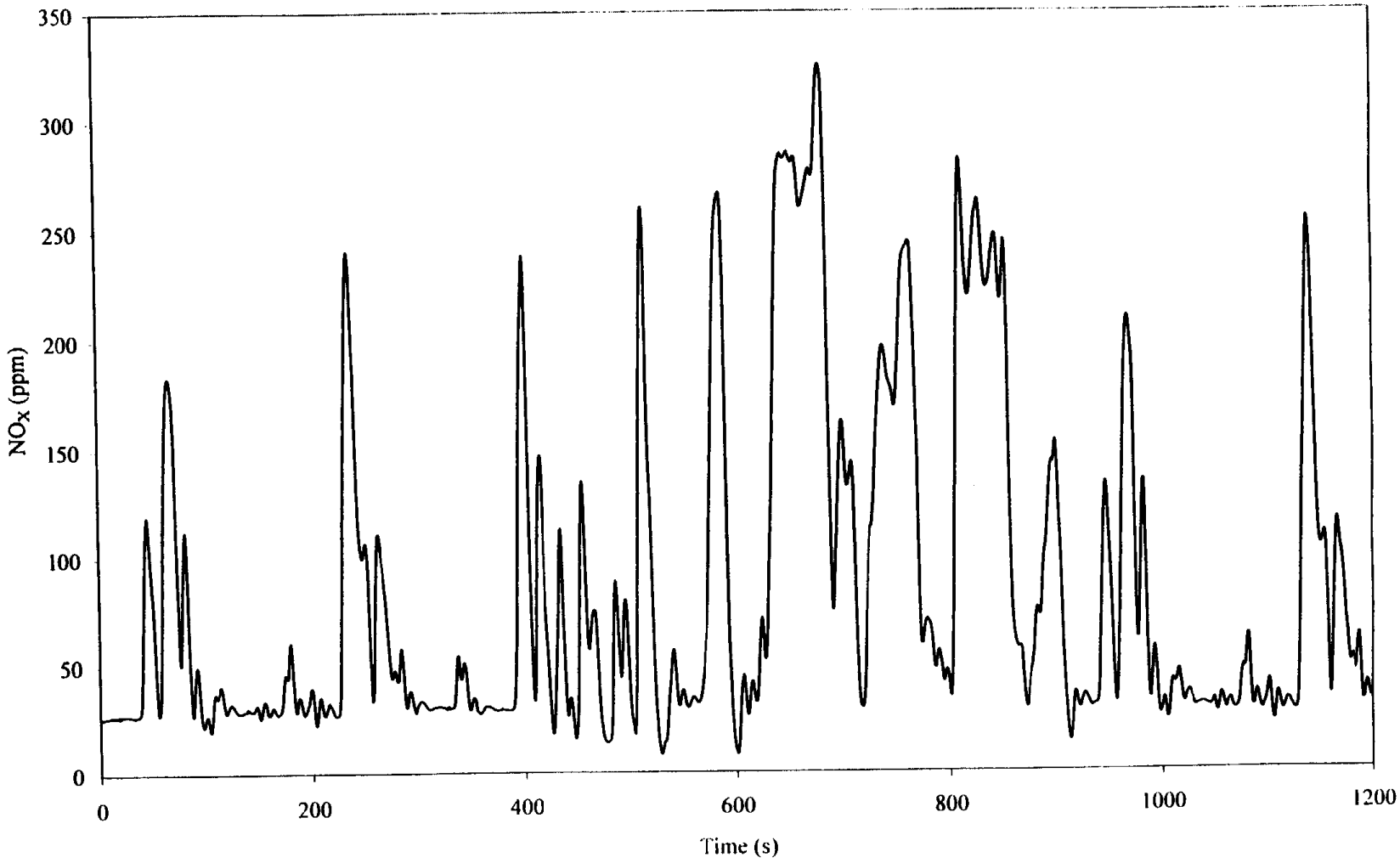

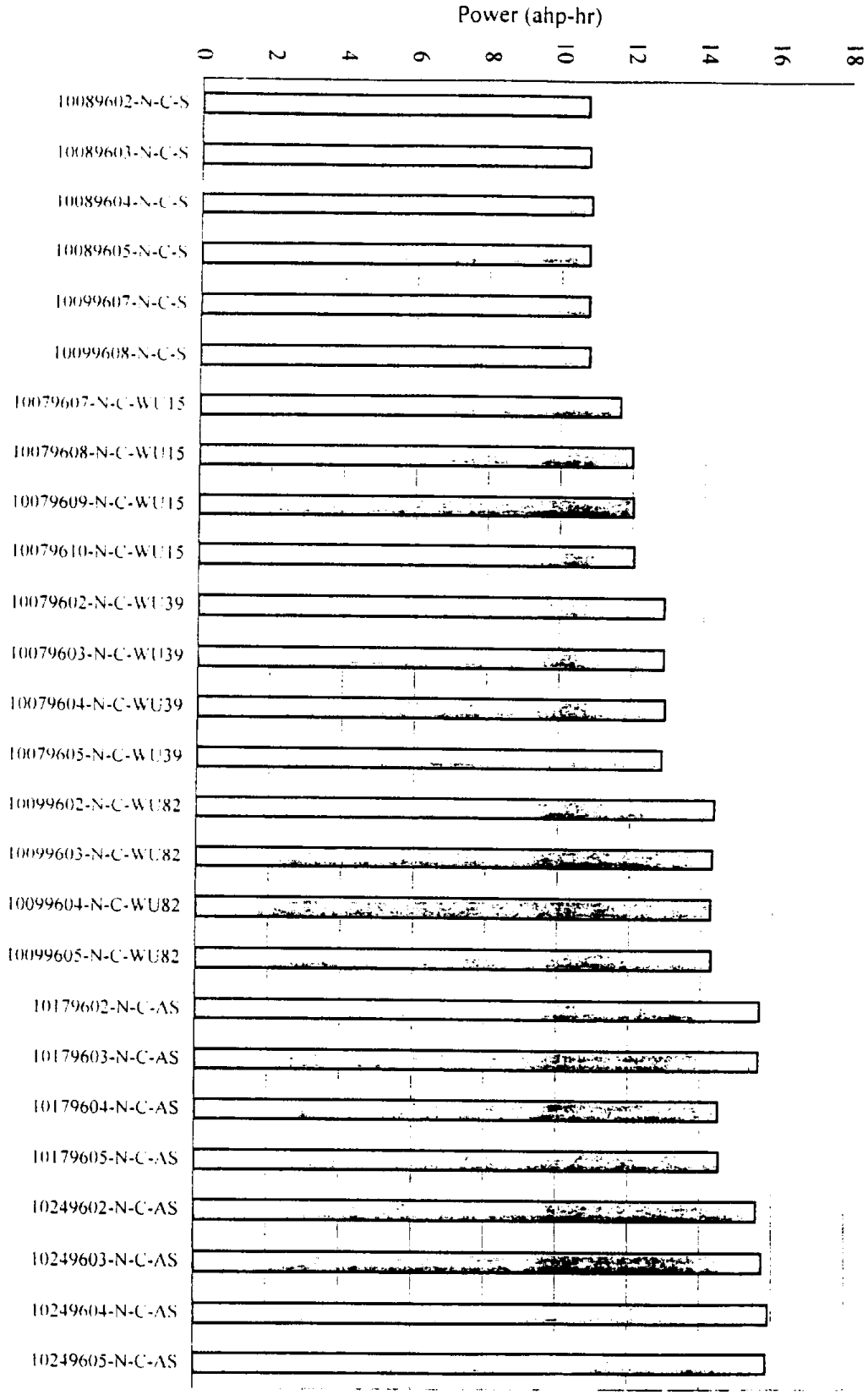

Figure 9.20 - Integrated axle power from Navistar transient chassis testing

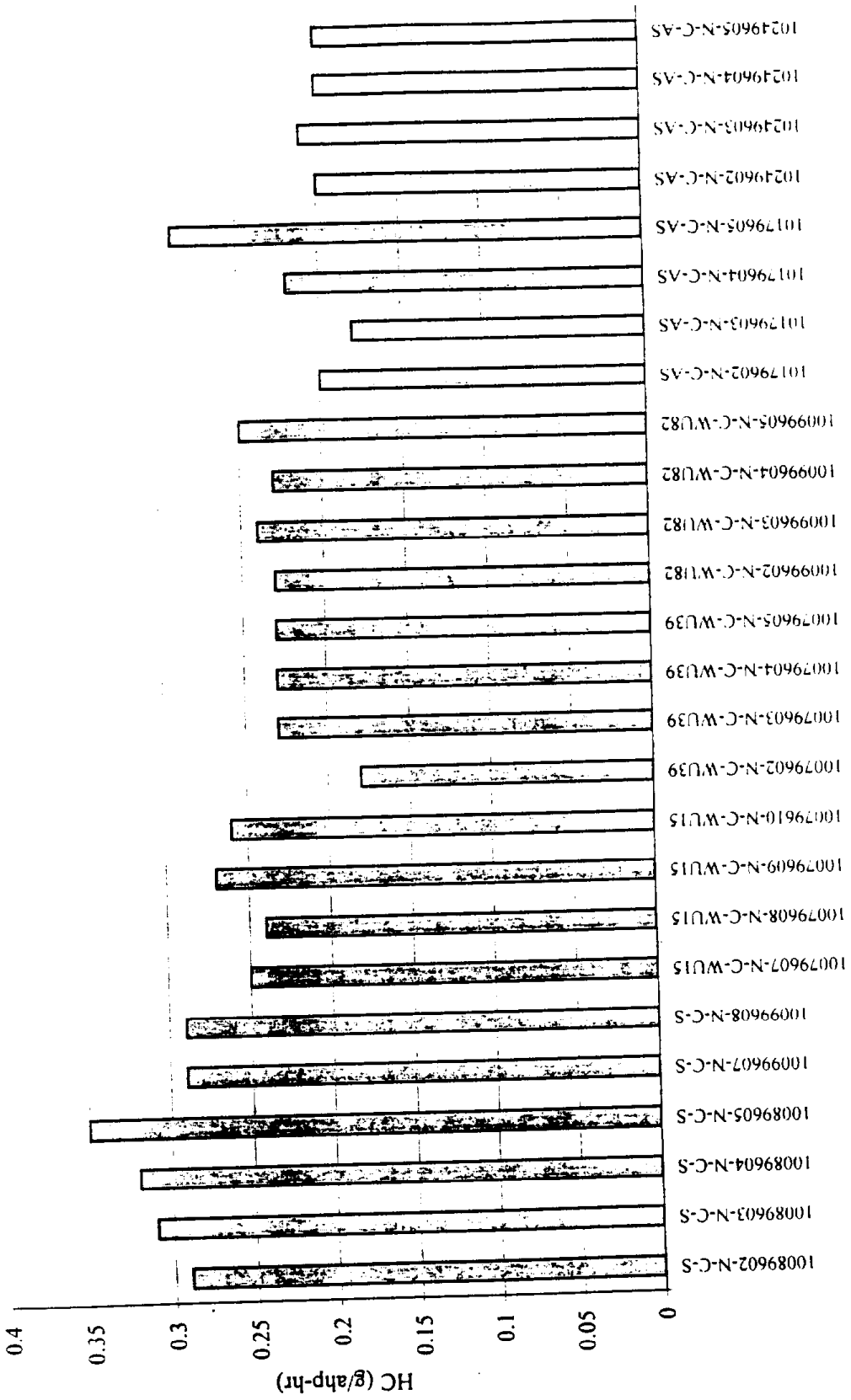

Figure 9.21 - Integrated hydrocarbon emissions from Navistar transient chassis testing

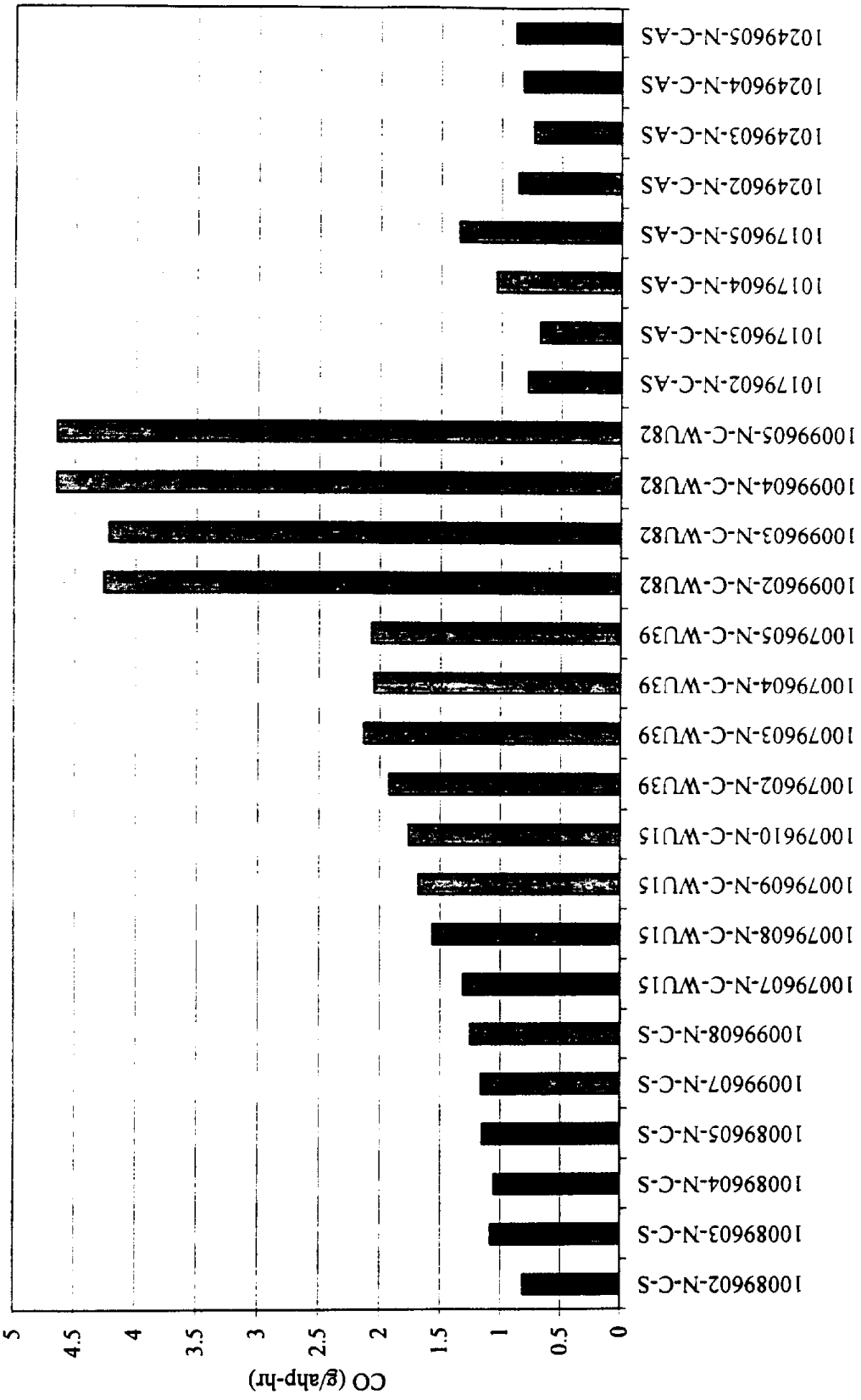

Figure 9.22 - Integrated carbon monoxide emissions from Navistar transient chassis testing

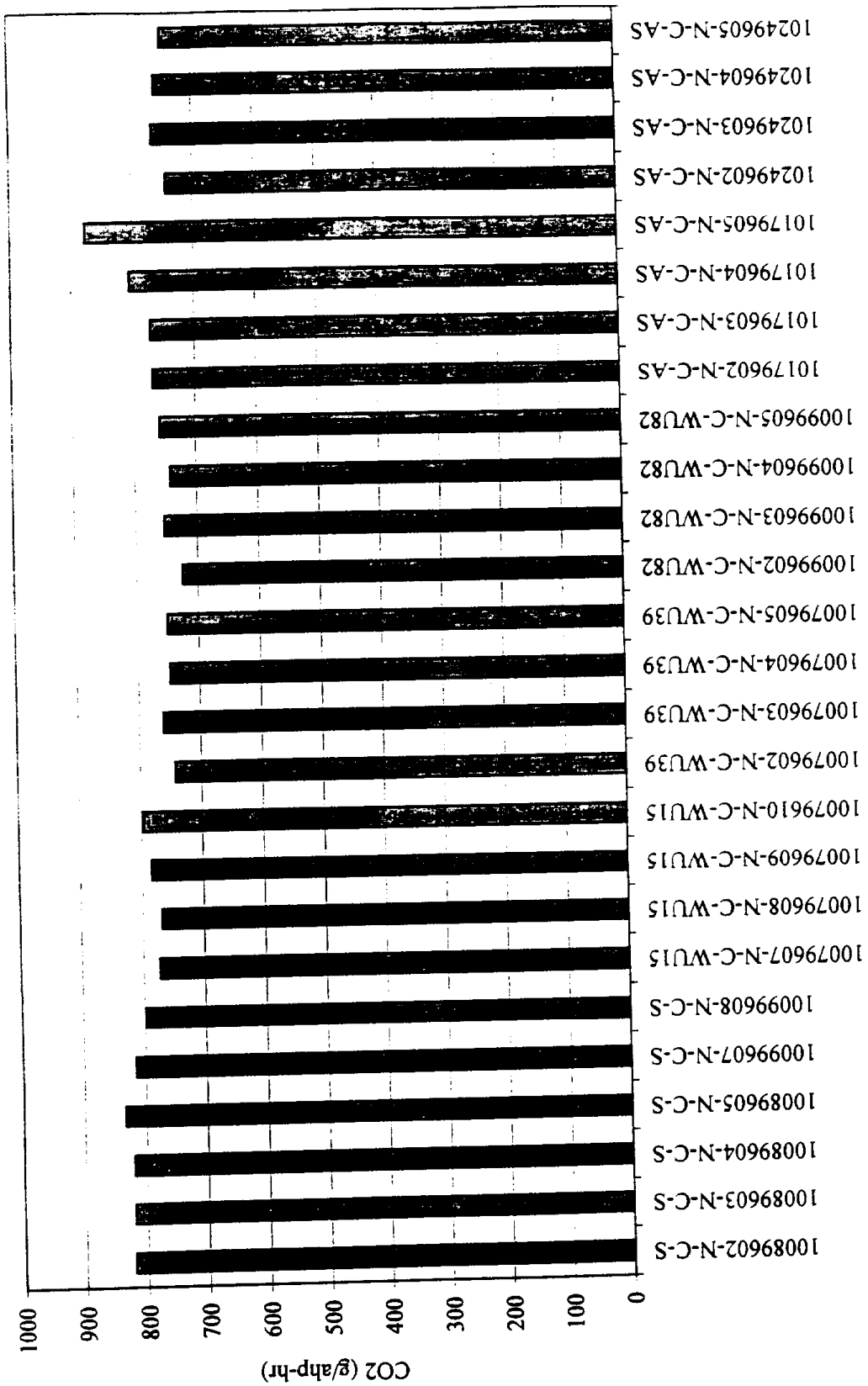

Figure 9.23 - Integrated carbon dioxide emissions from Navistar transient chassis testing

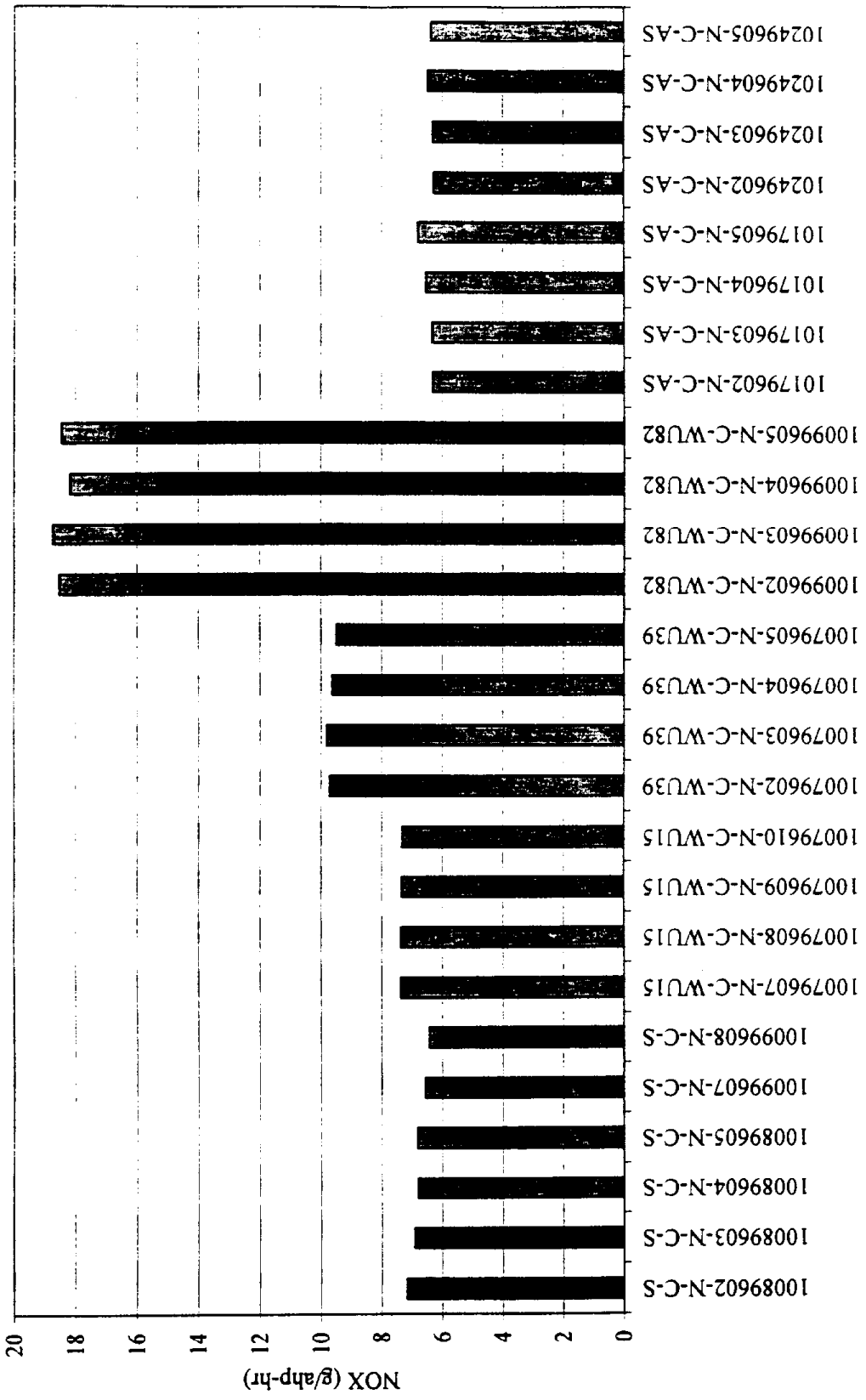

9.24 - Integrated oxides of nitgrogen emissions from Navistar transient chassis testing

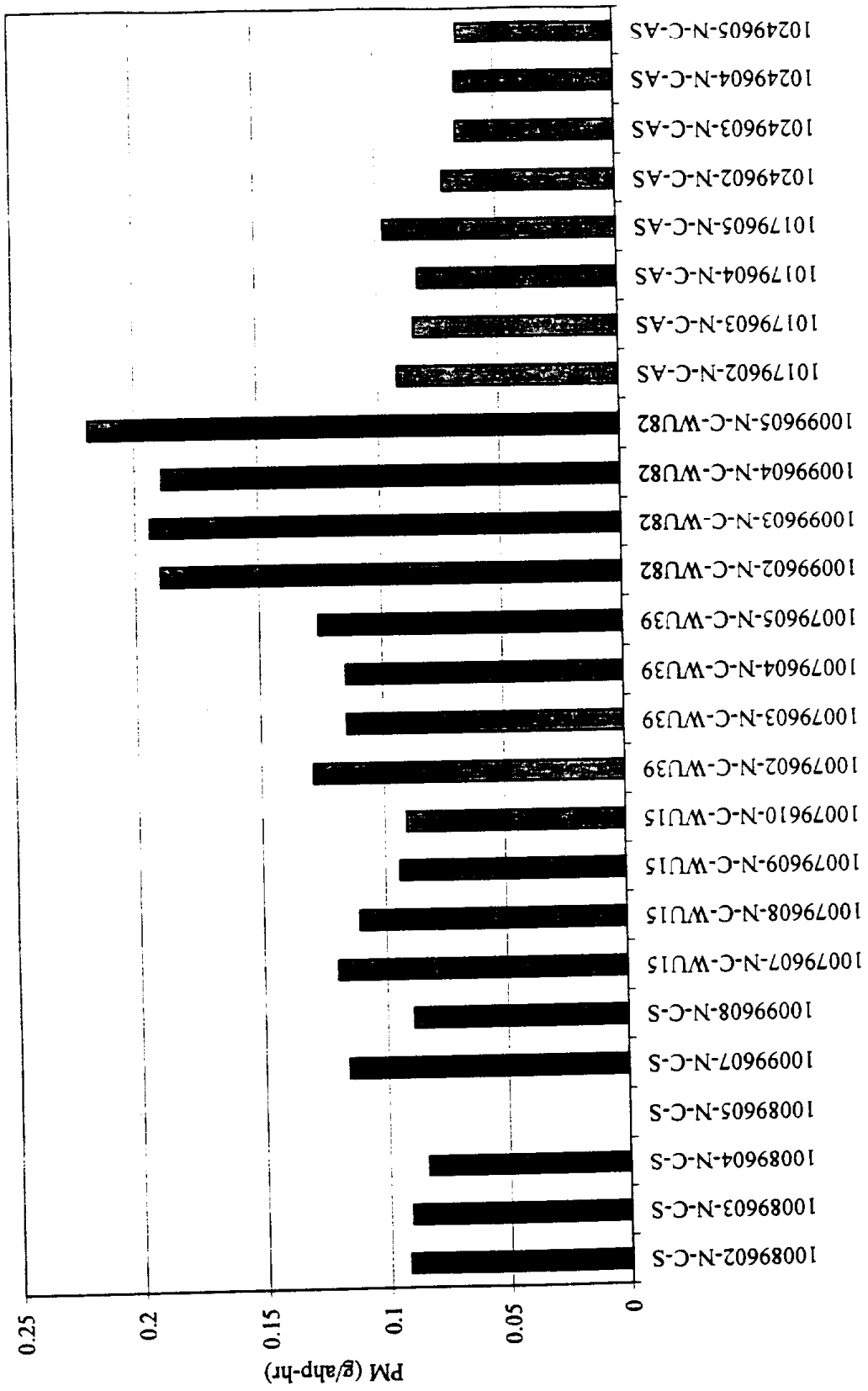

Figure 9.25 - Integrated particulate matter emissions from Navistar transient chassis testing

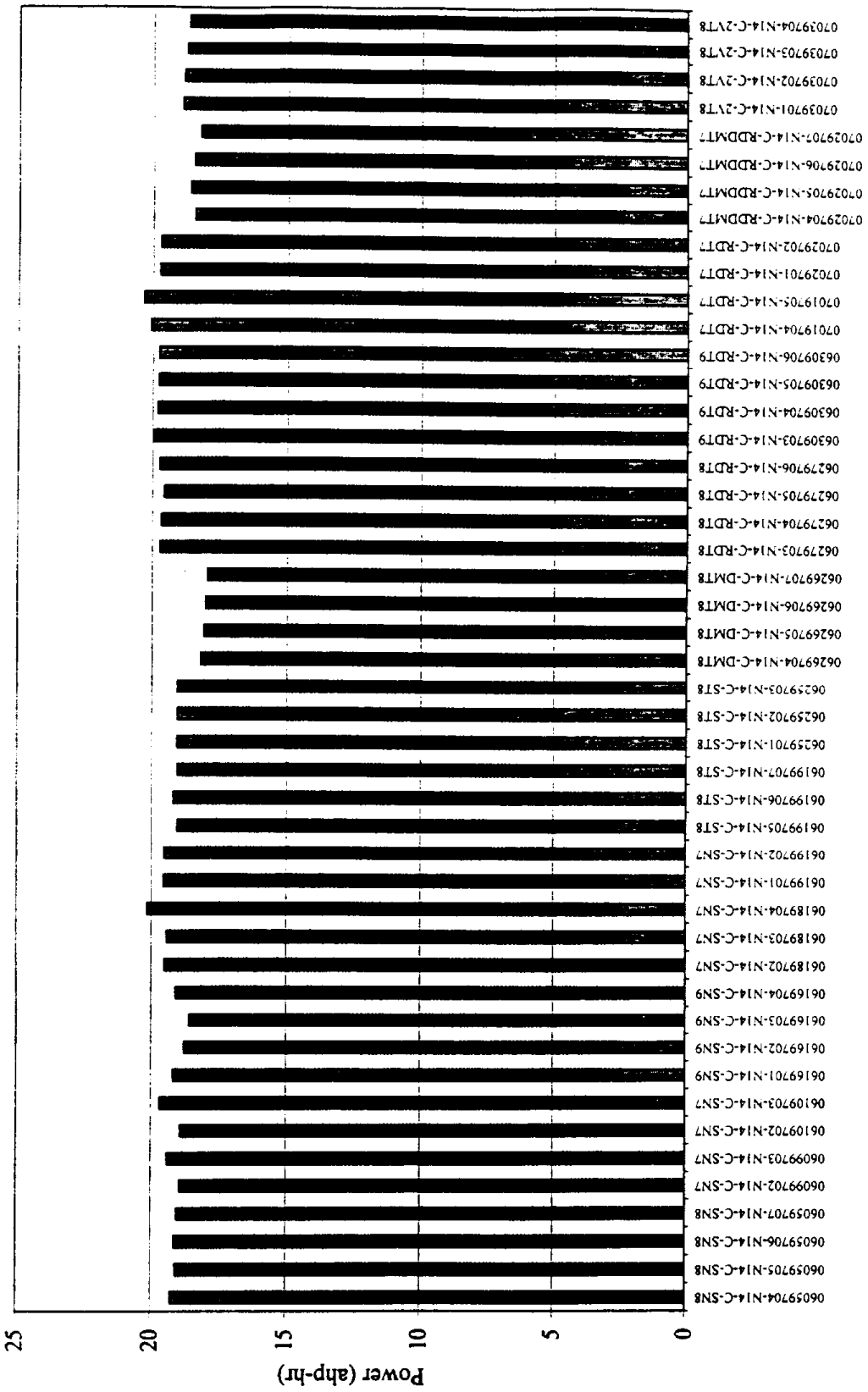

Figure 9.26 - Integrated axle power from Cummins transient chassis testing

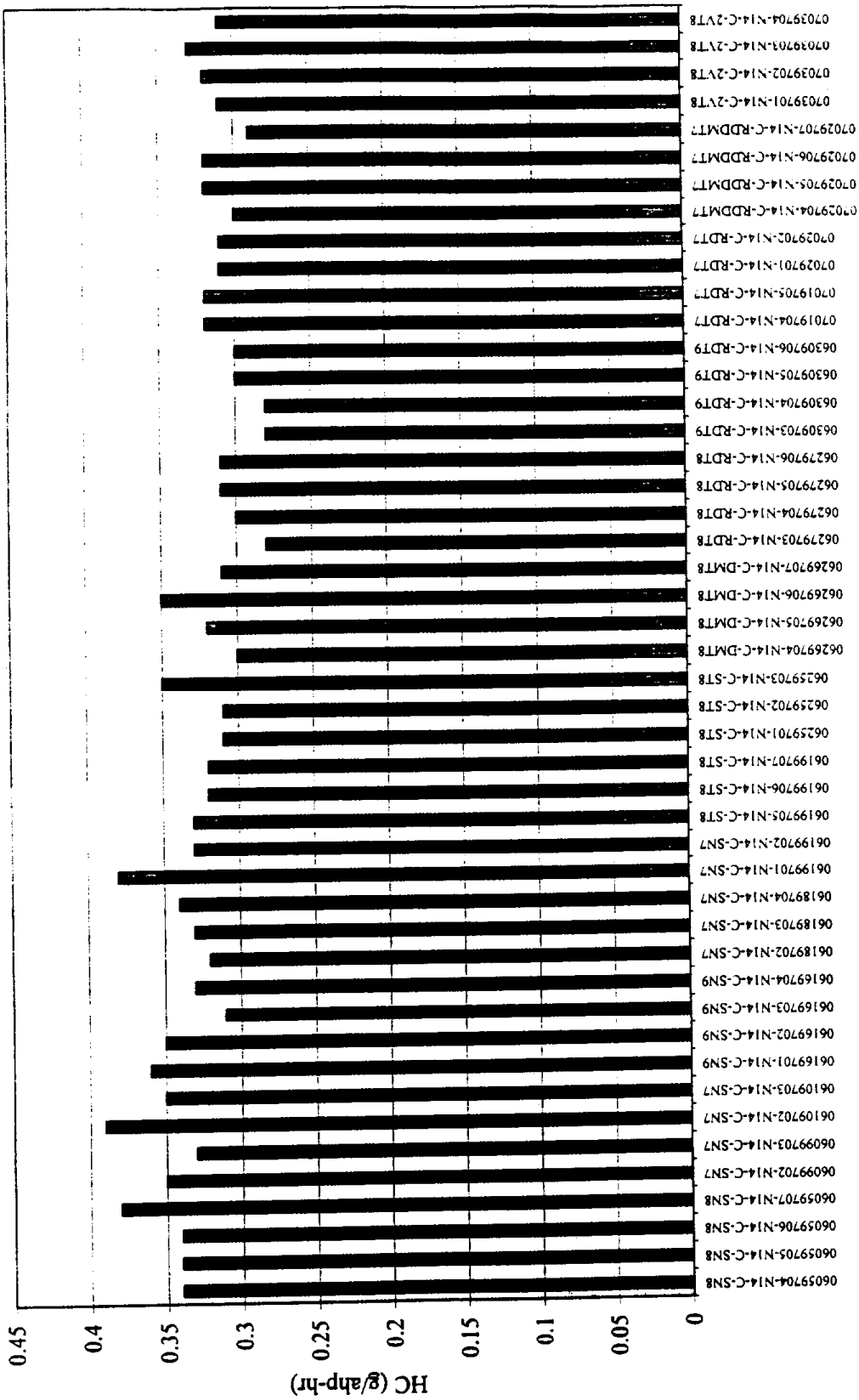

Figure 9.27 - Integrated hydrocarbon emissions from Cummins transient chassis testing

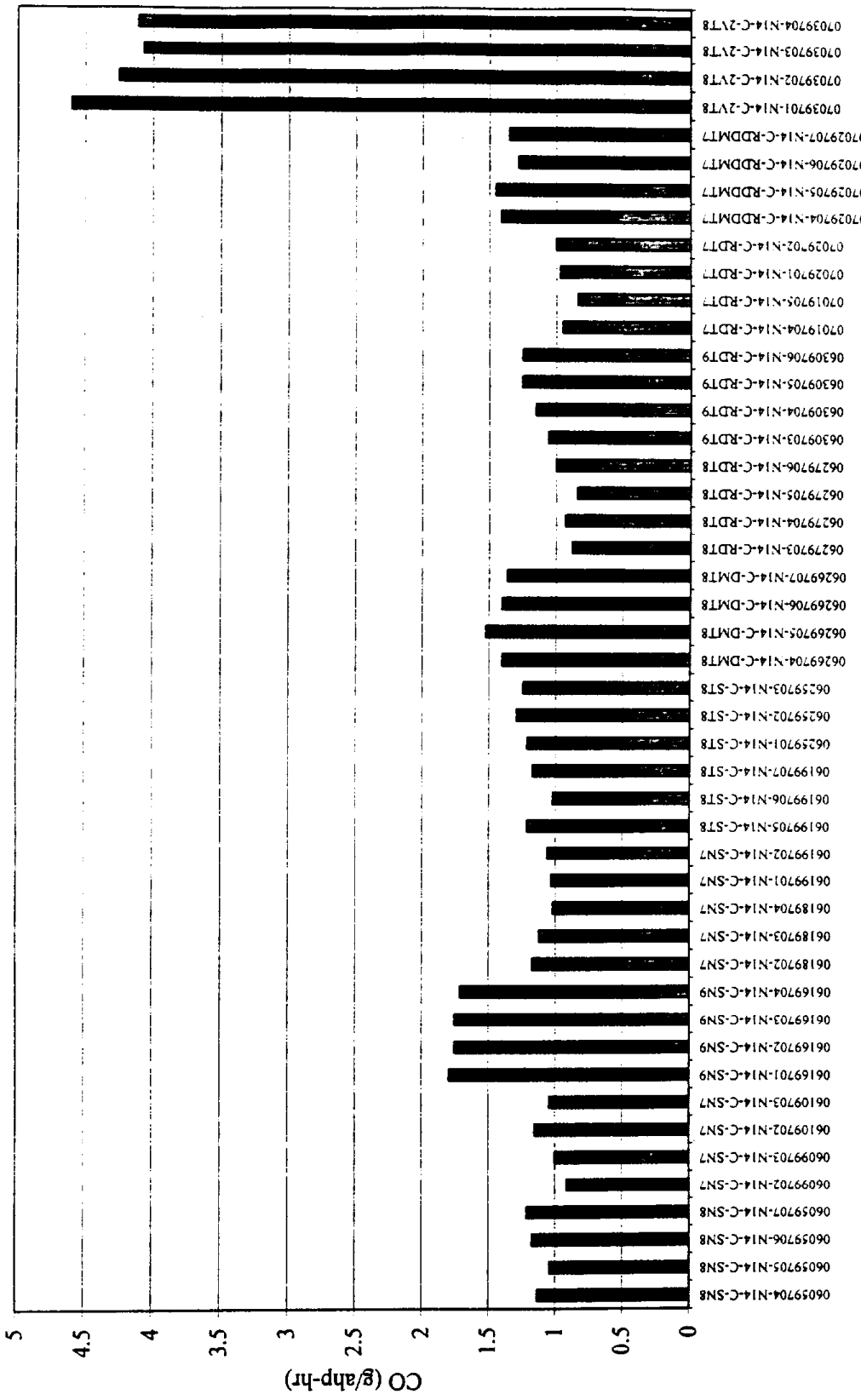

Figure 9.28 - Integrated carbon monoxide emissions from Cummins transient chassis testing

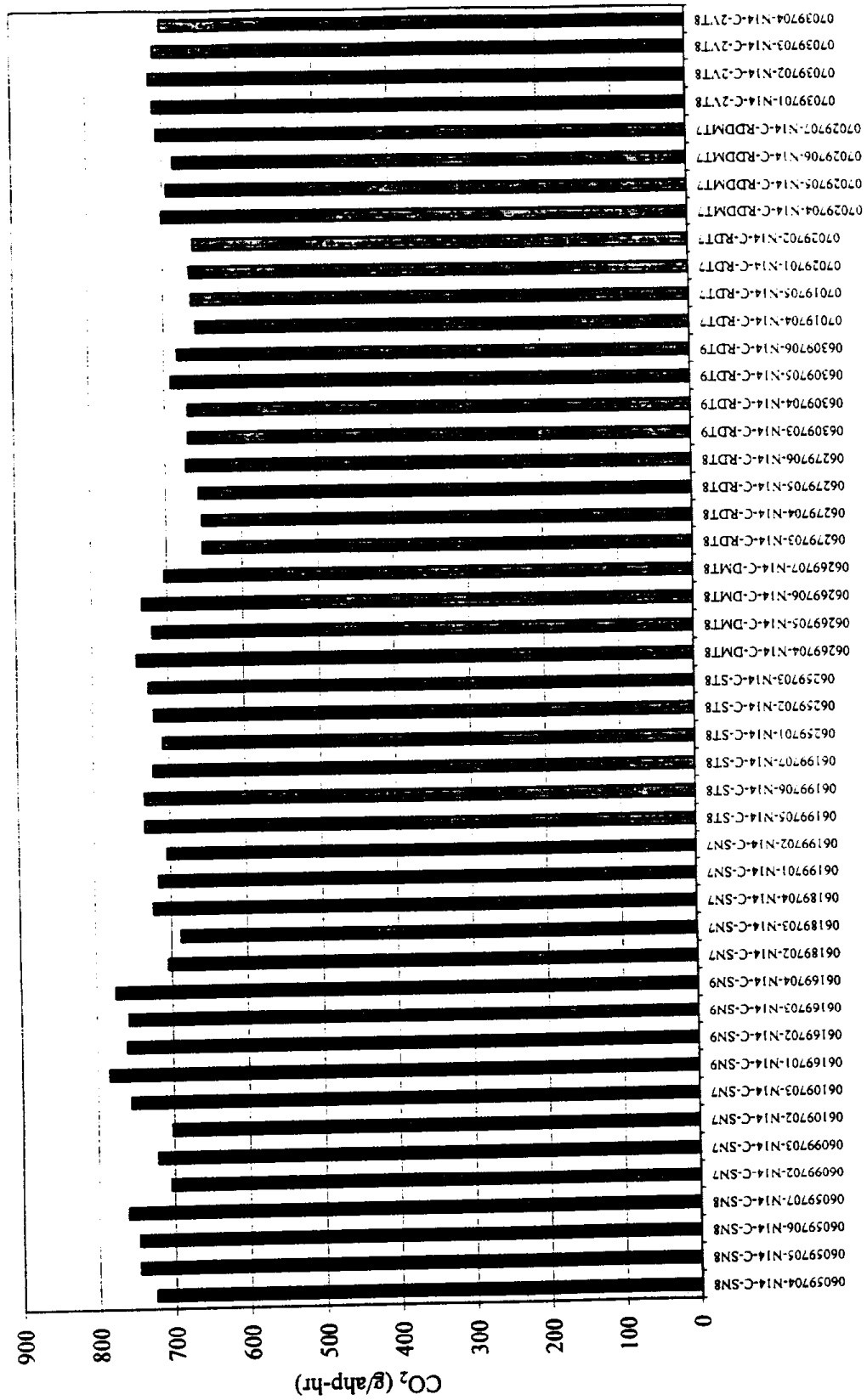

Figure 9.29 - Integrated carbon dioxide emissions from Cummins transient chassis testing

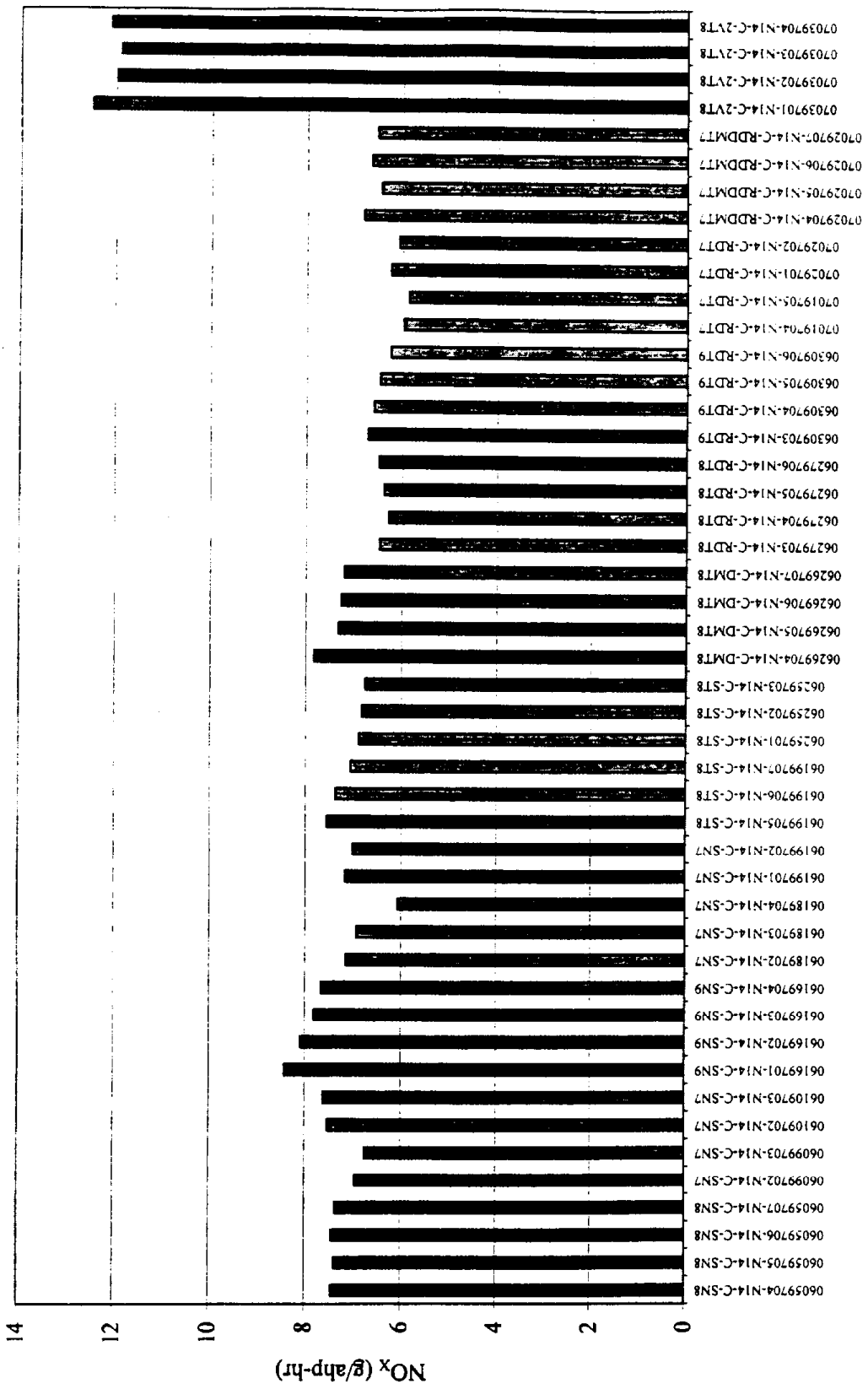

Figure 9.30 - Integrated oxides of nitrogen emissions from Cummins transient chassis testing

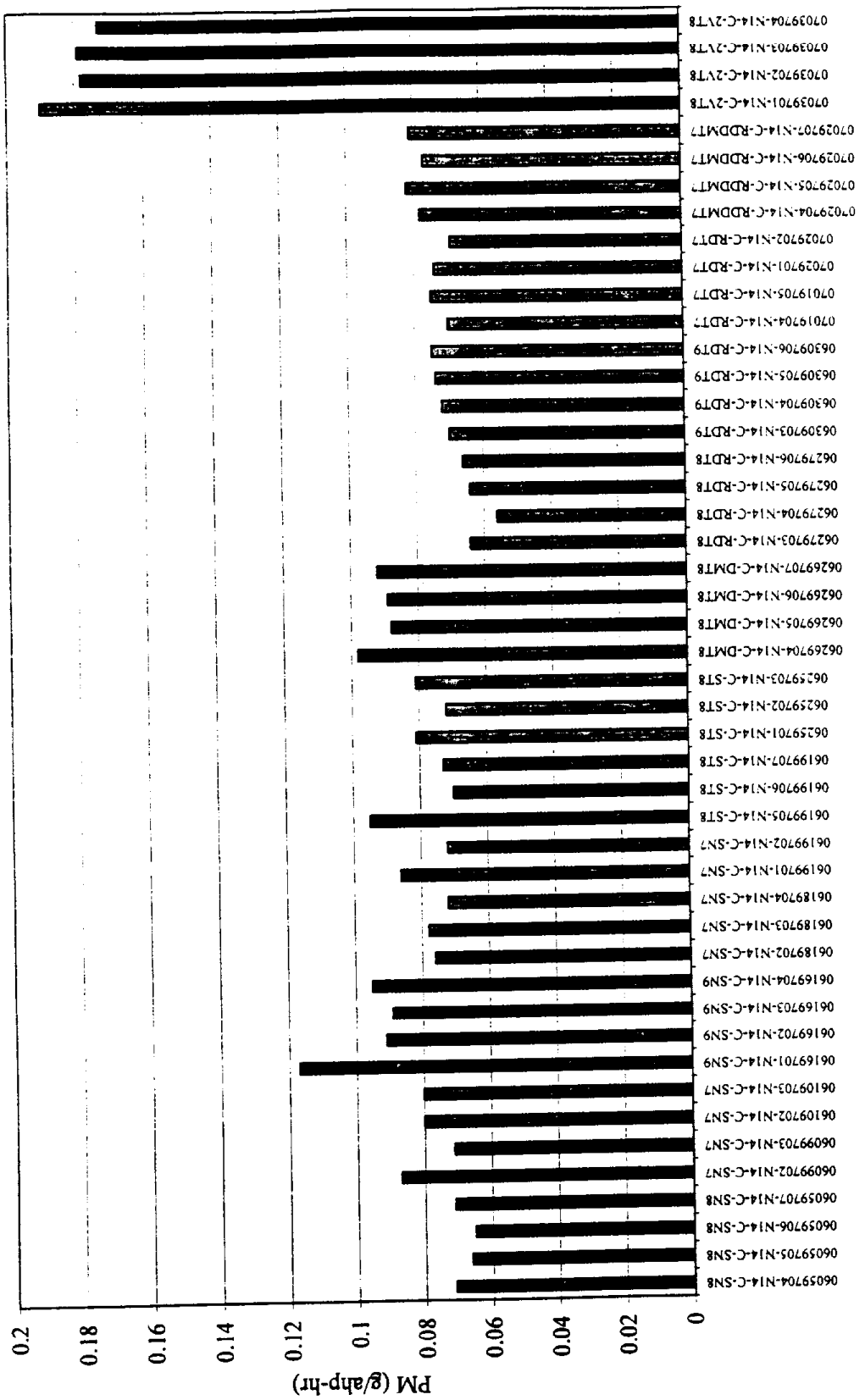

Figure 9.31 - Integrated particulate matter emissions from Cummins transient chassis testing

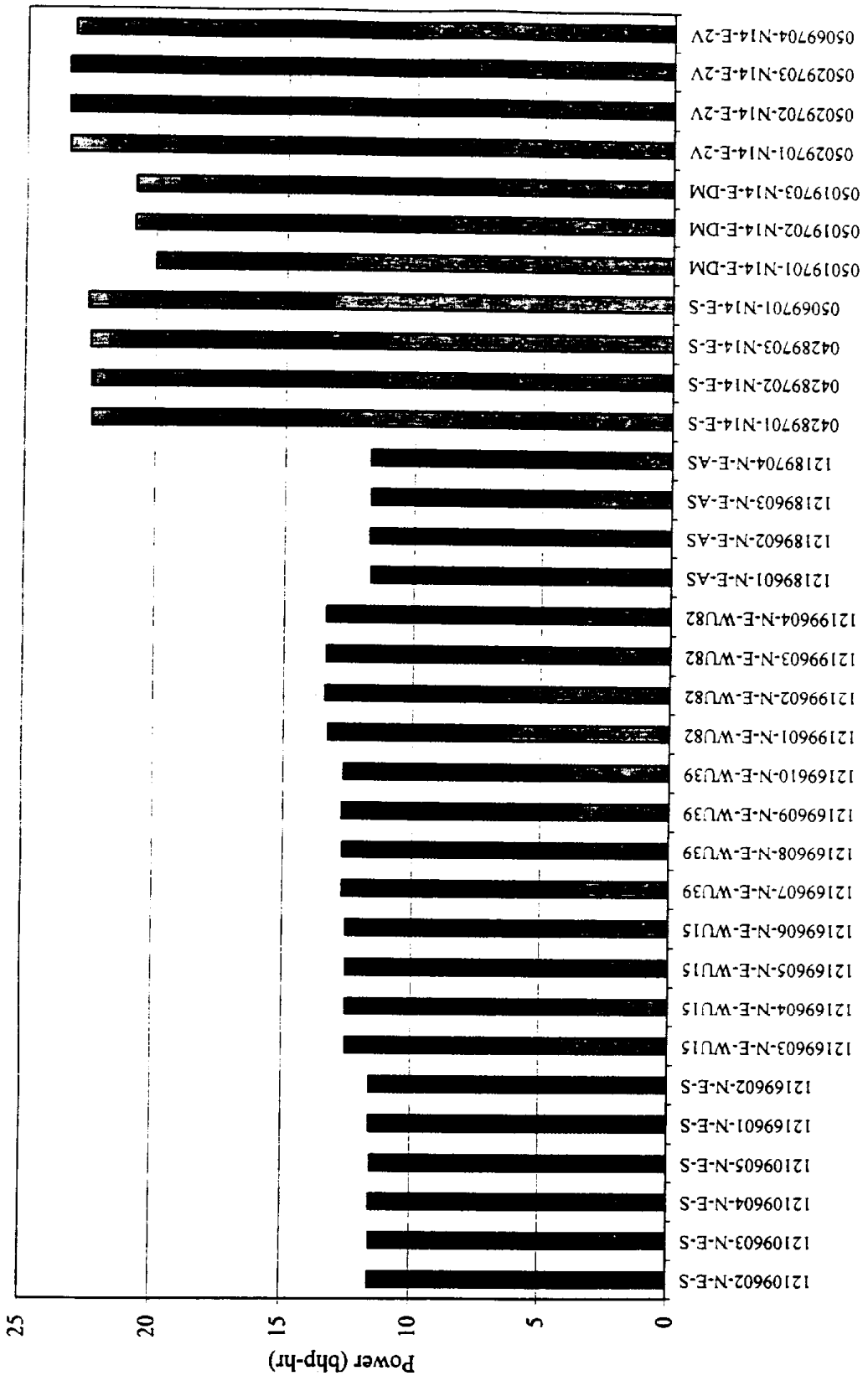

Figure 9.32 - Integrated power from transient tests of the Navistar and Cummins engines

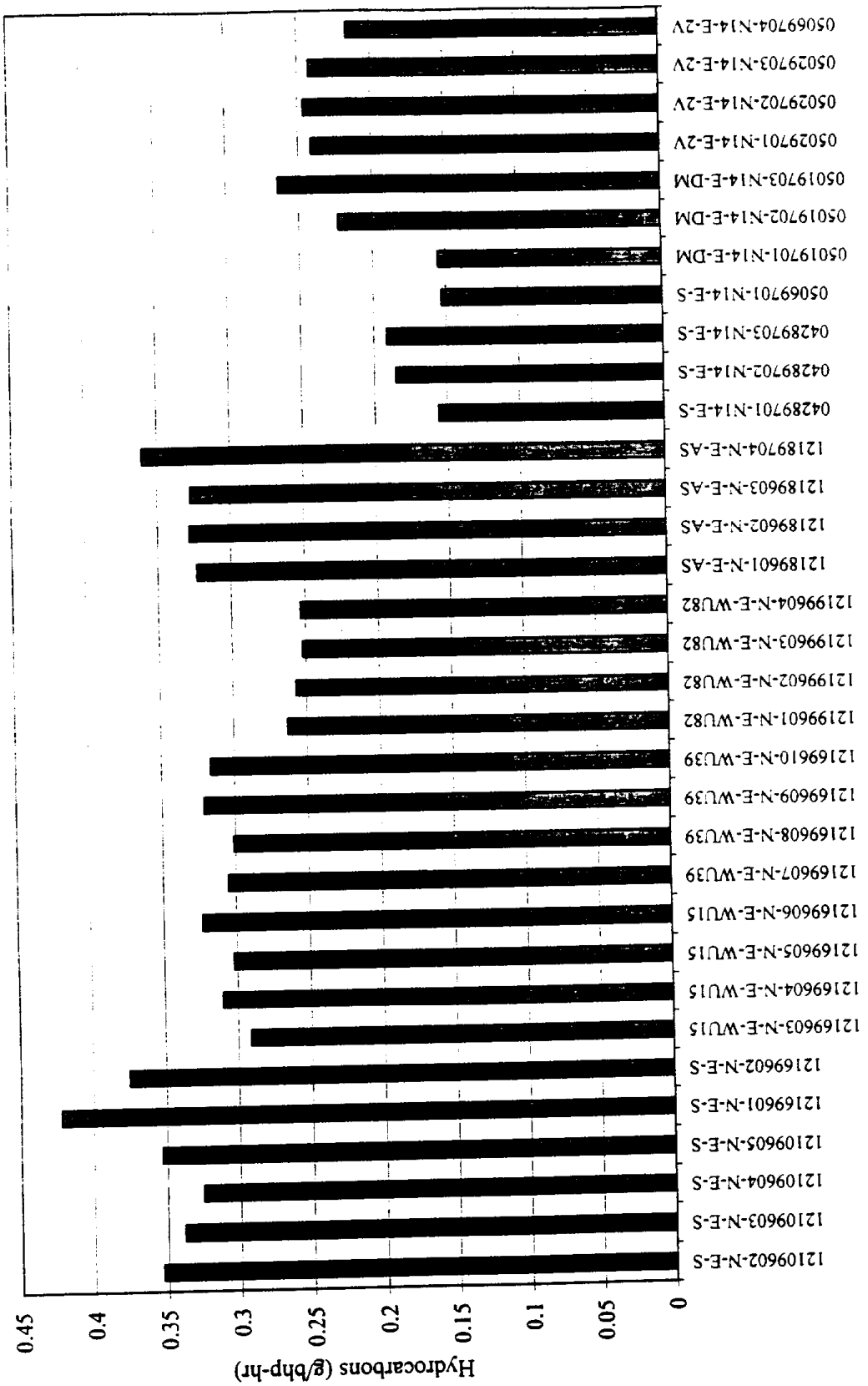

Figure 9.33 - Integrated hydrocarbon emissions from transient tests of the Navistar and Cummins engines

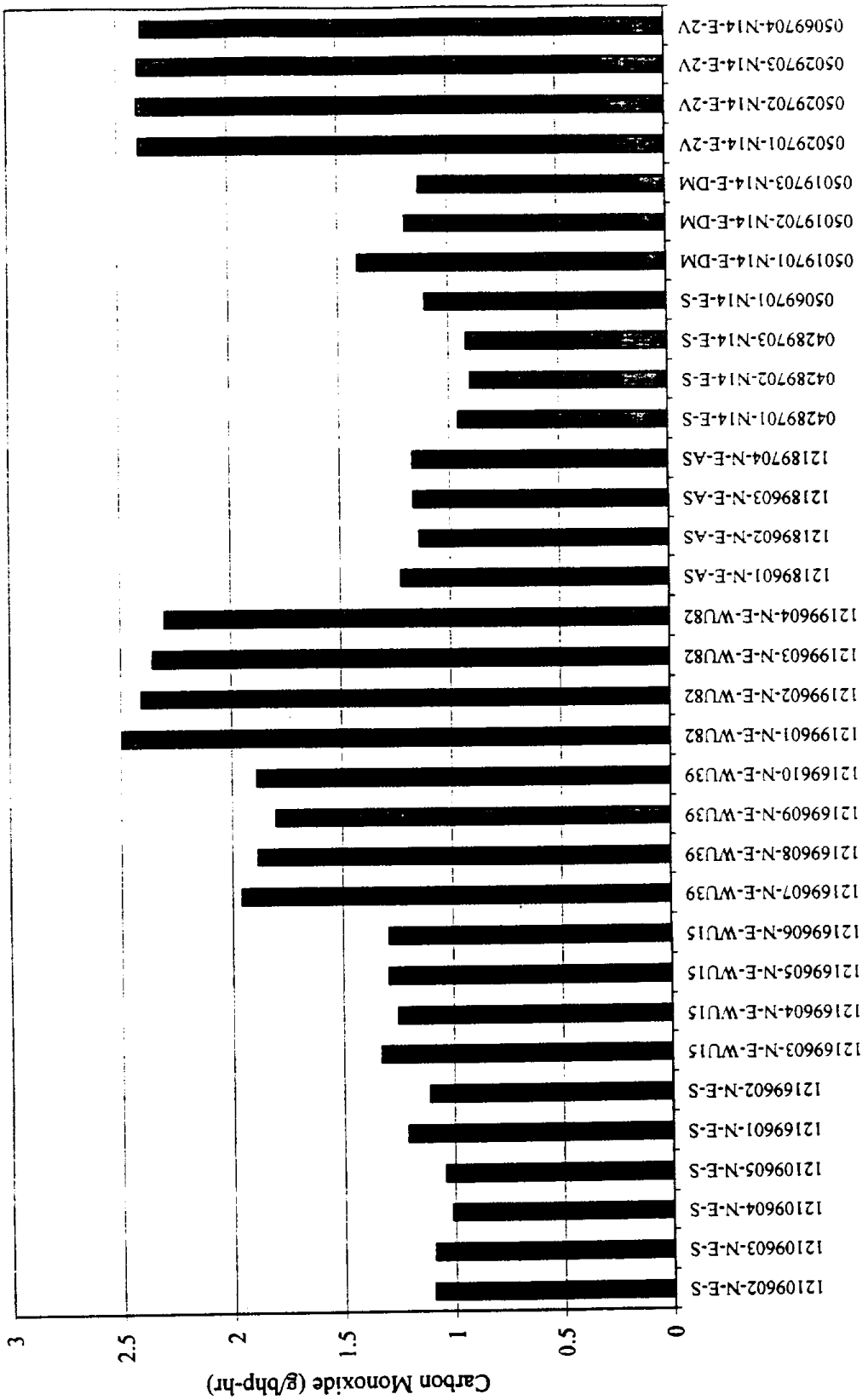

Figure 9.34 - Integrated carbon monoxide emissions from transient tests of the Navistar and Cummins engines

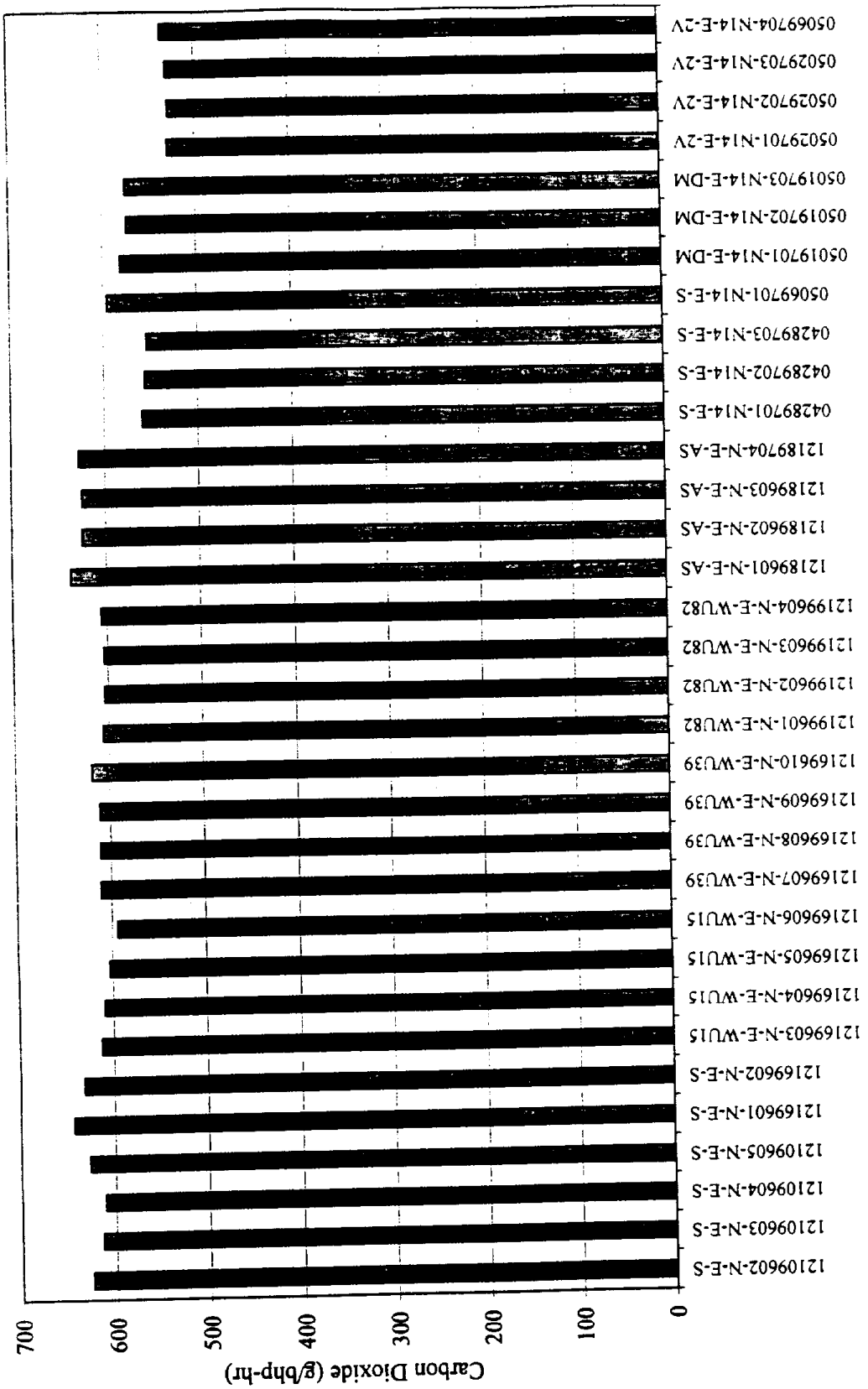

Figure 9.35 - Integrated carbon dioxide emissions from transient tests of the Navistar and Cummins engines

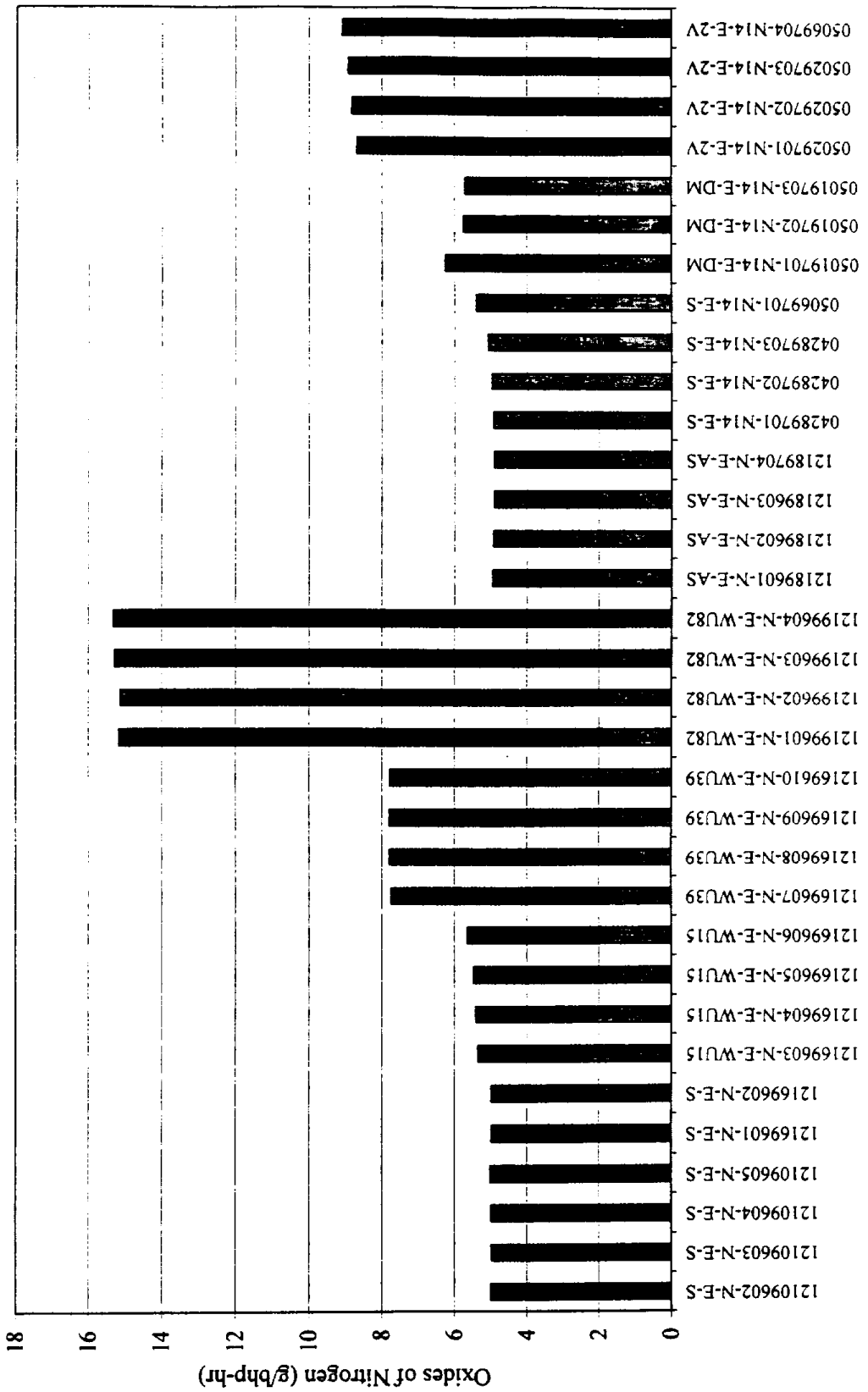

Figure 9.36 - Integrated oxides of nitrogen emissions from transient tests of the Navistar and Cummins engines

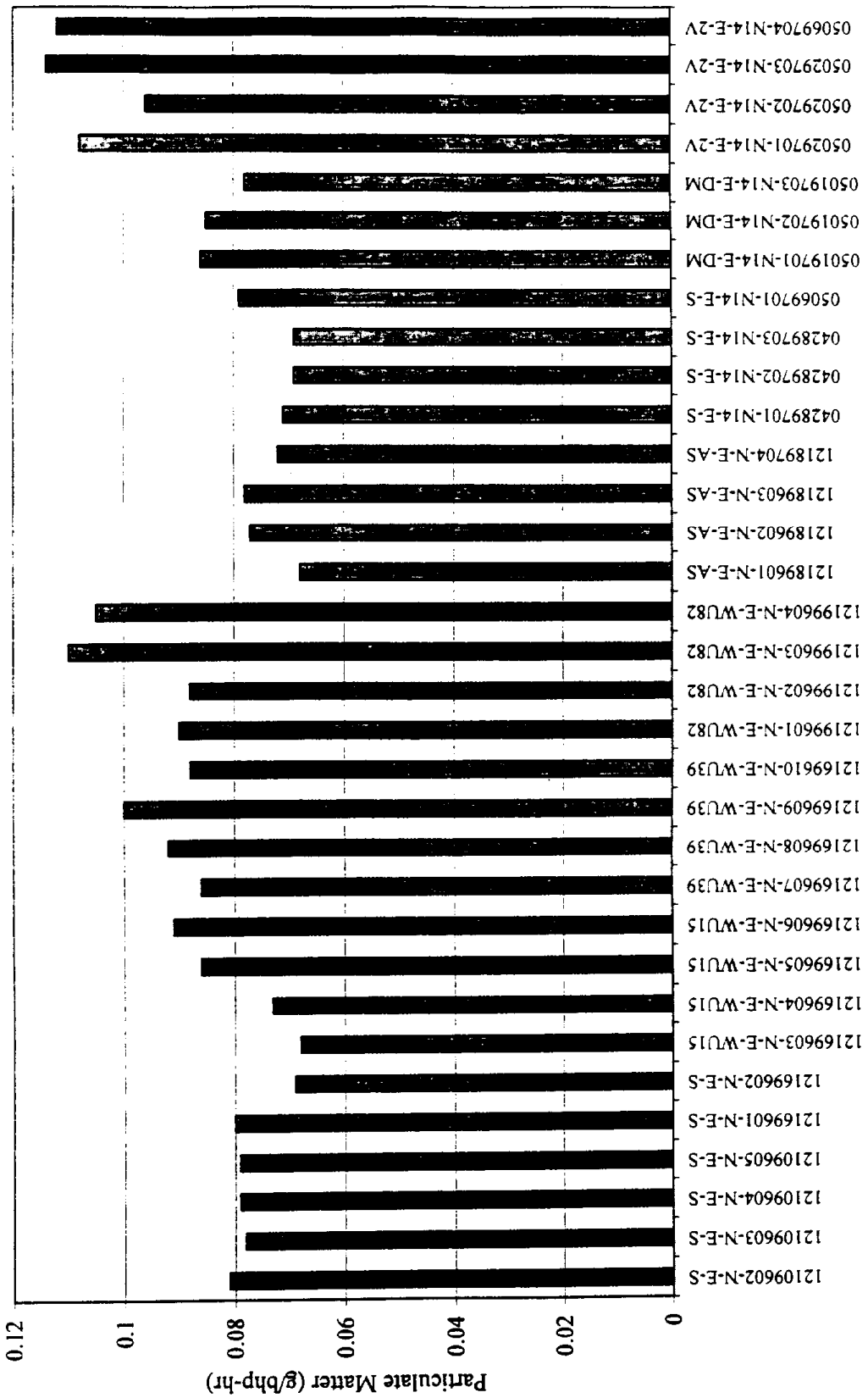

Figure 9.37 - Integrated particulate matter emissions from transient tests of the Navistar and Cummins engines

Figure 9.38 - Average work from transient engine tests

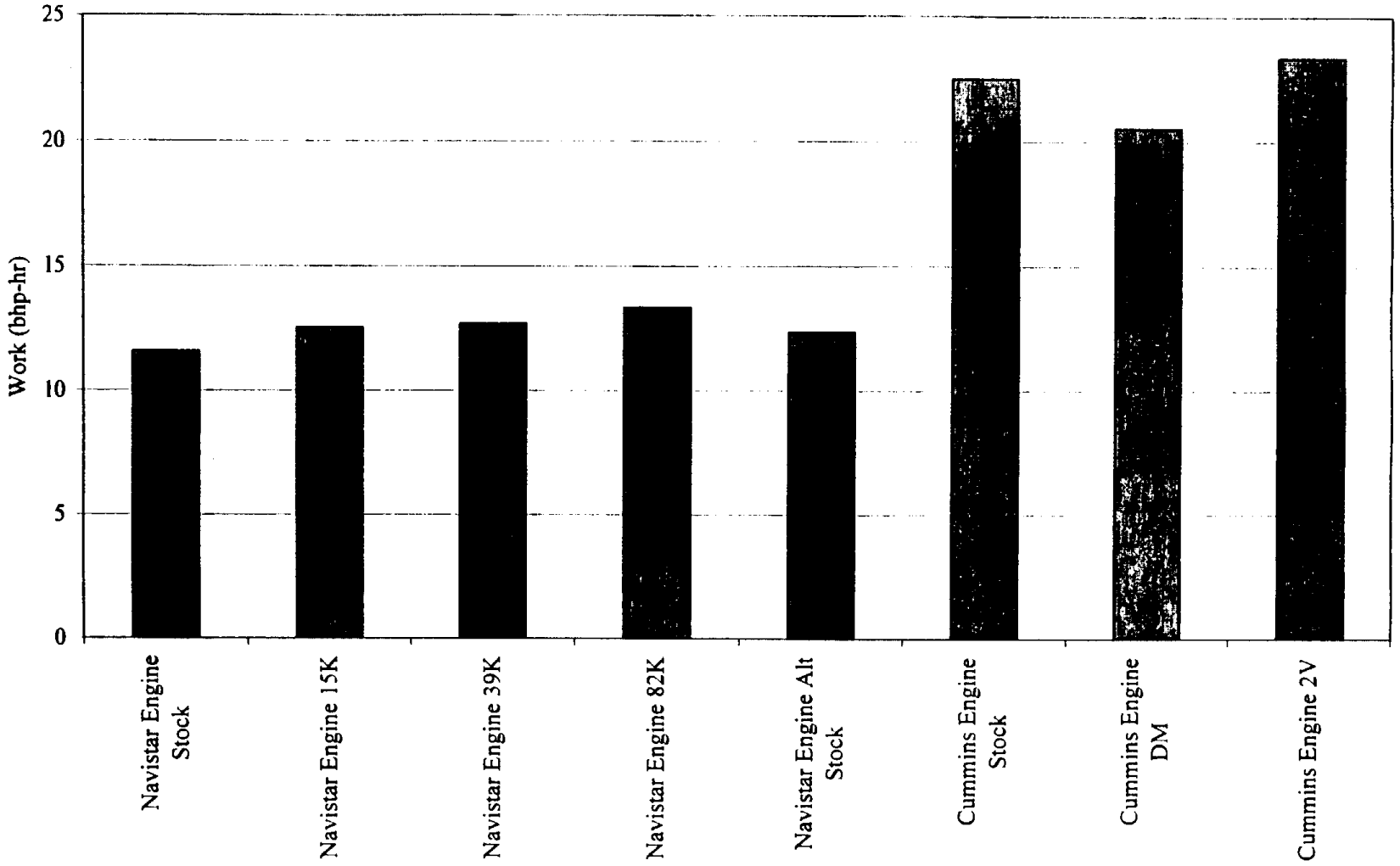

Figure 9.39 - Average hydrocarbon emissions from transient engine tests

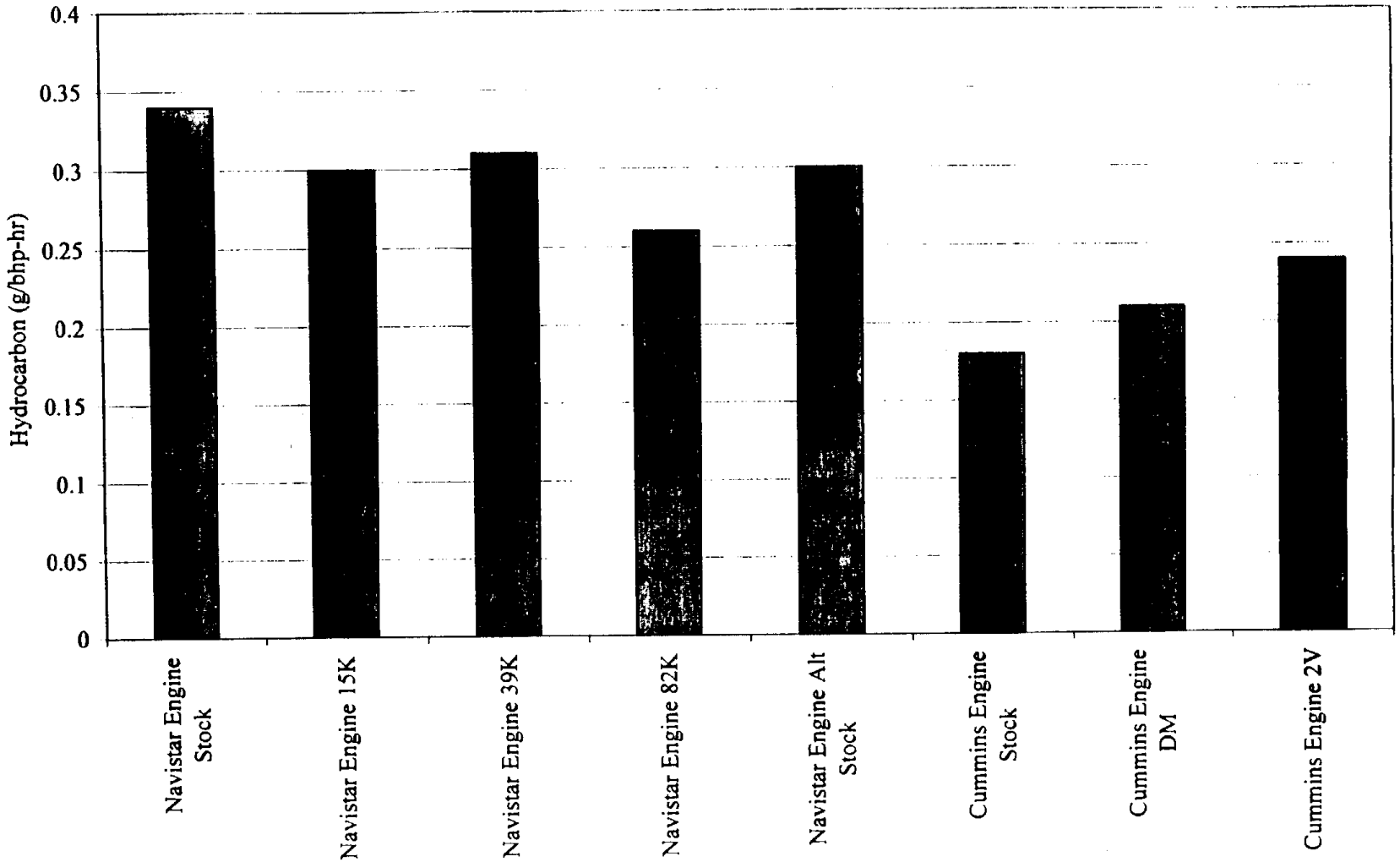

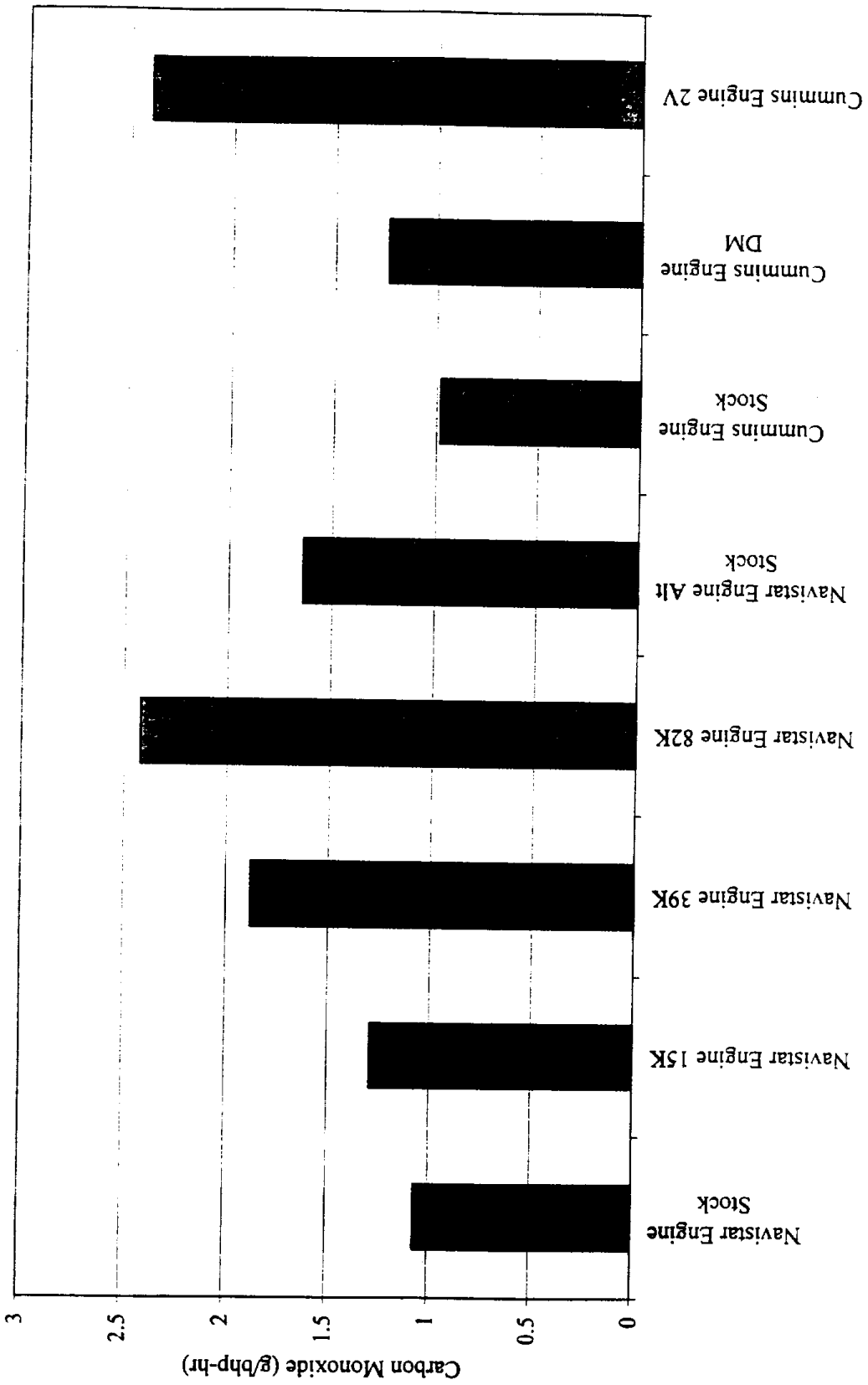

Figure 9.40 - Average carbon monoxide emissions from transient engine tests

Figure 9.41 - Average carbon dioxide emissions from transient engine tests

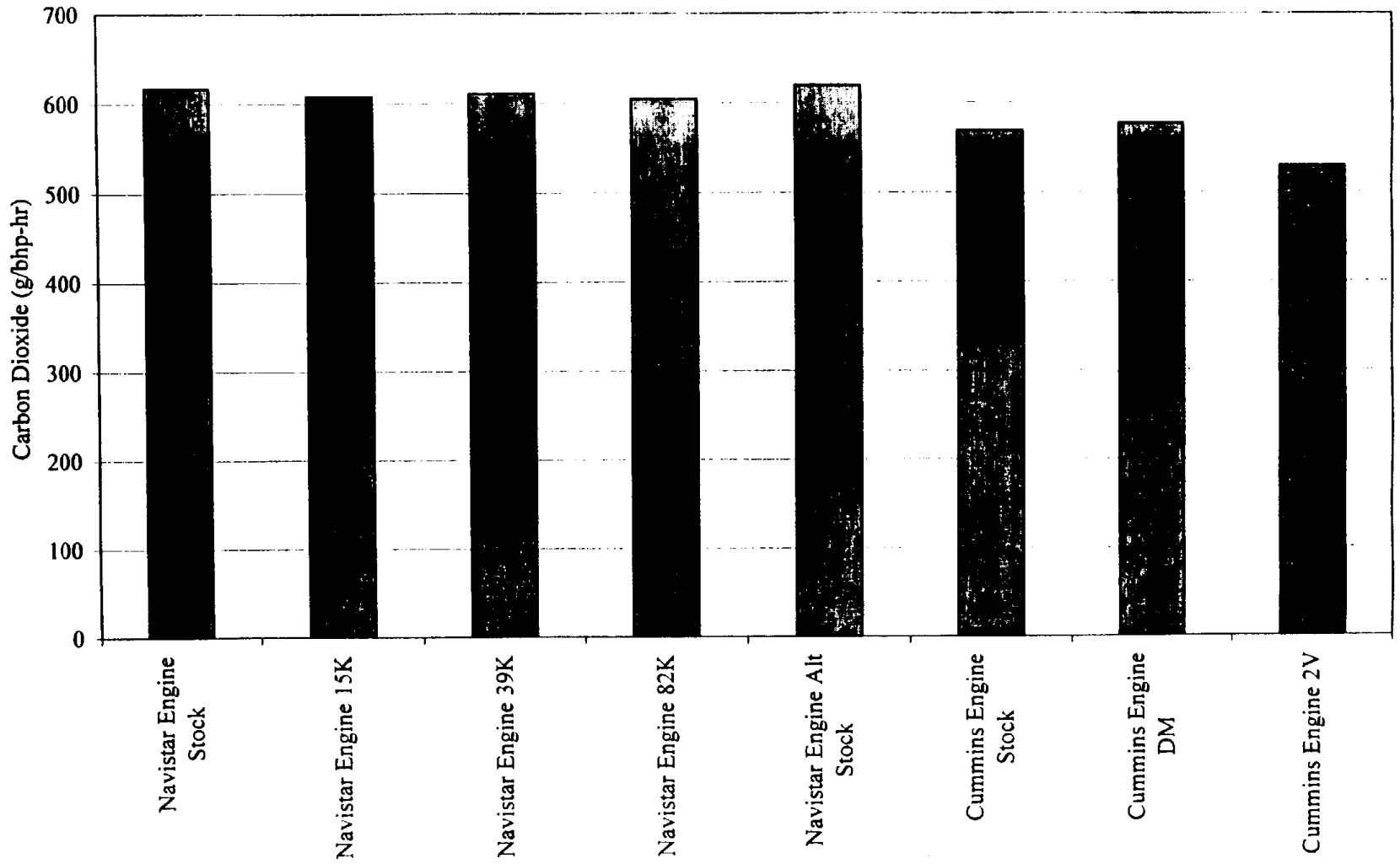

Figure 9.42 - Average oxides of nitrogen emissions from transient engine tests

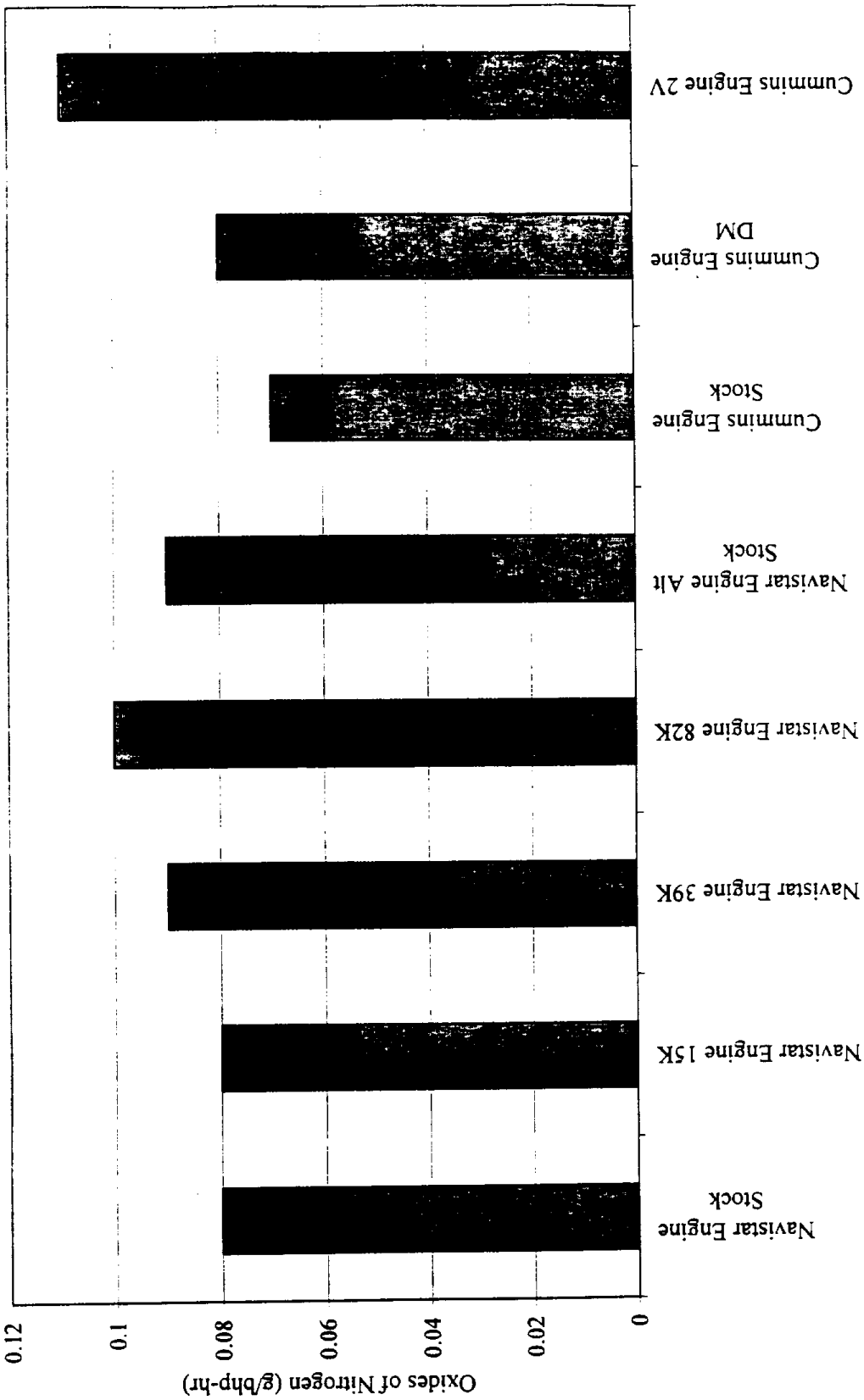

Figure 9.43 - Average particulate matter emissions from transient engine tests

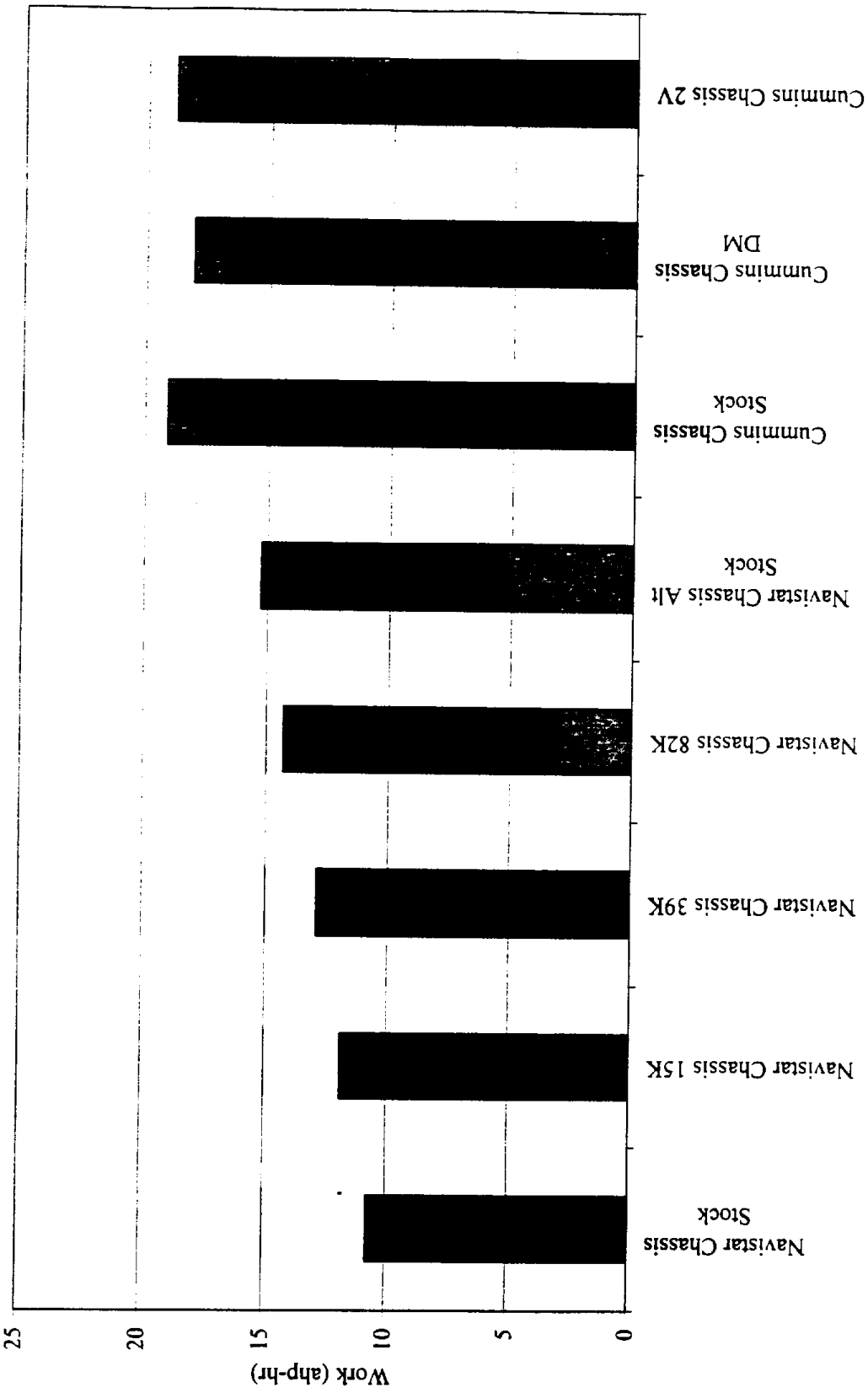

Figure 9.44 - Average work from transient chassis tests

Figure 9.45 - Average hydrocarbon emissions from transient chassis tests

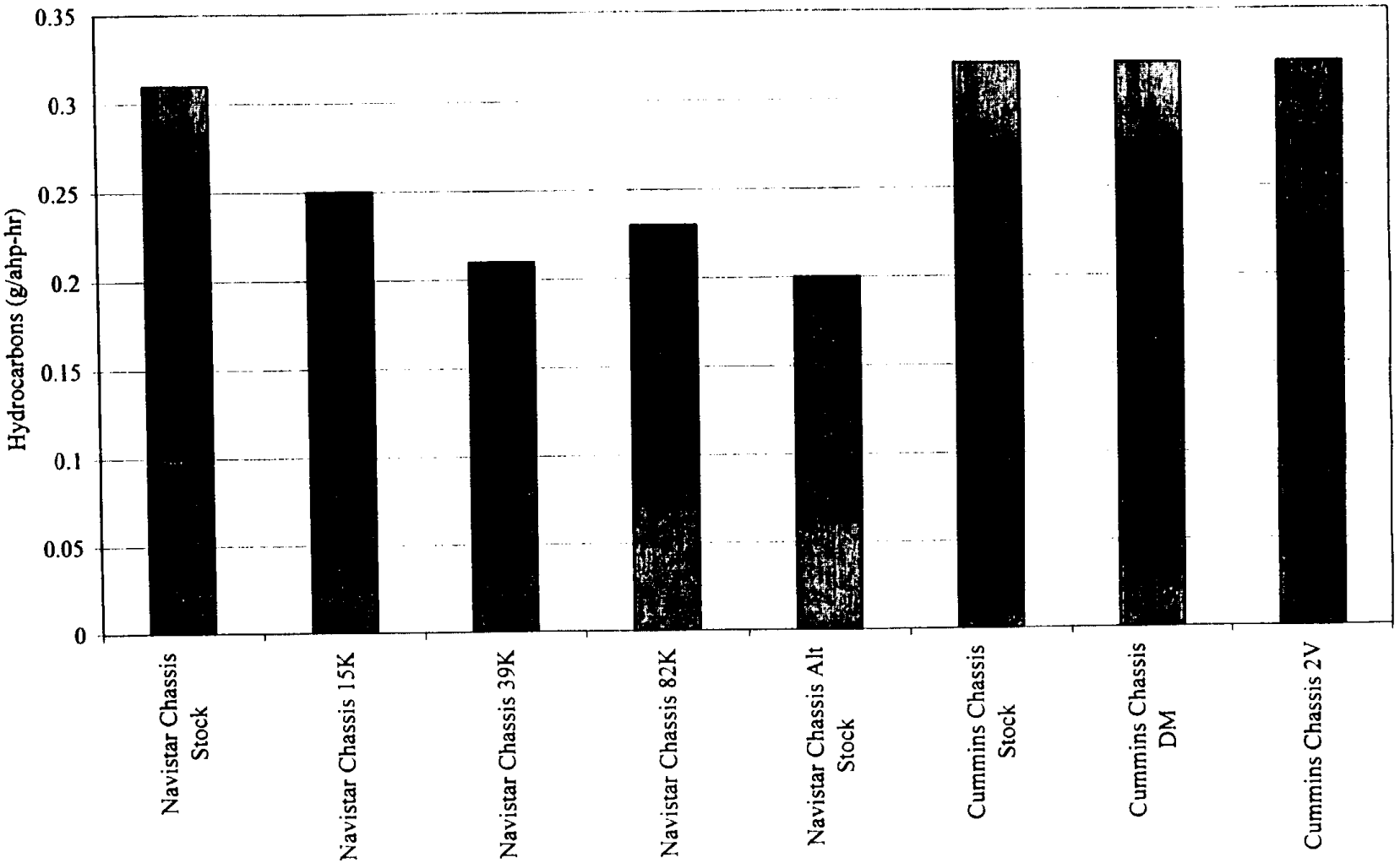

Figure 9.46 - Average carbon monoxide emissions from transient chassis tests

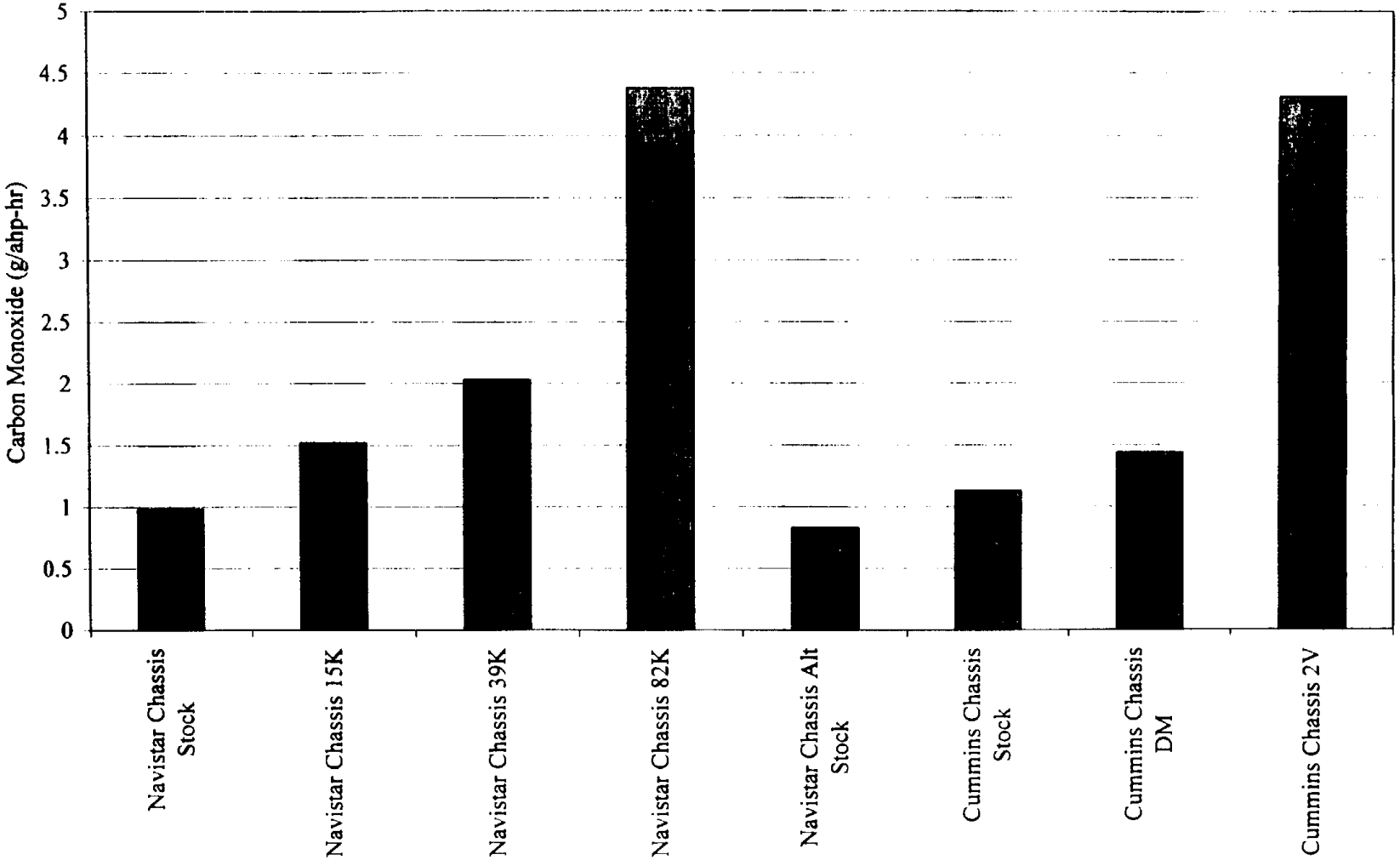

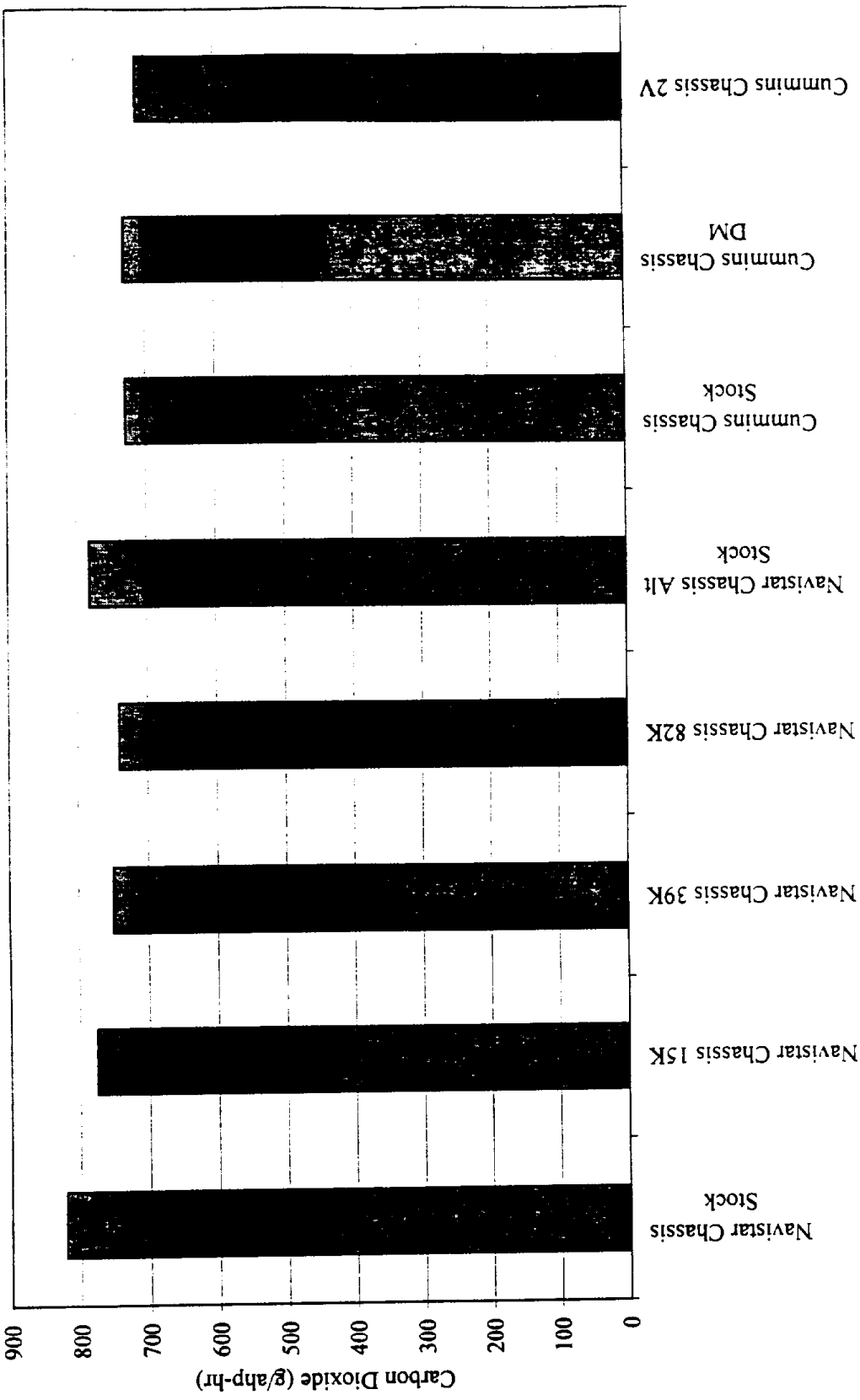

Figure 9.47 - Average carbon dioxide emissions from transient chassis tests

Figure 9.48 - Average oxides of nitrogen emissions from transient chassis tests

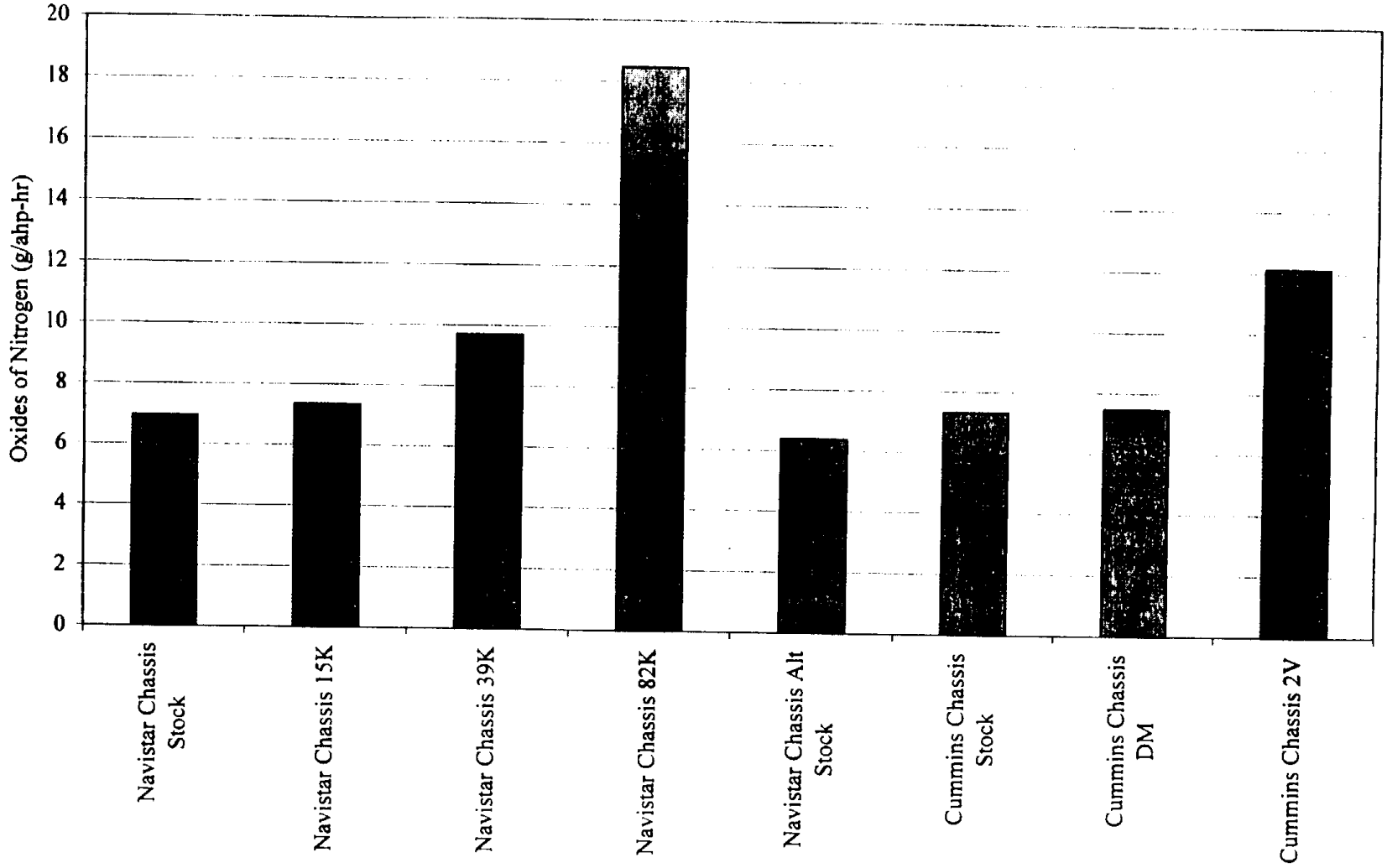

Figure 9.49 - Average particulate matter emissions from transient chassis tests

10. Electronic Throttle Control

Modern electronic engine controllers (ECM) use a pedal-operated potentiometer to signal torque demanded by the operator. When the engine is run in a "test cell" mode, this potentiometer can be replaced by an "electronic potentiometer" incorporating electrical isolation to obviate signal and ground mixing between the controlling computer and the ECM.

The device used in this implementation is the Analog Devices AD8402. This chip contains two 10k or potentiometers with 256 linear stops. By choosing suitable fixed resistors for the top and bottom of the "variable" resistor, an electrical equivalent of the pedal-operated potentiometer with 256 make-before-break taps can be constructed. In this implementation, a single pole change over relay is used. The relay is operated by the controlling computer at or near the lowest resistance values.

Figure 10.1 – Schematic of Electronic Control used in Cummins and Navistar Testing

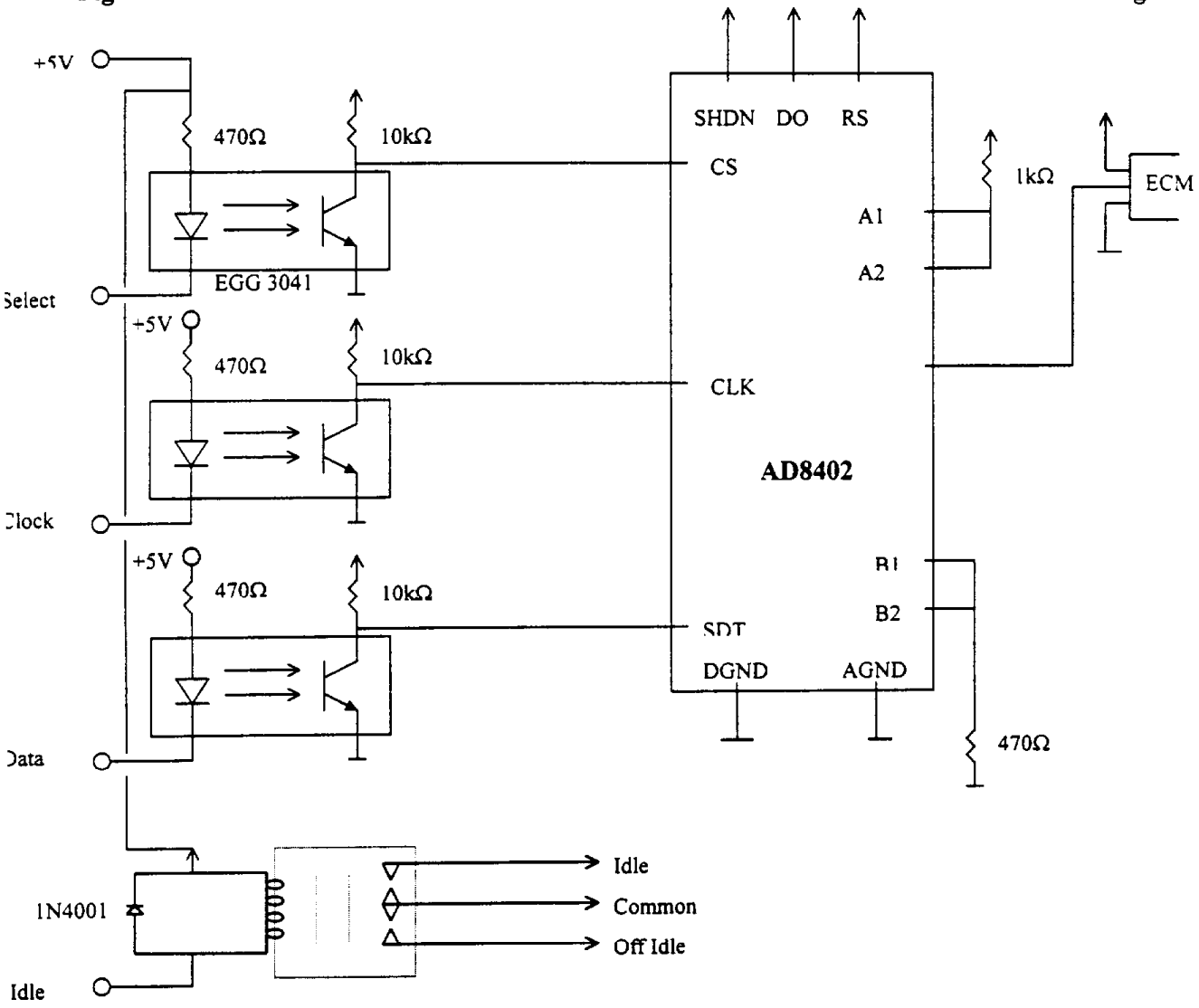

A software PI control was incorporated into the test software at both the engine and chassis emissions laboratories. This PI controller worked in conjunction with the digital throttle controller to modify pedal position according to the speed and load demand of the schedule. This was accomplished by comparing the engine speed and torque to that demanded by the schedule both as an proportional (difference) and an integral (summed difference). For points in the test where torque and speed were changing rapidly the proportional control was able to modify the pedal position rapidly to bring the engine close to the desired setpoint. As engine speed and torque approached the setpoint the influence of the proportional control lowered and the integral control modified the pedal position to more closely match the setpoint.

Use of this system, in conjunction with control of the dynamometers, allowed the engine both to follow the schedule closely and to maintain reproducibility between tests. This device was also instrumental in establishing the drivetrain efficiency through reproducible operation of the engine both on an engine dynamometer and installed in the vehicle chassis.